CHARACTERISATION OF ANTI-CANCER PROPERTIES OF BIOACTIVE COMPOUNDS IN SEA ANEMONE VENOM

MAHNAZ RAMEZANPOUR

(MSC MICROBIOLOGY)

Faculty of Medicine, Nursing and health Sciences

Flinders University of South Australia

A thesis submitted in fulfilment of the requirement for the degree of Doctor of Philosophy

July 2015

Thesis Summary

The potential of crude venom extracts, obtained by the milking technique from five sea anemones (*Heteractis crispa, Heteractis magnifica, Heteractis malu, Cryptodendrum adhaesivum* and *Entacmaea quadricolor*), to kill cancer cells was tested on three human cancer cell lines (A549 lung cancer; T47D breast cancer and A431 skin cancer). The level of cytotoxicity depended on which sea anemone venom extract was used and which cancer cell line was tested. The study then focused on *Heteractis magnifica* as its venom extract had significant inhibitory effects on the three cancer cell lines tested in the initial study. The *H. magnifica* venom displayed potent cytotoxic activity against human lung cancer A549 cells, with less effect on the survival of MRC5 human non-cancer lung cell line. This was evident by higher IC_{50} values (i.e. 18.17 µg/ml on the MRC5 cell line compared to 11.14 µg/ml on the A549 cancer cell line). *Heteractis magnifica* venom down-regulated cell cycle progression and induced apoptosis through the activation of caspases and mitochondrial membrane pathways in the A549 cancer cell line. Conversely, apoptotic cell death was not observed for MRC5 cells; instead, the cell death that occurred was by necrosis. Furthermore, *H. magnifica* venom significantly killed human adherent breast cancer cells T47D and MCF7. In contrast, an equivalent concentration of the venom exerted a lower effect on the survival of the 184B5 human non-cancer origin breast cell line. This was evident after 24 hours' (24h) treatment, with a higher IC_{50} value of 14.70 µg/ml on 184B5 (compared to values of 9.26 µg/ml on MCF7 and 5.67 µg/ml on T47D). The venom induced cell cycle arrest in T47D and MCF7 cell lines by apoptosis, through the activation of caspases and mitochondrial membrane pathways.

The crude venom was purified using size exclusion chromatography and mass spectrophotometry, and the amino acid sequence was partially determined. To provide sufficient material for functional investigation, recombinant protein was produced in a prokaryotic expression system and purified by affinity column. The peptide's cytotoxicity was evaluated by the MTT assay. The peptide decreased the survival of A549, T47D and MCF7 cancer cell lines. Conversely, an identical concentration of the peptide had significantly less effect on the survival of 184B5 cells. This was evident from higher IC_{50} values of 10.28 µg/ml on 184B5 (compared to 5.28 µg/ml on MCF7 and 6.97 µg/ml on T47D) after 24h treatment. The IC_{50} values for T47D and MCF7 (compared to values for 184B5) show support for selectivity against breast cancer cells. In addition, the IC_{50} value of T47D was much lower than published values for paclitaxel, the most common commercial drug currently used for breast cancer. These results clearly demonstrate that the purified recombinant peptide could be an excellent candidate for T47D breast cancer cell line if resistant to paclitaxel. The novel peptide identified has the potential for therapeutic development. It is able to decrease the survival of breast cancer cells in a dose-dependent manner, whereby the dose that targets and kills cancer cells has significantly less impact on non-cancer breast cells.

Table of Contents

List of Tables

List of Figures

List of Abbreviations

$\Delta\Psi$	mitochondrial membrane potential
ADC	adenocarcinoma
AIF	apoptosis-inducing factor
ALK	anaplastic lymphoma kinase
ALT	alanine transaminase
AMNH	American Museum of Natural History
ANOVA	analysis of variance
Ap-1	activator protein 1
Apaf-1	apoptosis protease-activating factor 1
AST	aspartate transaminase
AUC	area under the curve
BAC	bronchoalveolar carcinoma
BCA	bicinchoninic acid
BCC	basal cell carcinoma
BLAST	Basic Local Alignment Search Tool
BSA	bovine serum albumin
C. adhaesivum	*Cryptodendrum adhaesivum*
caspase	cysteine aspartate-specific protease
cDNA	complementary DNA
CVS	crystal violet staining (assays)
dH_2O	distilled water
DMEM	Dulbecco's minimum essential (or Dulbecco's modified Eagle) medium
DMSO	dimethyl sulfoxide
DNA	deoxyribonucleic acid
DNase	deoxyribonuclease
dNTPs	deoxynucleotides
DTT	dithiothreitol

E. coli	*Escherichia coli*
E. quadricolor	*Entacmaea quadricolor*
EDTA	ethylenediamine tetra acetic acid
EGFR	epidermal growth factor receptor
ELISA	enzyme-linked immunosorbent assay
FBS	foetal bovine serum
FDA	Food and Drug Administration (USA)
FITC	fluorescein isothiocyanate
FPLC	fast performance (pressure) liquid chromatography
h	hours (e.g. 24h = 24 hours)
H. crispa	*Heteractis crispa*
H. magnifica	*Heteractis magnifica*
H. malu	*Heteractis malu*
HCL	hydrochloric acid
HER2	human epidermal growth factor receptor 2
His	histidine
HMP	*Heteractis magnifica* peptide
HPLC	high-performance liquid chromatography
HSD	honestly significant difference (in Tukey's HSD post hoc test)
IC_{50}	50% inhibitory concentration
IPTG	isopropyl β-D-1-thiogalactopyranoside
K^+	potassium
KCl	potassium chloride
KDa	kilodalton
LB	lysogeny broth
MAP	mitogen-activated protein
ml	millimetre
mM	millimolar
MQ	Milli-Q water
mRNA	messenger RNA

MS	mass spectrometry
MS/MS	tandem mass spectrometry
MTT	3-(4,5-dimethylthiazol-2-yl)-2,5-diphenyl)tetrazolium bromide (or methylthiazol thiazolyl tetrazolium)
Na^+	sodium
NF-Kb	nuclear factor kappa-light-chain-enhancer of activated B cells
Ni	nickel
nm	nanometre
NSCLC	non-small cell lung carcinomas
OD	optical density
PARP	poly(ADP-ribose) polymerase
PBS	phosphate-buffered saline
PCR	polymerase chain reaction
PI	propidium iodide
RACE	rapid amplification of cDNA ends (RACE)
RLU	relative luminescence unit
RNase A	ribonuclease A
RNA	ribonucleic acid
rpm	revolutions per minute
RPMI	Roswell Park Memorial Institute
RT	room temperature
RT-PCR	reverse transcription polymerase chain reaction
SCC	squamous cell carcinoma
SCLC	small cell lung carcinomas
SEM	standard error of mean
SD	standard deviation
SDS	sodium dodecyl sulphate
SDS-PAGE	sodium dodecyl sulphate polyacrylamide gel electrophoresis
sp.	species
sp. nov.	new species

SPSS	Statistical Package for the Social Sciences (Version 18)
TE buffer	Tris/Borate/EDTA
TKIs	tyrosine kinase inhibitors
TNF	tumour necrosis factor
Tris-HCl	Tris hydrochloride
TRPV1	transient receptor potential cation channel, subfamily V, member 1
µg	microgram
µL	microlitre
USA/US	United States of America
UV	ultraviolet
VEGF	vascular endothelial growth factor
w/v	weight/volume percentage concentration

Declaration

I certify that this thesis does not incorporate, without acknowledgement, any material submitted for a degree or diploma in any university; and that, to the best of my knowledge and belief, it does not contain any material previously published or written by another person except where due reference is made in the text.

Mahnaz Ramezanpour

July 2015

Acknowledgements

I would like to pay principal acknowledgement to my supervisor Assoc. Prof. Barbara Sanderson for her professional guidance and support, and for her constructive criticisms of my study's experimentation, the manuscripts for publication and this thesis.

Thanks also go to my second supervisor Assoc. Prof. Karen Burke da Silva for her assistance, and for her helpful criticisms of my written work.

My deep gratitude goes to everyone in the Department of Medical Biotechnology, School of Medicine, Flinders University, beginning with Prof. Christopher Franco for his exemplary leadership and invaluable advice. My thanks go to Barbara Kupke and Angela Binns for looking after my safety in the lab, and keeping things running smoothly at all times. Thanks go to Dr Jing Jing Wang for always addressing my perplexities. Thanks also go to Jason who tolerated my many demands in the process of formatting my thesis and also for his friendship and supports.

An additional note of appreciation goes to Dr Timothy Chataway and Nousha Chegini for helping me to identify the peptide sequence by mass spectrometry and also guiding me in the use of the proteomics facilities. Thanks also go to Dr Shiwani Sharma and Sara Martin for their helpful assistance with the cloning technique. My thanks go to Mrs Sheree Bailey for her continuous help with flow cytometry. Thanks also go to Dr Sarah Vreugde and Dr Pallave Dasari for their friendship and support.

Special thanks go to my mother and my uncle for their unfailing love, care, sacrifices and support. Thanks go to my brothers for their understanding, encouragement and affection. Thanks also go to my friends Jason, Azadeh, Mojgan, Sarah, Clare and Shadi whose company and support have kept me going through these years.

Last but not least, I thank all those not mentioned here who have also shared moments of their time with me during my studies at Flinders University.

Publications and Presentations

Publications

Ramezanpour M, Burke da Silva K, Sanderson BJ (2012) Differential susceptibilities of human lung, breast and skin cancer cell lines to killing by five sea anemone venoms. JVAT 18(2):157–163.

Ramezanpour M, Burke da Silva K, Sanderson BJ (2013) The effect of sea anemone (*H. magnifica*) venom on two human breast cancer lines: death by apoptosis. Cytotechnology 65(4).

Ramezanpour M, Burke da Silva K, Sanderson BJ (2013) Venom present in sea anemone (*Heteractis magnifica*) induces apoptosis in non-small cell lung cancer A549 cells through activation of mitochondria-mediated pathway. Biotechnology Letters, doi: 10.1007/s10529-013-1402-4.

Ramezanpour M, Burke da Silva K, Sanderson BJ (2014) Marine bioactive products as anti-cancer agents: effects of sea anemone venom on breast and lung cancer cells. Cancer Cell and Microenvironment, doi: http://dx.doi.org/10.14800%2Fccm.29.

Publications in Submission

Ramezanpour M, Burke da Silva K, Sanderson BJ. Purification, cloning and characterization of bioactive peptide from *H. magnifica* venom.

Ramezanpour M, Burke da Silva K, Sanderson BJ. Significant anti-cancer activities of purified peptide from *H. magnifica* venom on human breast cancer cell lines.

Presentations

Venom 2 Drugs. May 2011. Queensland, Australia. “Cancer cell lines show differential sensitivity to killing by venom from sea anemone”.

ASMR SA Scientific Meeting June 2012. Adelaide, Australia. “Mechanism of action of *H. magnifica* venom on human lung cancer cell line”.

European Lung Cancer Conference (ELCC). Geneva, Switzerland. March 2014. "Cytotoxic effect of venom from sea anemones on human non-small cell lung cancer cell line".

Professional Memberships

American Association for Cancer Research (AACR)

European Society for Medical Oncology (EMSO)

CHAPTER 1: INTRODUCTION

1.1 Cancer

Unlike free-living cells such as bacteria, which compete to survive, the cells of a multicellular organism are usually committed to collaboration. To coordinate their behaviour, the cells send, receive and interpret an elaborate set of extracellular signals. In multicellular organisms, growth factors, hormones, neurotransmitters and extracellular matrix components are some of the many types of chemical signals used by cells (Bruce et al., 2007). These substances can exert their effects locally, or they might travel over long distances. As a result of complex signalling, each cell behaves in a locally responsible manner, either resting, growing, dividing, differentiating or dying as needed for the development or maintenance of the organism (Vander Molen et al., 1996). Molecular disturbances that upset this balance mean potential disease or damage for a multicellular organism (Bruce et al., 2007). A mutation may give one cell a selective advantage, allowing it to grow and divide more vigorously. It will then survive more readily than its neighbouring cells and can become a founder of a growing mutant clone (Albert, 2008). That mutant clone can become a tumour. The histological classification of tumours depends on a number of criteria including the identification of the basic cell type present and the tissue of origin, their behaviours and their appearance (Louis, 1978). Tumours can be triggered in a number of ways, including exposure to chemicals, certain viruses and radiation (Hanahan and Weinberg, 2011a). The first genetic alteration shown to contribute to cancer development is probably a mutation (a change in the primary structure of DNA) but it is also likely to be influenced by epigenetic events such as a shift

in gene expression (Friedberg et al., 2006). A role for mutational events in transformation is supported by the observations that most carcinogens are also mutagens and vice versa. In fact, cancer is considered a disease of mutant genes (Clive, 1991).

Tumours have different degrees of aggressive growth and can be subdivided into two groups, benign and malignant. Benign tumours grow slowly by expansion and local growth occurs without invasion of adjacent tissues. Therefore, benign tumours can be removed or destroyed easily to achieve a complete cure. In contrast, malignant tumours have the potential to invade and spread to nearby tissues and organs (Weinberg, 2013). They can become fixed to surrounding structures, have a tendency to metastasize and often recur locally after surgical removal. Invasiveness is an essential characteristic of cancer cells. It allows them to break loose, enter blood or lymphatic vessels, and form secondary tumours, called metastases, at other sites within the body (Weinberg, 2007, Nakamura et al., 1997, Albini et al., 1987). The process of carcinogenesis involving malignant tumours is outlined in subsection 1.1.1

1.1.1 Hallmarks of cancer and process of carcinogenesis

Carcinogenesis is a complex multistage process controlled by various signal transduction pathways linked to processes such as inflammation, cell differentiation and survival, and metastasis (Weinstein, 2000). Carcinogenesis is commonly depicted as proceeding in three distinct stages: initiation, promotion and progression. Initiation involves the formation of a mutated, preneoplastic cell from a genotoxic event. The formation of the preneoplastic, initiated cell is an irreversible, but dose-dependent process. Promotion involves the selective clonal expansion of the initiated cell by an increase in cell growth through either an increase in cell proliferation and/or a decrease in apoptosis in the target cell population. The events of this stage are dose dependent and reversible upon removal of the tumour promotion stimulus (Weinberg, 2013). Progression, the third stage, involves cellular and molecular changes that occur from the preneoplastic to the neoplastic state. This stage is irreversible, involves genetic instability, changes in nuclear ploidy and disruption of chromosome integrity (Barrett and Wiseman, 1987, Herceg and Hainaut, 2007, Klaunig and Kamendulis, 2004).

Most of the players of these pathways are interrelated, and irregularities in their crosstalk result in impairment of cellular functions leading to tumour generation and progression. Mutagens and tumour promoters play critical roles in the initiation and progression of carcinogenesis through their genetic and epigenetic

effects which may confer one or more growth advantages to the cell. Mutations result from damaged DNA if it is not repaired properly or if it is not repaired before replication occurs (Friedberg et al., 2006). One problem in understanding a cancer is to discover whether a particular heritable aberration is due to a genetic change. Specifically, is it due to an alteration in the DNA sequence of a cell, or to an epigenetic change, that is, a persistent change in the pattern of gene expression without a change in the DNA sequence (Albert, 2008).

The hallmarks of cancer that were first identified comprise six main biological capabilities acquired during the multistep development of human tumours (Hanahan and Weinberg, 2011) (Figure 1.1). These capabilities comprise: sustaining proliferative signalling; resisting inhibitory signals that might otherwise stop their growth; resisting their own programmed cell death; enabling replicative immortality; stimulating the growth of blood vessels to supply nutrients to tumours (angiogenesis); and invading local tissue and spreading to distant sites (metastasis). Each of these hallmarks can be a therapeutic target for anti-cancer treatment. For example, resisting programmed cell death makes induction of apoptosis a goal of novel drug development. Recently, the complexity of cancer is gradually being figured out and more detail on the hallmarks is being revealed (Hanahan and Weinberg, 2011a). These developments can offer possibilities to develop novel drugs with different modes of action and different molecular targets.

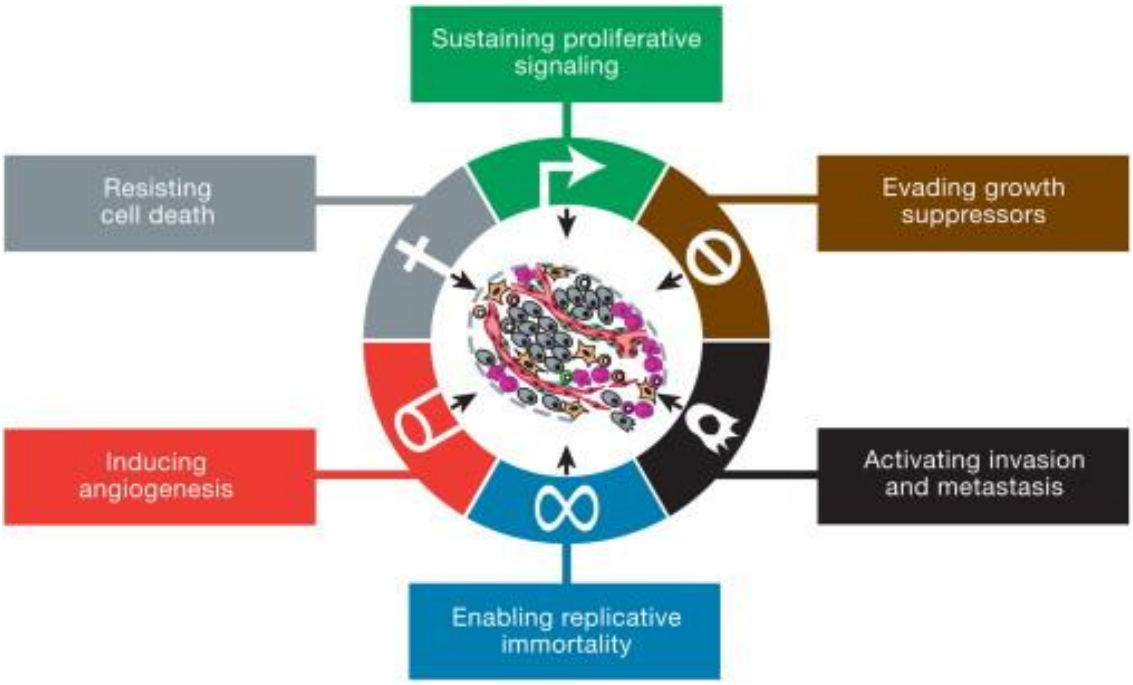

Figure 1.1: Six hallmarks of cancer

Note: As summarised by (Hanahan and Weinberg, 2011a). New therapeutic strategies can target each of the enabling characteristics and hallmarks.

1.1.2 Cancer classification

Cancers are classified according to the tissue and cell type from which they arise (Cooper, 2000). Carcinomas are cancers arising from epithelial cells: they are the most common cancer in humans. Sarcomas arise from connective tissue or muscle cells. Cancers that do not fit into either of these two broad categories include the various types of leukemia and lymphomas that are derived from white blood cells and their precursor cells (Albert, 2008). In parallel with the different types of malignant tumours, there are also several benign tumour types: an adenoma is a benign epithelial tumour with a glandular organization; the corresponding type of malignant tumour is an adenocarcinoma. Similarly, a chondroma and a

chondrosarcoma are, respectively, benign and malignant tumours of cartilage (Sarkar, 2009).

1.1.3 **Lung cancer**

Lung cancer is one of the most common cancers in the world (Maxwell, 2001). In 2002, 1.35 million people worldwide were diagnosed with lung cancer, and 1.8 million people died of lung cancer, with lung cancer accounting for more deaths each year than any other type of cancer (Chiller et al., 2002, Ray et al., 2010, Youlden et al., 2008). The overall prospects for survival are between 5% and 8% and patient survival is, on average, five years after diagnosis. In the United States (USA), lung cancer is gradually decreasing in men but is continuing to increase in women. Some studies have found that, in comparison to male smokers, female smokers are more sensitive to acquiring lung cancer (Khuder, 2001, Lee et al., 2011). Cigarette smoking is the principal risk factor for the development of lung cancer and the incidence of lung cancer is directly related to the number of cigarettes smoked (Bower and Waxman, 2010). The other factors that affect the development of lung cancer are exposure to asbestos and heavy metals, such as arsenic, nickel, copper and cadmium, as well as exposure to air pollution (Boffetta, 2004).

The two main types of lung cancer are small cell lung carcinomas (SCLC) and non-small cell lung carcinomas (NSCLC). Small cell lung carcinomas (SCLC) account for 15% of all bronchogenic malignancies and follow a highly aggressive clinical course (Toyooka et al., 2001). Less than 5% of patients currently survive

five years past the initial diagnosis, whereas the 5-year survival rate for patients diagnosed with NSCLC is 85% (Cancer Council, 2004). Small cell lung carcinomas (SCLC) are distinguished from NSCLC by clinical presentation, and response to chemotherapy and radiation therapy as well as certain biological characteristics. Non-small cell lung carcinomas (NSCLC) are the major histological type of lung cancer and include adenocarcinoma (and the bronchoalveolar carcinoma [BAC] subset), squamous cell carcinoma and large cell carcinoma. In the USA, the incidence of adenocarcinoma (ADC) indicates that it is the most frequent carcinoma (Mitsudomi et al., 2005, Ray et al., 2010).

1.1.3.1 Current therapies for lung cancer and their limitations

Surgery is one option for treatment of individuals with lung cancer. Up to 40% of patients with a complete surgical resection have a greater than 5-year survival rate. However, over 75% of patients who present with advanced or metastatic disease at the time of diagnosis are found unsuitable for surgery (Ray et al., 2010).

Radiation therapy is a treatment modality in both the curative and palliative management of patients with lung cancer. There are significant improvements in techniques for conformal radiotherapy of lung cancer, and improvements in survival have been observed in clinical trials of accelerated radiotherapy (Senan et al., 2004); however, some studies have reported an increase in normal tissue toxicity (Kominsky et al., 2002).

Chemotherapy is another treatment option for lung cancer. Platinum-based chemotherapy regimens are the standard therapy for NSCLC; however, such

regimens are associated with severe toxicities. In addition, efficacy of the treatment is limited due to the multiple drug resistance of NSCLC cells (Shepherd et al., 2000). Research efforts in the area of chemotherapy for lung cancer are focused on developing novel agents that target apoptosis, angiogenesis and tumour growth pathways in particular.

The only target therapies that are reaching a significant predictive effect, as compared with chemotherapy, are epidermal growth factor receptor (EGFR) mutations and anaplastic lymphoma kinase (ALK) rearrangements (Bergot et al., 2013b). Targeted inhibition of EGFR activity suppresses signal transduction pathways which control tumour cell growth, proliferation and resistance to apoptosis. Erlotinib and gefitinib were the first generation of tyrosine kinase inhibitors (TKIs) approved for the treatment of non-small cell lung carcinomas (NSCLC). The overall NSCLC patient population shows a 10–20% response to these treatments, and both erlotinib and gefitinib are approved as second- or third-line treatment agents (Ray et al., 2010). However, the effective targeting of EGFR to achieve significant clinical benefit is not straightforward, as many tumours acquire resistance to receptor inhibition (Wykosky et al., 2011). Anaplastic lymphoma kinase (ALK) is a validated tyrosine kinase target in non-small cell lung cancer (Shaw et al., 2013a). Crizotinib was the first-generation ALK inhibitor that has been shown to be superior to chemotherapy in the second-line setting and has resulted in significantly longer progression-free survival, a significant reduction in symptoms and a significant improvement in global quality of life (Bergot et al., 2013b). However, crizotinib has been associated with toxic

effects such as elevated aminotransferase levels and interstitial lung disease (Shaw et al., 2013a). A summary of current therapies is presented in Table 1.1.

Table 1.1: Current treatment for lung cancer

Current therapy	Target	Most common drugs used	Limitation	Side effect
Surgery			Early stage	Pain Tiredness Fatigue
Radiotherapy			Local control	Tiredness Nausea Sore skin Hair loss
Chemotherapy Platinum-based regimens		Cisplatin Carboplatin Paclitaxel Albumin-bound paclitaxel Docetaxel Gemcitabine Vinorelbine Irinotecan Etoposide Vinblastine Pemetrexed	Drug resistance	Cause severe toxicities
Target therapies	Targeting the epidermal growth factor receptor (EGFR)	Erlotinib Gefitinib	Resistance to receptor inhibition	Toxic effect
	Anaplastic lymphoma kinase (ALK)	Crizotinib	Resistance to receptor inhibition	Toxic effect

Sources: (Bergot et al., 2013a, Ray et al., 2010, Wykosky et al., 2011, Shepherd et al., 2000, Shaw et al., 2013c, Kominsky et al., 2002)

1.1.4 **Breast cancer**

Breast cancer is the second most frequent cancer affecting people worldwide (Maxwell, 2001, Saadat, 2008) and the most common cancer among females in the USA (Li et al., 2005)**.** "In Australia, 1 in 11 women will develop breast cancer over their lifetime" (Harnett et al., 1999). In 2010, 14,181 women and 127 men were diagnosed with breast cancer in Australia (Cancer Council, 2010). The structure of the normal breast is shown in Figure 1.2. The breast is composed of glandular and adipose tissue with varying properties. The glandular tissue consists of 15–20 lobules (milk-producing glands) and ducts (thin tubes that connect the lobules to the nipple). Virtually all carcinomas of the breast arise from the epithelia of the terminal ducts and lobules and only rarely do they develop from the stroma or other soft tissues (Baum and Schipper, 2005).

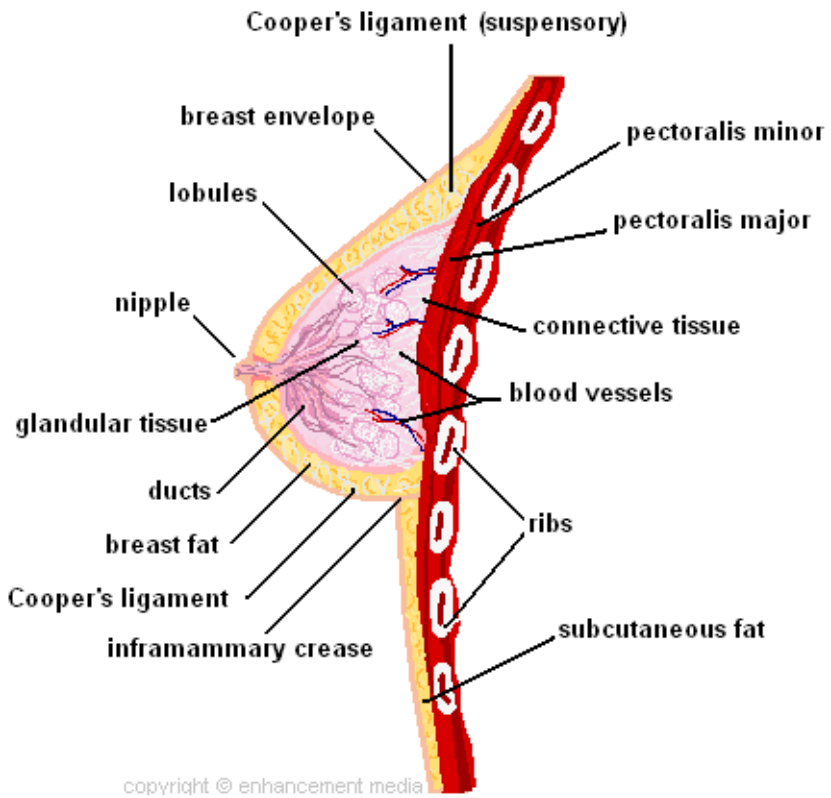

Figure 1.2: Structure of the breast

Note: The figure shows the lobules, milk ducts, fatty tissue (adipose), connective and glandular tissue, nipple/areola complex, underlying pectoral muscle and the ribs. The image is sourced from (http://www.breastlift4you.com/breast_anatomy.htm, 2014).

Breast cancer can be categorized in several ways, including by its clinical features, its expression of tumour markers and its histological type. Based on histological type, the two most common types are ductal and lobular carcinomas. Most breast cancers are ductal carcinomas, occurring in the ducts of the breast. A second but less common form of breast cancer is lobular carcinoma found in the lobules (Li et al., 2005).

Breast cancers can be broadly categorized as occurring with hormonal and non-hormonal risk factors. Oestrogen exposure is directly associated with hormonal

risk factors for developing breast cancer (Weinberg, 2013). Although the exact mechanisms have still to be fully elucidated, the alkylation of cellular molecules and the generation of active radicals that can damage DNA, together with the potential genotoxicity of oestrogen and some of its metabolites (the catechol oestrogens) have been implicated in causing breast cancer. Reducing exposure to oestrogen is thought to be protective against breast cancer, whereas prolonged exposure to oestrogen is associated with an increased risk for developing breast cancer (Martin and Weber, 2000b).

Other factors may contribute to individual variation in exposure to oestrogen. Obese post-menopausal women have lower serum concentrations of the sex hormone-binding globulin resulting in higher serum concentrations of bioavailable oestrogen. In addition, differences in exercise and the dietary intake of certain nutrients may influence exposure to oestrogen (Clemons and Goss, 2001).

A number of non-hormonal risk factors are associated with the development of breast cancer, such as: family history, exposure to ionizing radiation, alcohol consumption, and certain dietary factors including high dietary fat and “well-done” meat (Martin and Weber, 2000a, Clamp et al., 2003). A family history has been estimated to explain about 20–25% of the observed familial breast cancer risk. In addition to *BRCA1* and *BRCA2*, other genes such as *PALB2*, *CHEK2* and *ATM* can be considered well-established breast cancer susceptibility genes (Antoniou and Easton, 2006, Nickels et al., 2013).

1.1.4.1 Current therapies for breast cancer and their limitations

Surgery can be performed to reduce the risk of breast cancer in a woman who has a strong genetic link to breast cancer, such as having the *BRCA1* gene or the *BRCA2* gene, or a high-penetrance mutation in one of several other genes associated with breast cancer risk, such as *TP53* or *PTEN* (Domchek et al., 2010a). Bilateral prophylactic mastectomy has been shown to reduce the risk of breast cancer by up to 90% in women who have a strong family history of breast cancer (Meijers-Heijboer et al., 2001). However, surgery can also affect a woman's psychological well-being due to a change in body image and the loss of normal breast functions (Brandberg et al., 2008).

Radiation therapy uses high-energy x-rays to destroy cancer cells. This therapy usually follows lumpectomy, a focused surgery to eliminate any microscopic cancer cells in the remaining breast tissue. Early studies on the use of adjuvant radiotherapy are difficult to interpret owing to poor radiotherapy techniques, inappropriate dosage or a variety of confounding variables within a particular trial (Darby et al., 2011). In addition, radiotherapy may result in fatigue, dry or itchy skin, swelling, loss of appetite, nausea, digestive problems and a dry or sore throat (Cancer Council, 2012).

Chemotherapy is another important approach in treating breast cancer. In 1976, (Bonadonna et al., 1976d, Bonadonna et al., 1976a) reported the efficacy of an alkylating agent (cyclophosphamide) and antimetabolites (methotrexate, fluorouracil) as adjuvant treatment for node-positive breast cancer. The adjuvant treatment showed a positive effect in all subgroups of patients, although long-term

analysis of the trial over two decades showed no significant improvement in post-menopausal women, particularly those older than 60 years of age (Bonadonna et al., 1995). Anthracyclines were considered the gold standard of adjuvant chemotherapy until the late 1990s (Tarruella and Martín, 2009). However, long-term treatment had side effects, including cardiac toxicity fatigue, lowered blood counts, mouth ulcers and nausea which negated their benefits (Cancer Council, 2010). Although the precise role of taxanes is uncertain, it is reasonable to consider taxanes therapy in women when endocrine sensitivity is absent or incomplete (Bedard and Cardoso, 2008). Taxane side effects include: allergic reactions (paclitaxel); fatigue; hair loss; lowered blood counts; muscle aches and neurological damage (Cancer Council, 2014a).

Targeted therapy is the other major modality of medical treatment for breast cancer. Women with breast cancer who overexpress human epidermal growth factor receptor type 2 (*HER2*) are at greater risk of disease progression and death than women whose tumours do not overexpress *HER2* (Geyer et al., 2006b). Therapeutic strategies have been developed to block *HER2* signalling pathways in order to improve the treatment of this cancer. Trastuzumab and lapatinib both target *HER2* and have shown some beneficial effect when combined with docetaxel and platinum salts (Pegram et al., 2004) or paclitaxel and carboplatin (Perez et al., 2005, Robert et al., 2006). However, the use of *HER2* beyond first-line therapy is questioned due to potential resistance to this agent (Gunduz and Gunduz, 2011).

Vascular endothelial growth factor *(VEGF*) is a highly specific mitogen for vascular endothelial cells that increases endothelial proliferation and migration and inhibits endothelial apoptosis. Bevacizumab is a humanized monoclonal antibody directed against all isoforms of *VEGF* which, combined with paclitaxel, has shown significant improvement in progression-free survival (Miller et al., 2007). However, their benefit is limited by their severe toxic effect causing problems including cerebrovascular ischemia, fatigue, headache, hypertension, infection, sensory neuropathy and proteinuria (National Breast and Ovarian Cancer Centre, 2010).

Hormone therapy is another form of systemic therapy. Approximately, three-quarters of breast cancer cells express oestrogen and/or progesterone receptors, suggesting that they would be highly likely to respond to this form of treatment. The first targeted breast cancer therapy was antioestrogen, called tamoxifen. Although a positive effect of tamoxifen was demonstrated in early studies, adverse effects causing endometrial cancer and thromboembolism were later shown by (Fisher et al., 1994). Fulvestrant, a drug that blocks oestrogen receptors, is recommended for second-line therapy and was developed after the failure of tamoxifen (Pritchard, 2003). However, fulvestrant results in headaches, hot flushes, nausea and disturbance of menses (Young et al., 2008). Current treatments for breast cancer are summarised in Table 1.2.

Table 1.2: Common treatment for breast cancer

Current therapy	Class/agent	Side effect
Surgery		Change in body image Loss of normal breast functions
Radiation therapy		Fatigue, dry or itchy skin, swelling, loss of appetite, nausea
Chemotherapy	Alkylating agents (cyclophosphamide)	Bladder irritation, fatigue, hair loss, lowered blood counts, nausea/vomiting
	Anthracyclines (doxorubicin, epirubicin)	Cardiac toxicity, fatigue, lowered blood counts, mouth ulcers, nausea/vomiting
	Antimetabolites (capecitabine, gemcitabine, 5-fluorouracil, methotrexate)	Diarrhoea, fatigue, hand-foot syndrome, nausea, stomatitis
	Taxanes (docetaxel, paclitaxel, nab-paclitaxel)	Allergic reactions (paclitaxel), fatigue, hair loss, lowered blood counts, muscle aches, neurological damage
	Vinorelbine	Fatigue, injection site pain, hair loss (moderate), lowered blood counts, neuropathy
Targeted therapies	Bevacizumab	Cerebrovascular ischemia, fatigue, headache, hypertension, infection, sensory neuropathy, proteinuria
	Lapatinib	Diarrhoea, dyspepsia, fatigue, hand-foot syndrome, nausea/vomiting, rash
	Trastuzumab	Anaemia, cardiac dysfunction, infection, leukopenia, neutropenia
Hormone therapies	Tamoxifen	Causing endometrial cancer and thromboembolism
	Fulvestrant	Headaches, hot flushes, nausea, disturbance of menses and mood swings

Sources: (Darby et al., 2011, Fisher et al., 1994, Young et al., 2008, Cancer Council, 2014a, Pritchard, 2003, Gunduz and Gunduz, 2011, National Breast and Ovarian Cancer Centre, 2010, Geyer et al., 2006a, Bonadonna et al., 1995, Meijers-Heijboer et al., 2001, Domchek et al., 2010b)

1.1.5 **Skin cancer**

Skin cancer is a growing public health problem worldwide. The three main types of skin cancer are basal cell carcinoma (BCC), squamous cell carcinoma (SCC) and melanoma. One in two Australian men and one in three Australian women will be diagnosed with skin cancer by the age of 85 (Cancer Council, 2014c). Skin cancer can be induced by many factors, such as sun exposure, radiotherapy treatment, lowered immunity, exposure to chemicals and genetic conditions (Brash et al., 1991).

Treatment for skin cancer depends on the type and stage of the disease as well as the size and place of the tumour. Current therapies for treatment of skin cancers include surgical excision, radiation therapy, chemotherapy and targeted therapy. Surgical excision is an effective treatment; however, it is expensive and limited by the proximity of essential anatomical structures. Radiotherapy is another option; however, it may result in poor cosmetic results and wound healing problems (Petit et al., 2000). Dacarbazine, temozolomide, nab-paclitaxel, paclitaxel, carmustine, cisplatin, carboplatin and vinblastine are some examples of current chemotherapy drugs. Fluorouracil (5-FU) is the most widely used chemotherapy drug; however, it has a range of different side effects including nausea, diarrhoea, tiredness, hair loss and skin sensitivity to sunlight (Cancer Counsil, 2014).

Drugs that target cells with *BRAF* gene changes or *c-Kit* gene changes are considered to be a targeted therapy. Zelboraf and tafinlar attack the BRAF protein directly. The BRAF protein is an isoform of RAF mammalian serine/threonine

protein kinases that regulates cell proliferation, differentiation and survival (Gray-Schopfer et al., 2005). Vemurafenib and dabrafenib agents block the mitogen-activated protein (MAP) kinase pathway which is known to regulate the proliferation and survival of tumour cells in many cancers (Flaherty et al., 2012b).

A small portion of melanomas have been found to have changes in a gene called *c-Kit*. These *c-Kit* mutations are more common in mucosal and acral skin (soles, palms and nail beds), and in skin with chronic sun-induced damage. Some targeted drugs, such as imatinib and nilotinib, can affect cells with changes in the *c-Kit* gene (Curtin et al., 2006, Guo et al., 2011). Common side effects of targeted therapy are oedema, fatigue, anorexia, nausea, neutropenia and elevated aspartate transaminase (AST) and alanine transaminase (ALT) (Guo et al., 2011). The current therapy regimes are shown on Table 1.3.

Table 1.3: Common treatment for skin cancer

Current therapy	Target	Agent	Side effect
Surgery			Scars, wounds, pain
Radiation therapy			Hair loss, fatigue, nausea
Chemotherapy		Dacarbazine Temozolomide Nab-paclitaxel Paclitaxel Carmustine Cisplatin Carboplatin Vinblastine Fluorouracil	Hair loss Mouth sores Nausea Diarrhea or constipation Fatigue
Targeted therapy	Targeting *BRAF* gene changes	BRAF inhibitors (zelboraf, tafinlar) MEK inhibitors (vemurafenib, dabrafenib)	Oedema Fatigue Anorexia Nausea Neutropenia
	Targeting *c-Kit* gene	Imatinib Nilotinib	

Sources: (Petit et al., 2000, Cancer Counsil, 2014, Guo et al., 2011, Curtin et al., 2006, Flaherty et al., 2012a, Gray-Schopfer et al., 2005)

1.2 Marine Biodiscovery

The oceans cover about 70% of the earth's surface, and marine species comprise approximately half of the total biodiversity found on earth (Thakur et al., 2005). Marine organisms, therefore, provide a vast source from which useful therapeutics can be discovered (Suarez-Jimenez et al., 2012, Sithranga and Kathiresan, 2010). For example, fucoidan from seaweed has been shown to inhibit proliferation and induce apoptotic cell death in several types of tumour cells (Yamasaki-Miyamoto

et al., 2009). In addition, actinoporins isolated from the sea anemone were recently found to have cytotoxic activity against human cancer cell lines (Fedorov et al., 2010), and frondoside A (triterpenoid glycoside) isolated from the sea cucumber, *Cucumaria frondosa*, enhances the inhibition of lung tumour growth induced by the chemotherapeutic agent cisplatin (Attoub et al., 2013). During the period 1998–2006, the global marine preclinical pipeline included 592 marine compounds that showed anti-tumour and cytotoxic activity, and 13 marine-derived compounds were either in Phase I, Phase II or Phase III clinical trials (Mayer et al., 2010). However, although many agents have entered clinical trials for cancer treatment, only a few marine-derived products are currently on the market. These include cytarabine or cytosine arabinoside which has bioactive nucleosides that contain arabinose; trabectedin (ET-743) from the sea squirt, *Ecteinasidia turbinate*; eribulin from the marine sponge, *Halichondria okadai*; and brentuximab vedotin (an immunoconjugate derived from dolastatin 10, monomethylauristatin E), a secondary metabolite from a *symploca* species of cyanophyte, which are approved as marine-derived anti-tumour agents by the US Food and Drug Administration (FDA) for use in humans (Newman and Cragg, 2014).

Sea anemone toxins have attracted considerable interest since the 1970s (Frazão et al., 2012). Various studies *in vitro* and *in vivo* have demonstrated that more than 32 species of sea anemones produce lethal cytolytic peptides and proteins (Anderluh and Macˇek, 2002). Sea anemone venom has haemolytic activities (Lanioa et al., 2001b, Uechi et al., 2005a); immunomodulating activities (Pento et al., 2011a, Tytgat and Bosmans, 2007b); neurotoxic activities (Gondran et al.,

2002); and cardiotoxic properties (Bruhn et al., 2011). Sea anemone toxins are classified according to their primary structure and functional properties and are divided into four classes: (a) 5–8 kilodalton (kDa) peptides as found in two diverse species, *Tealia felina* and *Radianthus macrodactylus* with antihistamine activity; (b) ~20 kDa pore-forming proteins are most common and have been found to be inhibited by sphingomyelin (these have been found in a variety of species including *Actinia equina*, *Stichodactyla helianthus* and *Heteractis magnifica*; (c) ~30–45 kDa cytolysins, with or without phospholipase A_2-activity, found in *Aiptasia pallida*; and, finally, (d) the last group of 80 kDa proteins represented by *Metridium senile* cytolysin (Anderluh and Macˇek, 2002).

The cytotoxic mechanisms of sea anemone venoms work through various modes of action which are cell type dependent and venom structure related. Up-to-date cytotoxicity studies about the effects of compounds extracted from sea anemones on different cell lines are shown in Table 1.4 (Mariottini and Pane, 2014c). However, comparing the susceptibility of human cancer cell lines to different species of sea anemone venom has not been investigated. In this thesis, the susceptibility of different human cancers to different types of sea anemone venom was investigated with the aim being to understand the underlying mechanisms by which the venom had an effect. Furthermore, characterising the bioactive compound in sea anemone venom that is involved in killing cancer cells was a focus in the final chapter of the thesis (Chapter 5), so that future pharmaceutical work could be pursued based on the findings of this project.

Table 1.4: Cytotoxicity to different cell lines of compounds extracted from sea anemones

Species	Compound	Cells	Tissue/organ/histology	Organism	IC_{50}-ED_{50} (µg/ml)
Bunodosoma caissarum	Bc2	U8	Glioblastoma	Human	NI
		A172	Glioblastoma	Human	NI
Actinia equine	Equinatoxin II	V-79-379 A	Normal lung fibroblasts	Chinese hamster	8.8×10^{-10}
Actinia equine	Crude venom	V79	Normal lung fibroblasts	Chinese hamster	87.9×10^{3}
Actinia equine	Equinatoxin II-I18C mutant	MCF 7	Breast adenocarcinoma	Human	0.2–0.3
		ZR 751	Breast carcinoma	Human	5.8
		HT 1080	Fibrosarcoma	Human	14.2
Actinia equine	EqTx-II	U87	Glioblastoma	Human	NI
		A172	Glioblastoma	Human	NI
Aiptasia mutabilis	Crude venom	Vero	Normal kidney cells	Monkey	2000
		Hep-2	Epithelial carcinoma	Human	NI
Anemonia sulcate	Crude venom	V79	Normal lung fibroblasts	Chinese hamster	65.0×10^{3}
Heteractis crispa	Actinoporin RTX-A	HeLa	Promyelocytic leukemia	Human	1.06
		HL-60	Cervix carcinoma	Human	2.26
		THP-1	Monocytic leukemia	Human	1.11
		MDA-MB231	Breast cancer	Human	4.64
		SNU-C4	Colon cancer	Human	4.66
		Cl 41	Epidermal cells	Mouse	0.57
Sagartia rosea	Acidic actinoporin Src I	U251	Glioblastoma	Human	3.5
		NSCLC	Non-small cell lung carcinoma	Human	2.8
		BEL-7402	Liver carcinoma	Human	3.6
		BGC-823	Stomach adenocarcinoma	Human	7.4
		NIH/3T3	NIH Swiss embryo	Mouse	3.4
Urticina piscivora	Crude extract	KB	Epidermoid carcinoma	Human	6.54
		HEL299	Embryonic lung	Human	10.07
		L1210	Lymphocytic leukemia	Mouse	2.34
Urticina piscivora	UpI (protein)	KB	Epidermoid carcinoma	Human	40.32
		HEL299	Embryonic lung	Human	29.99
		L1210	Lymphocytic leukemia	Mouse	29.74

Source: (Anthozoa) (Mariottini and Pane, 2014a) Note: NI = not indicated

1.2.1 The marine phylum Cnidaria

The Cnidarians are a very large group of aquatic invertebrates that includes approximately 11,000 species (Hutton and Smith 1996). Cnidaria belong to the class Hydrozoan. Cnidarians are divided into several classes: Anthozoa; Cubozoa (box jellyfish); Hydrozoa (hydromedusae); Staurozoa (stalked jellyfish); Polypodiozoa; and Scyphozoans. Classes and orders in the phylum Cnidaria follow in Table 1.5 (Rocha et al., 2011a).

Table 1.5: Classes and orders in the phylum Cnidaria

Phylum	Class	Order
Cnidaria	Anthozoa	Actiniaria Antipatharia Ceriantharia Corallimorpharia Scleractinia Zoanthidea Alcyonacea Gorgonacea Helioporacea Pennatulacea
	Cubozoa	Carybdeida Chirodropida
	Hydrozoa	Anthoathecata Leptothecata Siphonophorae Actinulida Limnomedusae Narcomedusae Trachymedusae
	Scyphozoa	Coronatae Rhizostomeae Semaeostomeae
	Staurozoa	Stauromedusae

Source: (Rocha et al., 2011a)

Cnidarians can have one of two basic shapes: polyps (polypoid shape, e.g. sea anemones and corals) and medusae (medusolid shape, e.g. jellyfish). They are the simplest organisms at the tissue grade of organization. Their bodies are organized into two cell layers: the outer layer (ectoderm) and the inner layer (endoderm). In between the two cell layers is the mesoglea, a layer of jelly-like substance, which

contains scattered cells and collagen fibres (Seipel and Schmid, 2006). Cnidarians are generally passive predators that use tentacles with stinging cells in their tips to capture and subdue prey. The stinging cells are called cnidocytes and contain a structure called a nematocyst (Fautin, 2009). The nematocyst is a coiled thread-like stinger. When the nematocyst is called upon to fire, the thread is uncoiled, and the springs straighten. The nematocyst is fired either by the tentacle touching something or, in some cases, by a nerve impulse from the animal inducing it to fire (Fautin and Allen 1994). Cnidarian stinging can cause local and systemic symptoms such as coughing, nausea, vomiting, abdominal colic and diarrhoea. The damage induced by Cnidarian venoms has been essentially ascribed to a pore formation mechanism or to oxidative stress (Mariottini and Pane, 2014c).

The Cnidarian venom structure is known to contain a variety of active compounds that affect voltage-gated sodium (Na^+) and potassium (K^+) channels (Botana, 2014). Toxin-affecting sodium channel peptides are divided into three structural classes: type 1 peptides (mostly from the family Actiniidae); type 2 peptides (mostly from the family Stichodactylidae) containing between 45 and 50 amino acid residues; and type 3 peptides which are shorter peptides containing 27–32 amino acid residues. Toxin-affecting potassium channel peptides are divided into four structural classes: type 1 peptides consisting of 35–37 amino acid residues; type 2 peptides containing 58 or 59 amino acid residues; type 3 peptides containing 41–42 amino acid residues; and type 4 containing 28 amino acid residues. The lists of peptide toxins isolated from Cnidarian organisms are presented in Table 1.6 (Botana, 2014).

Table 1.6: Peptide toxins isolated from Cnidarian organisms

Type	Target	Current name	Type	Biological group	Species
Peptides	Na^+ channel toxins	Ac1	Type I	Sea anemone	*Actinia equina*
		AETX-I	Type I	Sea anemone	*Anemonia erythraea*
		ATX-I	Type I	Sea anemone	*Anemonia sulcata*
		ATX-II	Type I	Sea anemone	*Anemonia viridis*
		ATX-III	Type III	Sea anemone	*Anemonia sulcata*
		ATX-V	Type I	Sea anemone	*Anemonia viridis*
		Am-3	Type I	Sea anemone	*Antheopsis maculata*
		Anthopleurin A and B		Sea anemone	*Anthopleura xanthogrammica*
		Anthopleurin C		Sea anemone	*Anthopleura elegantissima*
		APE I (1-2) and APE 2 (1-2)		Sea anemone	*Anthopleura elegantissima*
		AFT I and II		Sea anemone	*Anthopleura fusc oviridis*
		Toxin HK(2,7,8,16)		Sea anemone	*Anthopleura species*
		Toxin PCR(1-7)		Sea anemone	*Anthopleura xanthogrammica*
		BcIII		Sea anemone	*Bunodosoma caissarum*
		Cangitoxin (0.2 and 3)		Sea anemone	*Bunodosoma cangicum*
		Neurotoxin Bg 2,3		Sea anemone	*Bunodosoma granulifera*
		Calitoxin(1,2)		Sea anemone	*Calliactis parasitica*
		CgNa	Type I	Sea anemone	*Condylactis gigantea*
		Cp I	Type I	Sea anemone	*Condylactis passiflora*

		Ca I	Type II	Sea anemone	*Cryptodendrum adhaesivum*
		Halcurin	Type II	Sea anemone	*Heteractis carlgreni*
		Rm(1-5)	Type II	Sea anemone	*Heteractis crispa*
		Toxin Rc-I	Type I	Sea anemone	*Heteractis crispa*
		Hh X	Type II	Sea anemone	*Heterodactyla hemprichii*
	Na^+ channel toxins	Neurotoxin Nv I	Type II	Sea anemone	*Nematostella vectensis*
		Pa-TX		Sea anemone	*Parasicyonis actinostoloides*
		Rp-II-III	Type II	Sea anemone	*Radianthus paumotensis*
		Sh I	Type II	Sea anemone	*Stichodactyla helianthus*
		Gigantoxin, 2-3	Types I and II	Sea anemone	*Stichodactyla gigantea*
		SHTX-4	Type II	Sea anemone	*Stichodactyla haddoni*
		Ta I	Type II	Sea anemone	*Thalassianthus aster*
	K^+ channel toxins	Shk	Type I	Sea anemone	*Stichodactyla helianthus*
		BgK	Type I	Sea anemone	*Bunodosoma granulifera*
		BDS I and II	Types II and III	Sea anemone	*Anemonia viridis*
		APETx 1 and 2	Type III	Sea anemone	*Anthopleura elegantissima*
		AeK	Type I	Sea anemone	*Actinia equina*
		AETX-K	Type I	Sea anemone	*Anemonia erythraea*
		SA5II	Type II	Sea anemone	*Anemonia viridis*
		Kalicludin(1-3)	Type II	Sea anemone	*Anemonia viridis*
		Kaliseptin	Type I	Sea anemone	*Anemonia viridis*

		Am-2	Type III	Sea anemone	*Antheopsis maculata*
		Bc-IV	Type III	Sea anemone	*Bunodosoma caissarum*
		Bc-V	Type III	Sea anemone	*Bunodosoma caissarum*
		Toxicon Bcg III	Type III	Sea anemone	*Bunodosoma cangicum*
		Polypeptide HCI	Type II	Sea anemone	*Heteractis crispa*
		Kunitz-type trypsin inhibitors IV	Type II	Sea anemone	*Heteractis crispa*
		Metridium	Type I	Sea anemone	*Metridium senile*
		HmK	Type I	Sea anemone	*Radianthus magnifica*
		SHPI-1,2	Type II	Sea anemone	*Stichodactyla helianthus*
		SHTX-1/SHTX-2 and 3	Types I and II	Sea anemone	*Stichodactyla haddoni*
	Phospholipases A2	Acpla2		Sea anemone	*Adamsia palliata*
		Cationic protein C1		Sea anemone	*Bunodosoma caissarum*
		Phospholipase A2		Sea anemone	*Condylactis gigantea*
		UcPL A2		Sea anemone	*Urticina crassicornis*
		Milleporin-1		Fire coral	*Millepora platyphylla*
		Proteins		Fire coral	*Millepora complanata*
	Cytolytic protein	Cytolysin RTX-A-S-II	Type I	Sea anemone	*Heteractis crispa*
		Equinatoxin (I,II,III,IV,V)	Actinoporin	Sea anemone	*Actinia equina*
		Stycholysin (I,II, III)	Actinoporin	Sea anemone	*Stichodactyla helianthus*
		AvT (I,II)	Actinoporin	Sea anemone	*Actineria villosa*
		Fragaceatoxin C	Actinoporin	Sea anemone	*Actinia fragacea*
		Tenebrosin (A,B,C)	Actinoporin	Sea anemone	*Actinia tenebrosa*

		Bandaporin	Actinoporin	Sea anemone	*Anthopleura asiatica*
		Actinoporin (A,G)	Actinoporin	Sea anemone	*Oulactis orientalis*
		PsLx-20A	Actinoporin	Sea anemone	*Phyllodiscus semoni*
		HMG (I,II,II)	Actinoporin	Sea anemone	*Radianthus magnifica*
		Haemolytic toxin	Actinoporin	Sea anemone	*Radianthus magnifica*
		Cytolysin Src-1	Actinoporin	Sea anemone	*Sagartia rosea*
		Up-1	Type III	Sea anemone	*Urticina piscivora*
		Uc-1	Type III	Sea anemone	*Urticina crassicornis*
		Urticinatoxin	Type III	Sea anemone	*Urticina crassicornis*
		PaTX-60 (A,B)		Sea anemone	*Phyllodiscus semoni*
		AvTX-60A		Sea anemone	*Actineria villosa*
		Hydralazine		Hydra	*Chlorohydra viridissima*
		Cytotoxins		Fire coral	*Millepora tenera*
		Cytotoxins		Fire coral	*Millepora alcicornis*
		Millepora cytotoxin MCTx-1		Fire coral	*Millepora tenera*
		Proteins		Fire coral	*Millepora platyphylla*
		Physalitoxin		Hydrozoa	*Physalia physalis*
		PCrTX-I,II,III		Box jellyfish	*Carybdea rastoni*
		CrTX-A-B		Box jellyfish	*Carybdea rastoni*
		CaTX-A-B		Box jellyfish	*Carybdea alata*
		CAHI		Box jellyfish	*Carybdea alata*
		CqTX-1		Box jellyfish	*Chiropsalmus quadrumanus*
		CfTX-1,2		Box jellyfish	*Chironex fleckeri*

		Four major proteins	40,45,80 and 160 KDa	Box jellyfish	*Carukia barnesi*
		Bioactive proteins	10-30 KDa; 40-50 KDa; 120 and 170 KDa	Box jellyfish	*Chironex fleckeri*
		CARTOX + 1neurotoxin + 3cytolysins	107 KDa + 120 KDa + 220, 139 and 36 KDa	Box jellyfish	*Carybdea marsupialis*

Source: (Botana, 2014)

1.2.1.1 Actiniaria

The subclass Hexacorallia (Zoantharia) of the Cnidarian class Anthozoa currently contains six orders: Actiniaria (sea anemones); Antipatharia (black corals); Ceriantharia (tube anemones); Scleractinia (stony corals); Corallimorpharia (corallimorpharians); and Zoanthidea (zoanthids) (Daly et al., 2003). Morphological features of all orders are summarised in Table 1.7.

Table 1.7: Summary of diagnostic morphological features for class Anthozoa

Order	Exoskeleton	Habit	Mesenterial filament	Siphonoglyph	Marginal sphincter muscle	Mesentery arrangement
Actiniaria	Absent	Solitary or clonal	Unilobed or trilobed	None to two or more	Endodermal, mesogloeal, or none	Monomorphic or dimorphic
Antipatharia	Proteinaceous	Colonial	Unilobed	Two	None	Monomorphic coupled pairs
Ceriantharia	Absent	Solitary	Trilobed	One	None	Monomorphic couples
Coralli-morpharia	Absent	Solitary or clonal	Unilobed	None	None	Monomorphic coupled pairs
Scleractinia	Calcareous	Solitary or colonial	Unilobed	None	None	Monomorphic coupled pairs
Zoanthidea	Absent	Solitary or colonial	Trilobed	One	Endodermal, mesogloeal, or none	Dimorphic coupled pairs

Source: (Daly et al., 2003)

Actiniaria (sea anemones) comprise approximately 1,200 species in 46 families (Dalay et al., 2008). They are one of the most ancient predatory animals on the earth. Named after a flower, they have a central mouth surrounded by tentacles with studded nematocysts (Bosmans and Tytgatb, 2007). Sea anemones attach themselves to a substrate such as rock, sand or mud, using an adhesive foot. They are likely to stay in the same place but if the conditions become unsuitable or a predator attacks they will detach themselves and move to a more suitable place (Karthikayalu et al., 2010).

Sea anemone venom contains complex biologically active substances, such as protein substances and neurotransmitters that are used for protection against predators, for hunting and for competitive interaction (Andreev et al., 2008f). Sea

anemones eat small fishes and crustaceans by paralysing them with stinging tentacles and then transfer their prey to their mouth (Bosmans and Tytgatb, 2007). It is fortunate that a relatively small number of sea anemone species are harmful to humans and that the stinging incidence is low, perhaps because sea anemone nematocysts are often too small to penetrate far into human skin (Burke, 2002, Kem et al., 1999).

The older classification of the order Actiniaria, according to (Carlgren, 1949), was followed by four suborders: Endocoelantheae, Nyantheae, Protantheae and Ptychodacteae. However, the new classification of Actiniaria, according to (Rodríguez et al., 2014), included two suborders: Anenthemonae (Edwardsiidae and Actinernoidea) and Enthemonae (Actinostoloidea, Actinoidea and Metridioidea). Suborders, superfamilies and families in the order Actiniaria are represented in Table 1.8 (Rodríguez et al., 2014).

Table 1.8: A new higher-level classification for the order Actiniaria

Order	Suborders	Superfamilies	Families
Actiniaria	Anenthemonae	Edwardsioidea (members of the family Edwardsiidae, which have only eight perfect mesenteries)	Edwardsiidae
		Actinernoidea (members of the former suborder Endocoelantheae, in which secondary cycles of mesenteries arise in the endocoels	Actinemidae Halcuriidae
	Enthemonae	Actinostoloidea (members of the former family Actinostolidae sensu)	Actinostolidae Exocoelactinidae
		Actinoidea (members of the former Endomyaria and Ptychodacteae plus some former members of Athenaria)	Actiniidae Actinodendridae Andresiidae Capneidae Condylanthidae Haloclavidae Homostichanthidae Losactinidae Limnactiniidae Liponematidae Minyadidae Oractinidae Phymanthidae Preactiniidae Ptychodactinidae Stichodactylidae Thalassianthidae
		Metridioidea (acontiate actiniarians plus several families that have lost acontia, including members of former sub- and infra-orders Protantheae and Boloceroidaria, respectively)	Acontiophoridae Actinoscyphiidae Aiptasiidae Aiptasiomorphidae Aliciidae Amphianthidae Andvakiidae Antipodactinidae Bathyphelliidae Boloceroididae

			Diadumenidae Gonactiniidae Halcampidae Haliactinidae Haliplanellidae Homathiidae Isanthidae Kadosactinidae Metridiidae Mimetridiidae Nemanthidae Nevadneidae Octineonidae Ostiactinidae Phelliidae Ramireziidae Sagartiidae Sagartiomorphidae

Source: (Rodríguez et al., 2014)

The identification of sea anemones is mainly dependent on their morphological features including the body shape, size, colour, distribution of nematocysts and arrangement of tentacles in relation to internal anatomy (Fautin and Allen, 1994). In 2008, (Daly et al., 2008) analysed sequences from two mitochondrial markers (partial 16S and 12S rDNA) and two nuclear markers (18S and partial 28S rDNA) to define the diagnostic features and constituents of each family. Specimens were identified using polyp anatomy and the distribution and size of cnidae in various regions of the polyp. Voucher specimens in formalin were deposited at the American Museum of Natural History (AMNH) (see Appendix II). In 2014, (Rodríguez et al., 2014) modified the diagnostic features of Actiniaria (see Appendix I).

This study focused on five species from the order Actiniaria, suborder Enthemonae and superfamily Actinoidea: *Heteractis magnifica*, *Heteractis malu* and *Heteractis crispa* (species of sea anemone in the family Stichodactylidae); *Entacmaea quadricolor* (species of sea anemone in the family Actiniidae); and *Cryptodendrum adhaesivum* (species of sea anemone in the family Thalassianthidae). The morphology of these species does differ from each other, primarily in overall size and in tentacle length (Table 1.9) (Nedosyko et al., 2014a).

Table 1.9: Morphological characteristics of each species

Species	Tentacle length (mm)	Oral disc diameter (mm)
Entacmaea quadricolor	100	50
Heteractis magnifica	100	500
Heteractis crispa	75	1000
Heteractis malu	40	200
Cryptodendrum adhaesivum	5	300

Source: (Nedosyko et al., 2014)

Heteractis magnifica

Heteractis magnifica belongs to the family Stichodactylidae (Yamaguchi et al., 2010a). It is found in open areas and typically is attached to hard substrate such as coral boulder. *Heteractis magnifica* occurs in blue, green, red, white and brown

colours. The oral disc of *H. magnifica* is typically yellow, brown or green coloured and is well populated with approximately 300–500 mm long finger-shaped tentacles that hardly taper to a blunt or slightly swollen end (Fautin, 1981). The tentacles and oral disc are usually of the same colour, typically purplish, but may be red, white/tan, brown, green or blue. Tentacles approach the mouth to within 20–30 mm and usually are only visible in the centre due to the contraction of the anemone. *Heteractis magnifica* can be widely found ranging from the Indo-Mid-Pacific; East Africa; French Polynesia; Indonesia; Fiji, Malaysia and the Red Sea to Australia (Fautin and Allen 1994).

Figure 1.3: *Heteractis magnifica*

Source: (http://www.anemone-clown.fr/photos/g/amphiprion-akallopisos-heteractis-magnifica.jpg, 2006)

Heteractis crispa

Heteractis crispa, commonly known as the leathery or sebae sea anemone, is a member of the family Stichodactylidae (Madhu and Madhu, 2007). *Heteractis*

crispa is usually light tan to brown in colour, and has numerous long, slender tentacles that end in points with an entered pink dot (Fautin, 1981). The oral disc is extremely wide, around 200 mm. They have a grey leathery column, with adhesive verrucae which is a unique feature among host Actinians. The pedal disc attaches to coral branches and the oral disc lies at the surface. They are known to have very long lives, and slow rates of reproduction/replacement (some not asexually), but the record of success in captive care is low (Fautin and Allen 1994). They are found in locations ranging from French Polynesia, Micronesia, and Melanesia to the Red Sea, and from Australia to Japan.

Figure 1.4: *Heteractis crispa*

Source: (http://atj.net.au/Dive20079229Anemone_Bay.html, 2014)

Heteractis malu

Heteractis malu belongs to the family Stichodactylidae (Nedosyko et al., 2014b). *Heteractis malu* has brown or purplish sparse tentacles of stumpy appearance which end in points with radial markings. It has a narrow column which is cream

or yellow in colour, with longitudinal rows of adhesive verrucae (Fautin, 1981). The oral disc is widely flared at the surface and is as much as 200 mm in diameter. They are distributed from the Hawaiian Islands to Australia and northwards to Japan and are located in sediment in shallow quiet waters (Fautin and Allen 1994).

Figure 1.5: ***Heteractis malu***

Source: (http://www.interhomeopathy.org/sea_anemone_must_protect_by_withdrawal_inwardly, 2009)

Crytodendrum adhaesivum

Cryptodendrum adhaesivum belongs to the family Thalassianthidae (Frazão et al., 2012). It was previously called *Stoichactis digitata*, and is commonly known as the pizza sea anemone due to its smooth rounded rim which gives it the appearance of a pizza. The body column may be brightly coloured, ranging from green to grey, purple or yellow. The tentacles on the oral disc are stubby and colourful, and the stalk and tips may differ in colour (Fautin, 1981).

Cryptodendrum adheasivum has two types of tentacles: the tentacles on the oral disc are short, tiny and tightly packed, while those near the edge are simple elongated bulbs about 1 mm diameter. With the two distinct types of tentacles in *C. adheasivum*, it is entirely covered with tentacles except around the mouth. It is a large flattened anemone and its oral disc is commonly 300 mm or larger (Fautin and Allen 1994). They are distributed ranging from Australia to southern Japan and Polynesia, Micronesia and Melanesia, and westward to Thailand, the Maldives, and the Red Sea.

Figure 1.6: *Cryptodendrum adhaesivum*

Source: (http://www.fishchannel.com/saltwater-aquariums/reefkeeping/keeping-marine-anemones.aspx, 2013)

Entacmaea quadricolor

Entacmaea quadricolor is known as the bubble-tip or bulb-tentacle sea anemone. *Entacmaea quadricolor* belongs to the family Actiniidae (Changa et al., 2011). The bulb tips that form towards the ends of the anemone's tentacles are the

signature of this anenome. Brown or green are the most common colours of the anemone, with the same colour for both the oral disc and tentacles. In shallow water, each polyp is relatively small, but clusters remain next to one another so their tentacles are confluent; however, in deep water, solitary larger forms can also be found (Fautin, 1981). *Entacmaea quadricolor* like to have their foothold inside a crevice in the rock or coral with their tentacles in the light. The distribution is widespread, ranging across northern Australia, eastern South Africa, the Red Sea, the Persian Gulf, India and the Maldives, and across to South East Asia and Japan, New Caledonia and Fiji (Fautin and Allen 1994).

Figure 1.7: *Entacmaes quadricolor*

Source: (https://www.meerwasser-lexikon.de/tiere/882_Entacmaea_quadricolor.htm, 2009)

1.3 Scope and Aims

The overall aim of this study was to investigate and characterise the anti-cancer properties of bioactive compounds extracted from sea anemone venom. The outline of the scope of this study is presented in Figure 1.8.

To understand the anti-cancer activity of five sea anemone venoms, the initial study used three human cancer cell lines as *in vitro* models: human skin cancer (squamous carcinoma) A431; human breast cancer (ductal carcinoma) T47D; and human lung cancer (non-small cell lung cancer) A549 cell lines. The potential cytotoxicity of the five different crude venom extracts from *H. crispa, H. magnifica, H. malu, C. adhaesivum* and *E. quadricolor* were determined via MTT and crystal violet assays (see Chapter 2).

A more detailed study was then carried out using *H. magnifica* because it showed a significant cytotoxic effect on the cancer cell lines, and as it is a large anemone from which is easy to obtain venom.

The cellular and molecular mechanisms of the cytotoxicity of *H. magnifica* on human breast cancer cells T47D (ductal carcinoma, an endogenously expressing mutant p53 cell line) and MCF7 (adenocarcinoma, a p53 wild type cell line) (see Chapter 3), and on A549 cancer cells (a human lung cancer [NSCLC] cell line) (see Chapter 4) were studied. In addition, two non-cancer origin cell lines were used as controls to study efficacy: human lung fibroblast MRC5 and human breast epithelial 184B5 cell lines. Firstly, the effect of *H. magnifica* on cell lines was studied by MTT assay; furthermore, cycle progression was measured by propidium iodide (PI) staining and the endpoint detected by flow cytometry. Secondly, the apoptotic effect of the *H. magnifica* venom was measured by PI and annexin V-FITC (fluorescein isothiocyanate) staining and detected by flow cytometry. Thirdly, an investigation was conducted to determine whether venom

induced apoptosis via activation of the cysteine aspartate-specific proteases (caspases) cascade and/or mitochondrial membrane pathways.

The *H. magnifica* crude venom was purified by gel filtration chromatography and tandem mass spectometry (MS/MS). To provide sufficient material for functional investigation, the polymerase chain reaction (PCR) product was cloned into an expression vector and used to make recombinant protein. Finally, the cytotoxicity of the recombinant peptide were determined against human lung cancer cell line A549 and human breast cancer cell lines T47D and MCF7, as well as human breast non-cancer cell line 184B5 by MTT assay (see Chapter 5).

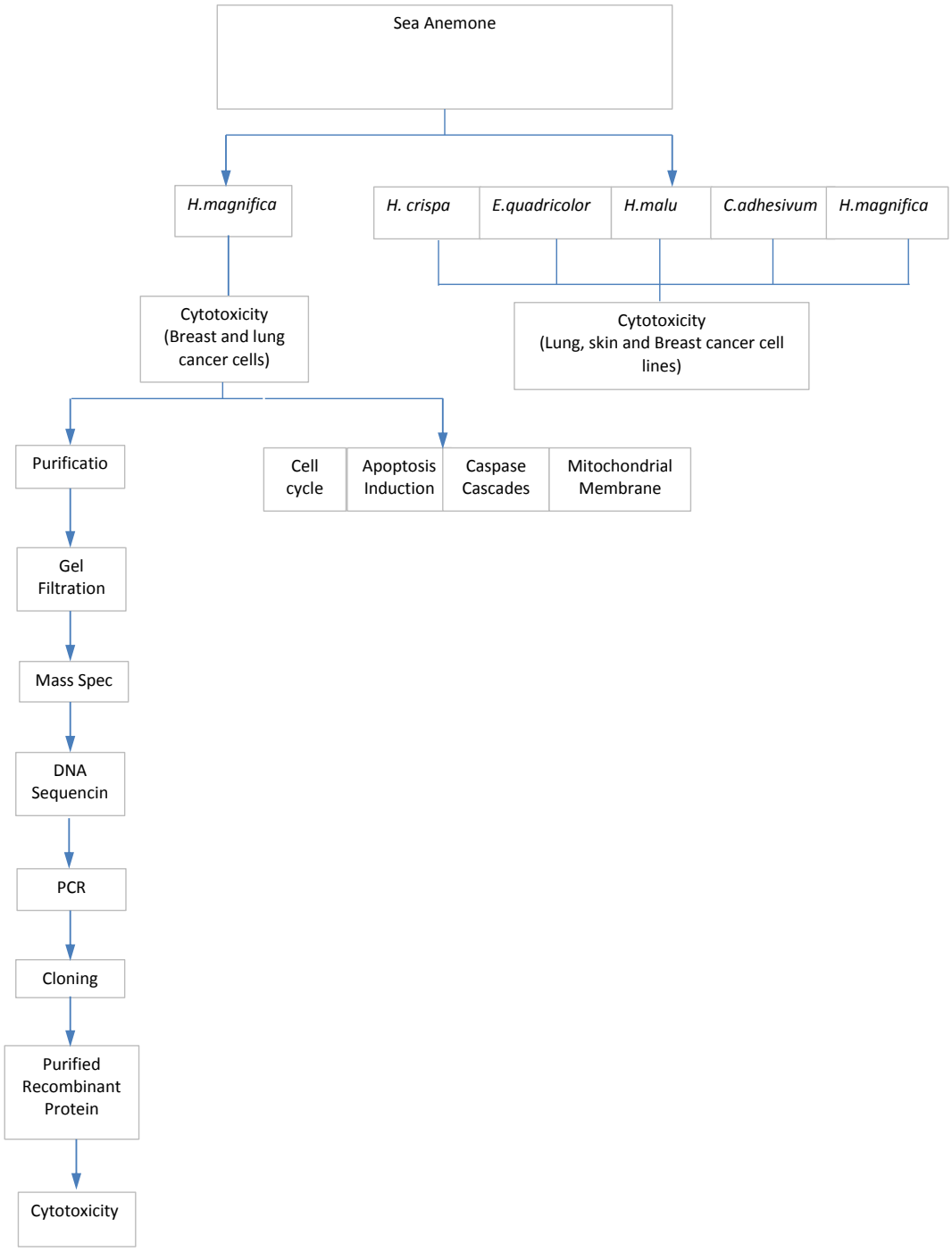

Figure 1.8: Brief outline of scope of thesis for the study of potential cytotoxicity of sea anemone venoms and their mechanism of action

CHAPTER 2: FIVE SEA ANEMONE VENOMS DIFFERENTIALLY KILL HUMAN LUNG, BREAST AND SKIN CANCER CELL LINES

2.1 Introduction

Sea anemones (order Actiniaria) are a rich source of biologically-active proteins and polypeptides (Rocha et al., 2011c) from which several cytolytic toxins, neuropeptides and protease inhibitors have been identified. Compared to other Cnidarians (typically jellyfish toxins), sea anemone toxins are relatively stable (Honma and Shiomi, 2006). Therefore, a number of toxins from various species of sea anemones have been isolated and extensively characterised (Andreev et al., 2008a). Sea anemones possess a variety of peptide and protein toxins that affect ion channels in electrically responsive cells (Santos et al., 2013). The anemone toxin binds to the influx site on sodium channels and slows down the process of sodium inactivation. Some anemones also contain smaller peptide toxins that selectively block specific potassium channels. It is thought that structural analysis of the K^+ channel peptide toxin from sea anemones would provide basic information which could allow immunosuppressant drugs to be designed (Kem et al., 1999). Most anemones also contain potent cytolytic proteins called actinoporins which permeabilize cell membranes and ultimately cause cell death (Kem et al., 1999, Gordon et al., 1996). Sea anemone compounds exhibit toxicity activity as was shown in Chapter 1 on Table 1.6.

Most investigations on sea anemones have focused on the purification and isolation of venom. Hence, the aim of the study presented in this chapter was to evaluate the *in vitro* cytotoxic effect of the crude venoms obtained from five anemones (*Cryptodendrum adhaesivum; Entacmaea quadricolor; Heteractis magnifica; Heteractis crispa and Heteractis malu*) on human lung cancer A549;

breast cancer T47D; and skin cancer A431 cells. Cell viability was assessed by MTT and crystal violet assays. The MTT assay determines the metabolic activity of viable cells (Mosmann, 1983) while the crystal violet assay relies on detection of the number of live cells that are adhered to the plate (because dead cells are non-adherent and washed away during the assay procedure) (Chiba et al., 1998). The susceptibility of the three cancer cell lines to being killed by the five different sea anemone venom extracts was determined.

2.2 Materials and Methods

2.2.1 Reagents

The reagents 3-(4,5-dimethylthiazol-2-yl)-2,5-diphenyltetrazolium bromide (MTT, 97.5%); crystal violet powder; acetic acid and sodium dodecyl sulphate (SDS, 99%); bicinchoninic acid (BCA) solution; copper (II) sulphate pentahydrate solution 4% (weight/volume percentage concentration [w/v]); and protein standard solution (bovine serum albumin) were purchased from Sigma-Aldrich (USA). Methanol was purchased from Merck (Germany). The MTT was dissolved in phosphate-buffered saline (PBS) at 5 mg/ml, then filtered (0.2 μm) to sterilize it prior to use and then stored at -20°C.

2.2.2 Venom extraction

Five different sea anemone species (*H. crispa, H. magnifica, H. malu, C. adhaesivum* and *E. quadricolor*) that have a symbiotic relationship with clownfish were collected from the Great Barrier Reef near Cairns, Queensland, Australia. They were housed in the marine aquaria in the animal house facility at

Flinders University. The anemones were kept in a tropical sea water aquarium and fed weekly with prawns, but then were fasted for a week prior to venom collection. A crude extract was obtained by milking, a technique that does not appear to cause serious harm to the anemone (Sencic and Macek, 1990). Crude venom was obtained by transferring the sea anemone from an aquarium into a clean plastic aquarium bag. Each individual was then milked by gently massaging tentacles to release venom one to three times. Venom samples were lyophilized and stored at –80°C until required for assays. When needed, the lyophilized venoms were dissolved in Milli-Q water at 100 mg/ml.

2.2.3 Protein determination

The total level of protein in the crude extract was determined by the bicinchoninic acid (BCA) protein assay (Walker, 1996, Smith et al., 1985). Bovine serum albumin (BSA) solutions were used as protein standards at the following concentrations: 1000, 800, 600, 400, 200 and 0 μg/ml, each of which was obtained from a 20 mg/ml stock solution. A quantity of 25 microlitres of each standard was added to a 96-well flat-bottom plate in triplicate. Bicinchoninic acid (BCA) (Concentration A) and copper (II) sulphate (Concentration B) were mixed at a ratio of 50:1 and added to each well at a volume of 200 μl. The plate was covered and incubated at 37°C for 30 minutes. The optical density (OD) was determined on a spectrophotometric plate reader at 562 nanometres (nm) (Model 550 with Microplate Manager Software, Bio-Rad, USA).

2.2.4 Cell lines and cell culture

2.2.4.1 Cell lines

The A549 cell line derived from a carcinoma of the lung; the T47D cell line derived from a ductal carcinoma of the mammary gland breast tissue; and A431 cell line derived from an epidermoid carcinoma of the skin were obtained from the American Type Culture Collection. The details of the cell lines are listed in Table 2.1.

Table 2.1: Summary of the human cell lines used in this study

Cell line	ATTC number	Origin and cell type	Age/gender of donor
A549	CCL-185	Lung	58/M
T47D	CRL-2865	Breast epithelial	54/F
A431	CRL-155	Skin epithelial squamous	85/F

2.2.4.2 Cell culture

The A431 cell line was maintained in Dulbecco's minimum essential (or Dulbecco's modified Eagle) (DMEM) medium (Appendix II), and the T47D and A549 cell lines were maintained in Roswell Park Memorial Institute (RPMI) 1640 medium (Appendix II). All were supplemented with 10% foetal bovine serum and 1% penicillin/streptomycin. Cells were seeded at 1×10^6 cells/ml in sterile T-75 cm^2 tissue culture flasks and incubated at 37°C in a 5% CO_2 fully humidified incubator. All cell lines were subcultured when they reached 80% confluence.

2.2.5 Cell viability assays

2.2.5.1 Identification of viable cell numbers with crystal violet assay

To identify viable cells in the culture at the end of the experiments, the crystal violet assay was conducted which stains and fixes the nuclei of live cells only. Cells were seeded at 10^4 cells per well in 100 µl in quadruplicate wells of 96-well flat-bottom plates and incubated for 24h (37°C, 5% CO_2) to allow attachment of the cells (Kueng et al., 1989). All wells other than the treatment wells of each plate contained 0.1 ml sterile PBS to prevent evaporation from the inner treatment wells. The lyophilized venoms were dissolved in Milli-Q water at 100 mg/ml. The media were replaced with 180 µl of fresh media plus 20 µl of the extract of each type of venom (*H. crispa, H. magnifica, H. malu, C. adhaesivum* and *E. quadricolor*) and 200 µl of media was used as a negative control. The cells were incubated with each extract at final protein concentrations of 0.1, 1, 10 and 40 µg/ml (which were equal to 2.5, 25, 250 and 1000 µg/ml of mass concentration) for 24h, 48h and 72h. In addition, for a negative control, the media alone were used. After treatment, the medium was removed, followed by two PBS washes and the addition of 50 µl of 0.5% crystal violet in 50% methanol to each well. The plate was incubated for 10 minutes at room temperature to stain the cells. Excess dye and dead cells were washed out gently with distilled water. The plate was allowed to dry overnight; 50 µl of 33% acetic acid was then added for 10 minutes to de-stain the cells. The OD at 570 nm was measured on an enzyme-linked immunosorbent assay (ELISA) plate reader (Bio-Tek Instruments Inc, USA) (Saotome et al., 1989).

2.2.5.2 The MTT Cell Viability Assay

The MTT assay was performed to identify viable cells at the end of the experiment by measuring the metabolic function of mitochondria within living cells. Cells were seeded at 10^4 cells per well in 100 µl in quadruplicate wells of 96-well flat-bottom plates and incubated for 24h (37°C, 5% CO_2) to allow attachment of the cells. The lyophilized venoms were dissolved in Milli-Q water at 100 mg/ml. Treatment was as for the crystal violet assay (subsection 2.2.5.1). Then, 100 µl of MTT at a final concentration of 0.5 mg/ml (a soluble tetrazolium salt) in media was added to each well. After 4h, 80 µl of 20% SDS 0.1 M hydrochloric acid (HCl) was added to each well: plates were incubated over night in the dark at room temperature. The plates were read on an ELISA plate reader (Bio-Tek Instruments Inc., USA) using a wavelength of 570 nm, with a reference wavelength of 630 nm (Mosmann, 1983, Young et al., 2005).

2.2.6 Statistical analysis

Experiments were conducted at least three independent times (n = 3). The effects of sea anemone extract on the viability of A431, T47D and A549 cell lines were analysed by one-way analysis of variance (ANOVA), followed by Tukey's honestly significant difference (HSD) post hoc test for equal and unequal variances as appropriate. All data were analysed using SPSS software (Version 18). Differences were considered statistically significant when *p*-values were less than 0.05.

2.3 Results

2.3.1 Protein determination

Protein concentration was determined using the bicinchoninic acid assay (BCA assay). The total protein concentration in the crude extracts of *H. magnifica* and *H. crispa* was 400 μg/ml. The protein concentrations in the crude extracts of *H. malu*, *C. adhaesivum* and *E. quadricolor* were 598 μg/ml, 1387 μg/ml and 1176 μg/ml, respectively.

2.3.2 Cell viability assays

2.3.2.1 Cell viability assay on A549 non-small cell lung cancer cell line

The induction of cell killing was determined by two methods: MTT assay (relative viability) and crystal violet assay (relative cell number). Venom extracts (*H. magnifica, H. crispa, H. malu, E. quadricolor* and *C. adhaesiuvm*) were tested on A549 lung cancer cell lines. In the MTT assay, significant differences were found after treatment with *H. malu*, *C. adhaesivum*, *E. quadricolor* and *H.magnifica* at 40 μg/ml at all endpoints.

Heteractis crispa significantly reduced the viability of the A549 cell line at 40 μg/ml at 48h and 72h (Figure 2.1, Appendix IV). The toxic effects of the extracts determined by the MTT assay were slightly increased for *E. quadricolor* at 24h, 48h and 72h.

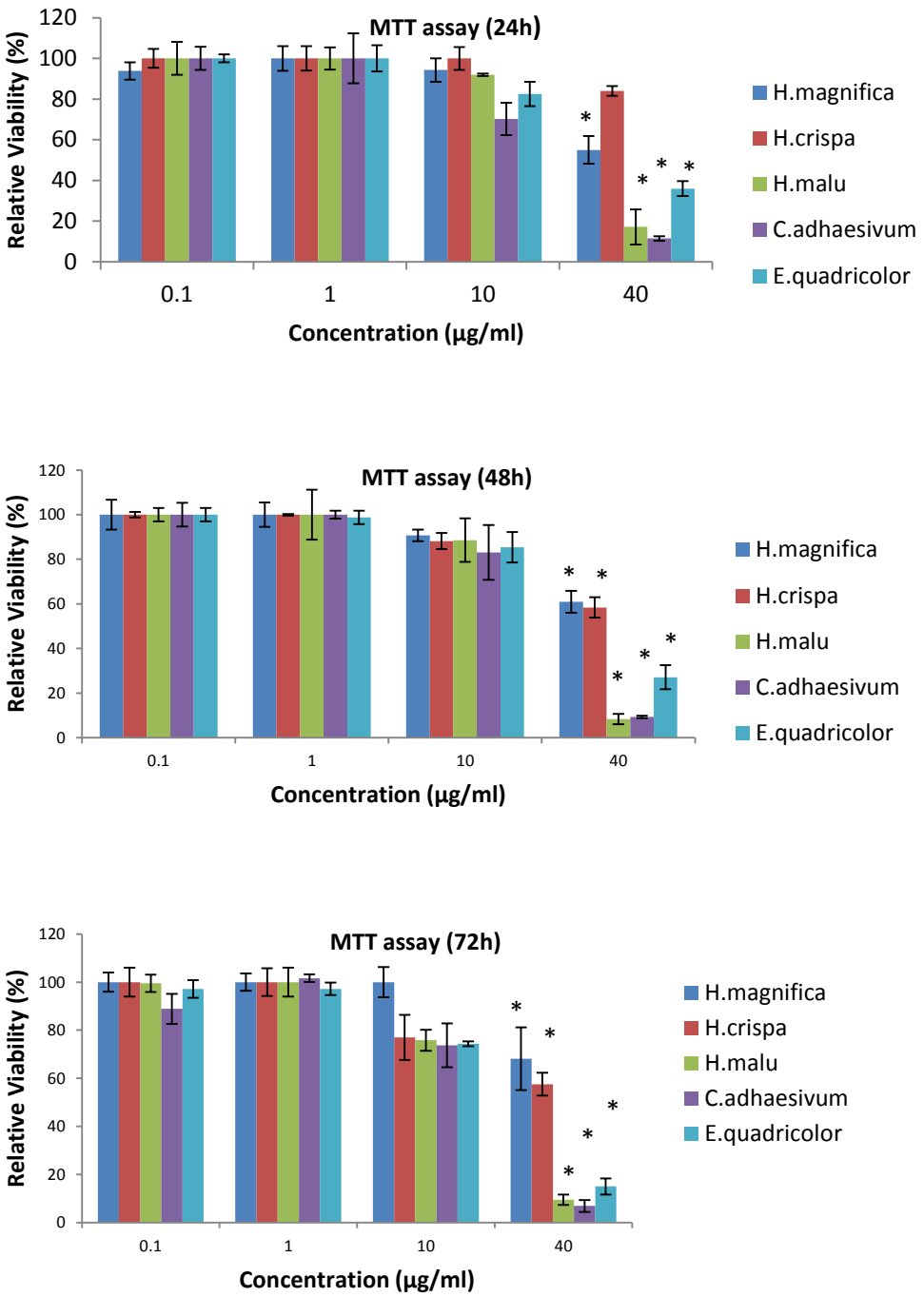

Figure 2.1: Relative cell viability (%) of A549 cells estimated by MTT assay

Notes: In 96-well plates after 24h, 48h and 72h of exposure to *H. magnifica*, *H. crispa*, *C. adhaesivum*, *E. quadricolor* and *H. malu* venom extract. Data shown as mean ± SEM, n = 3. * = treatments significantly different from the 0 µg/ml untreated control at $p < 0.05$.

The crystal violet assay indicated significant differences after treatment with *H. malu*, *C. adhaesivum* and *E. quadricolor* at 40 µg/ml. In contrast, *H. crispa* did not show any significant effect at 24h, 48h and 72h. *Heteractis magnifica* had a significant killing effect on A549 cells after 24h exposure (Figure 2.2, Appendix IV). Statistical analyses are shown in Appendix III.

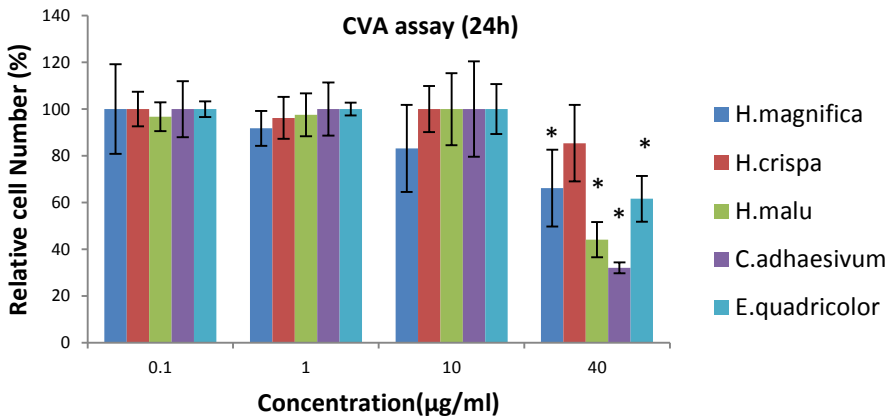

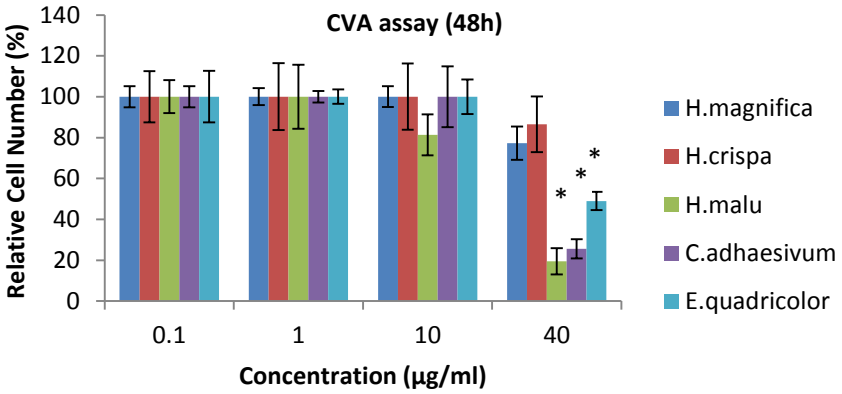

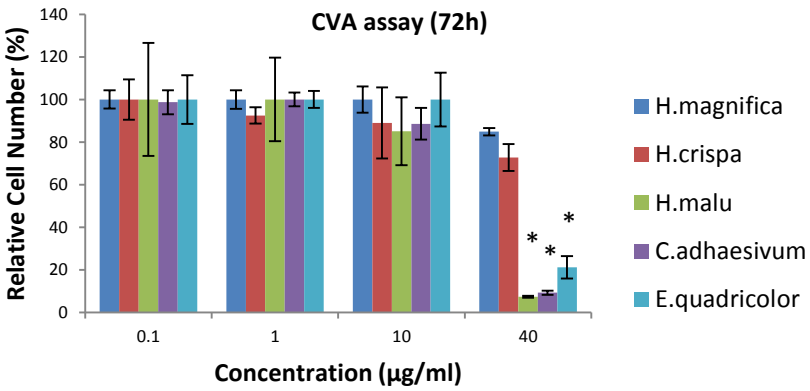

Figure 2.2: Cell number (%) of A549 cells estimated by crystal violet assay

Notes: In 96-well plates following 24h, 48h and 72h exposure to *H. magnifica*, *H. crispa*, *C adhaesivum*, *E. quadricolor* and *H. malu* venom extract. Data shown as mean ± SEM, n = 3. * = treatments significantly different from the 0 µg/ml untreated control at $p < 0.05$.

2.3.2.2 Cell viability assay on T47D cell line

Venom extracts of all five sea anemone species (*H. magnifica, H. crispa, H. malu, E. quadricolor* and *C. adhaesiuvm*) were tested by the MTT assay (relative cell viability) and crystal violet assay (relative cell number) on the T47D breast cancer cell lines. Among these venom extracts, *H. malu* showed the most significant cytotoxicity effect on T47D at 40 µg/ml and also had a significant inhibitory effect on cell viability at 24h, 48h and 72h.

Cryptodendrum adhaesivum showed a significant decrease in relative cell viability after 48h and 72h; however, no significant effect was shown at the dose of 40 µg/ml after 24h.

Entacmaea quadricolor showed a significant effect after 72h. No significant effect was found using *H. magnifica* and *H. crispa* extract on T47D cells after 24h, 48h and 72h (Figure 2.3, Appendix IV).

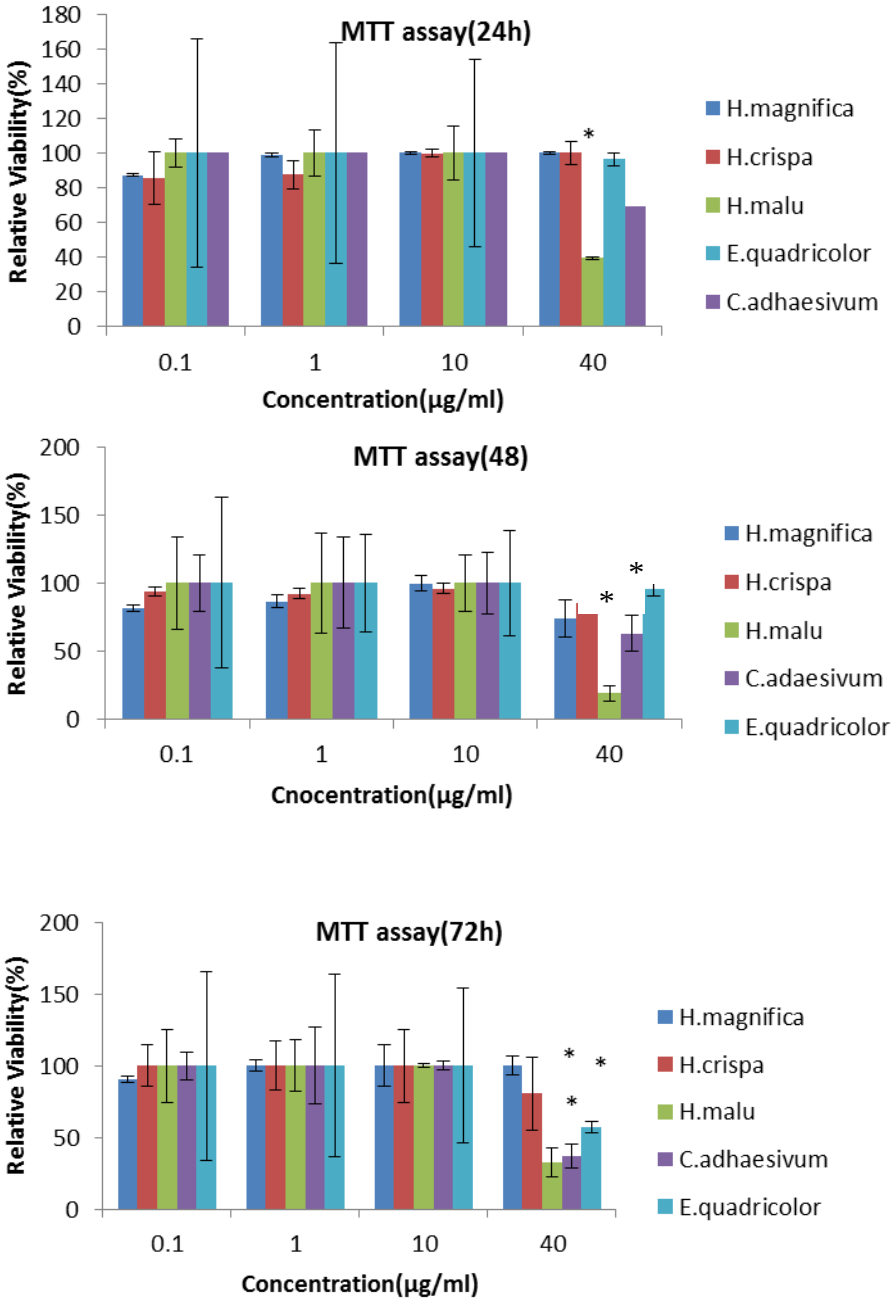

Figure 2.3: Effect of *H. magnifica, H. crispa, C. adhaesivum, E. quadricolor* and *H. malu* venom extract on growth of T47D cells measured by MTT assay

Notes: At 24h, 48h and 72h. Data shown as mean ± SEM, n = 3. * = treatments significantly different from the 0 µg/ml untreated control at $p < 0.05$.

Using the crystal violet assay, a toxic effect was detected for the venom extract from two anemone species (*C. adhaesivum* and *H. malu*) on T47D cell line at the dose of 40 µg/ml. However, *H. magnifica*, *H. crispa* and *E. quadricolor* had no significant effect on the T47D breast cancer cell line (Figure 2.4, Appendix IV). Statistical analyses are shown in Appendix III.

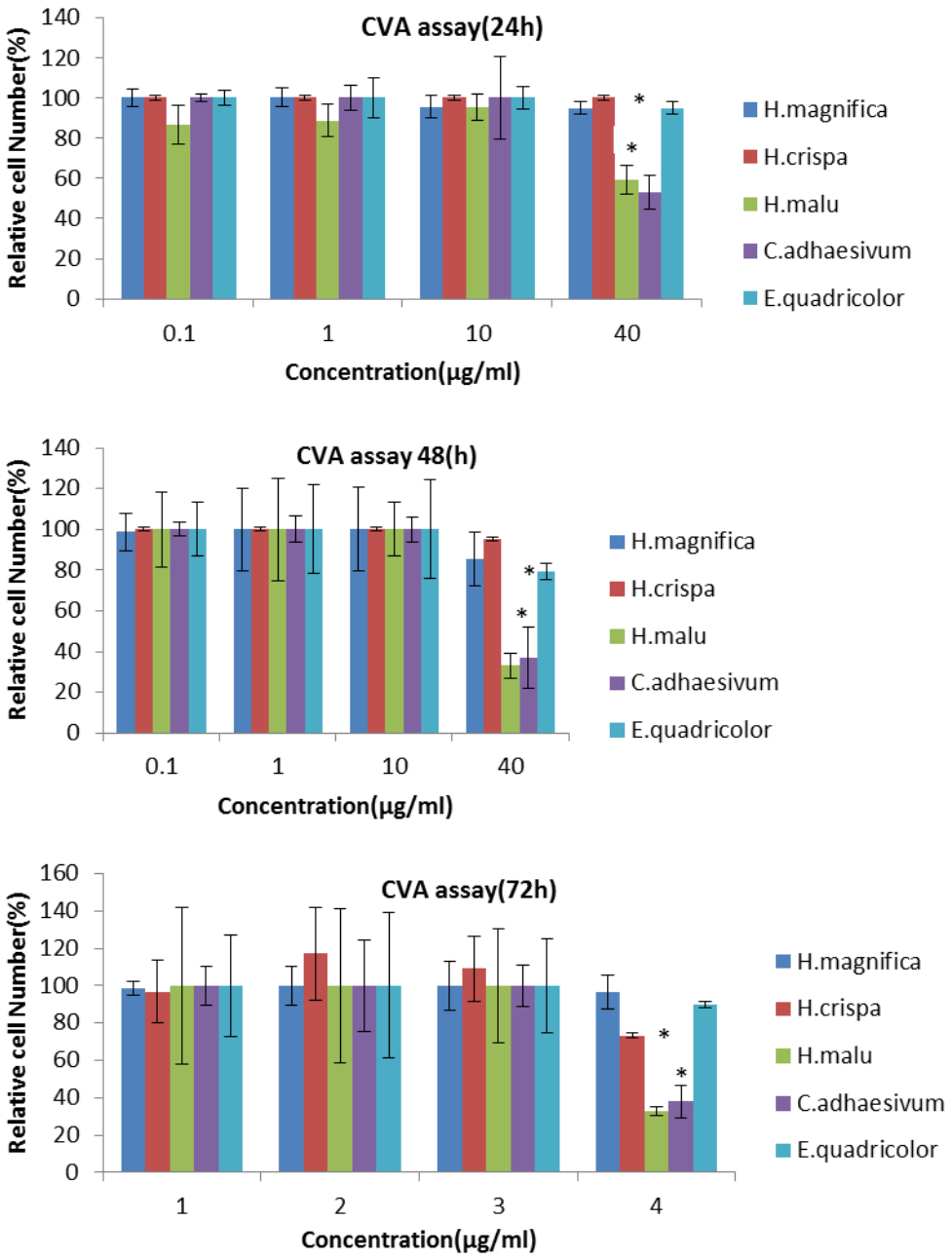

Figure 2.4: Effect of *H. magnifica, H. crispa, C. adhaesivum, E. quadricolor* and *H. malu* venom extract on growth of T47D cells measured by crystal violet assay

Notes: At 24h, 48h and 72h. Data shown as mean ± SEM, n = 3. * = treatments significantly different from the 0 µg/ml untreated control at $p < 0.05$.

2.3.2.3 Cell viability assay on A431 cell line

Sea anemone venom extracts (*H. magnifica, H. crispa, H. malu, E. quadricolor* and *C. adhaesiuvm*) were tested by the MTT assay (relative cell viability) and crystal violet assay (relative cell number) on A431 skin cancer cell lines. In A431 cells, treatment with *H. malu, C. adhaesivum* and *E. quadricolor* reduced the relative viability of cells at the dose of 40 μg/ml in the MTT assay. Of these, *H. malu* showed the most marked cytotoxicity on A431 cells at 24h, 48h and 72h.

Heteractis magnifica had a significant inhibitory effect on the proliferation of A431 cells after 24h and 72h treatment using the MTT assay. *Heteractis crispa* had no significant dose-dependent effect on the A431 cancer cell line (Figure 2.5, Appendix IV).

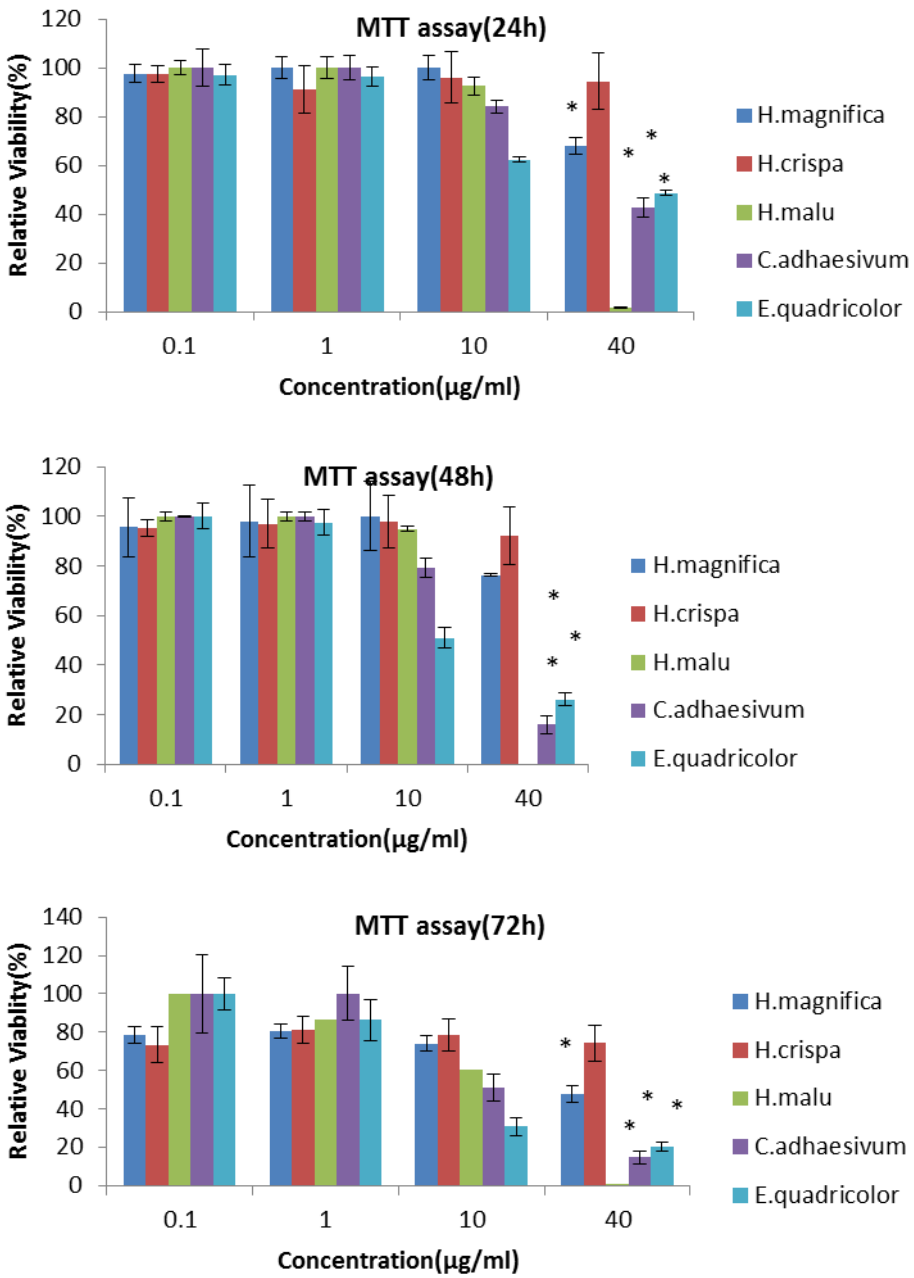

Figure 2.5: Cytotoxic effect of *H. magnifica, H. crispa, C. adhaesivum, E. quadricolor* and *H. malu* venom extract on A431 cell line measured by MTT assay

Notes: At 24h, 48h and 72h. Data shown as mean ± SEM, n = 3. * = treatments significantly different from the 0 µg/ml untreated control at $p < 0.05$.

In the crystal violet assay, the extracts *H. malu*, *C. adhaesivum* and *E. quadricolor*, but not *H. magnifica* and *H. crispa*, presented a significant time-dependent response on A431 cells with decreasing survival as the exposure time increased (Figure 2.6, Appendix IV). Statistical analyses are shown in Appendix III.

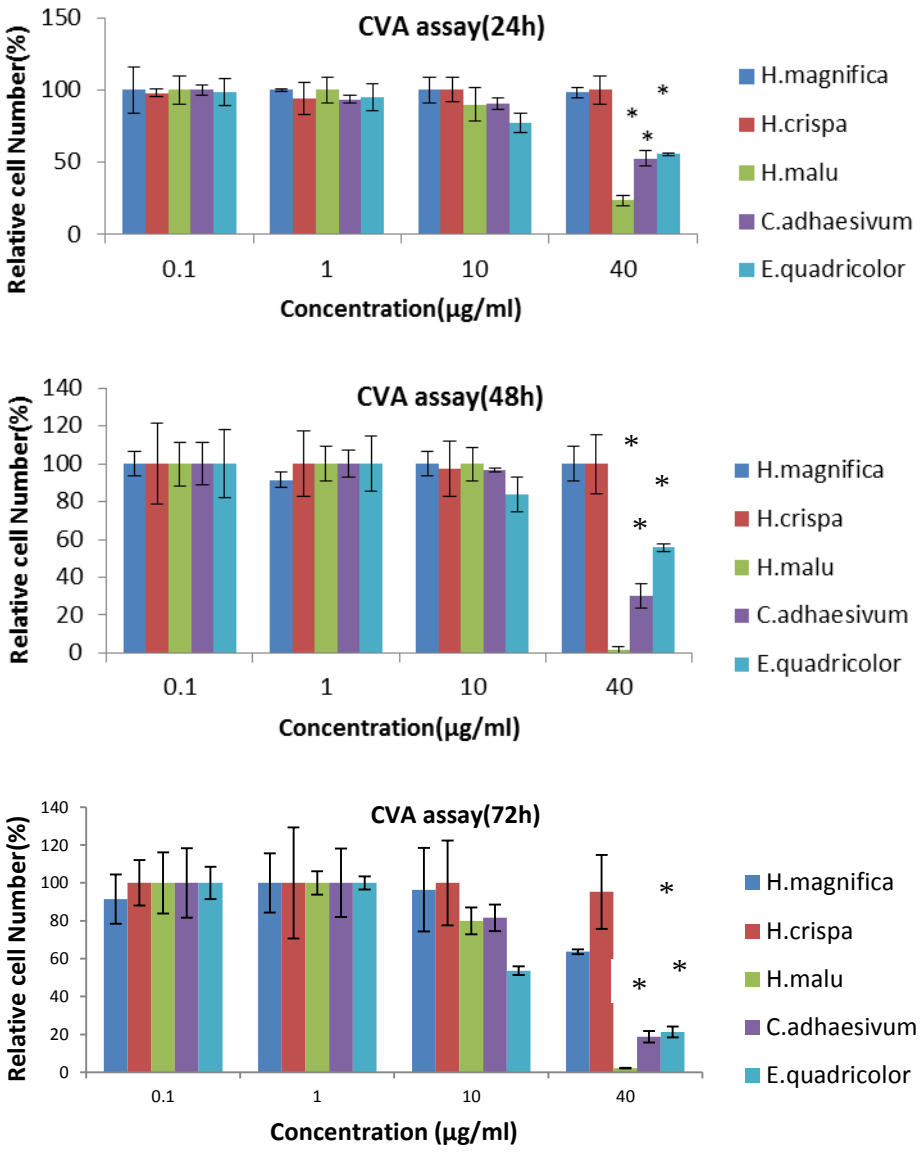

Figure 2.6: Cytotoxic effect of *H. magnifica*, *H. crispa*, *C. adhaesivum*, *E. quadricolor* and *H. malu* venom extract on A431 cell line measured by crystal violet assay

Notes: At 24h, 48h and 72h. Data shown as mean ± SEM, n = 3. * = treatments significantly different from the 0 µg/ml untreated control at $p < 0.05$.

2.4 Discussion

In this study, the potential of five sea anemone venoms (*Heteractis magnifica, Heteractis crispa, Heteractis malu, Cryptodendrum adhaesivum* and *Entacmaea quadricolor*) to kill cancer cells was tested on three different cancer cell lines: A549 lung cancer, T47D breast cancer and A431 skin cancer. The A549 cell line was the most sensitive and showed a significant reduction in relative cell viability as observed at 40 µg/mL. *Heteractis malu* and *C. adhaesivum* crude venom showed higher cytotoxic activity on three cancer cell lines as compared with *H. magnifica*, *H. crispa* and *E. quadricolor*. *Heteractis crispa* venom was the least cytotoxic of the five venoms.

Gigantoxins are newly discovered peptides that have been isolated from the sea anemone *Stichodactyla gigantea* (Honma and Shiomi, 2006). Gigantoxins II and III were found to be potently lethal to crabs with respective LD_{50} levels of 70 µg/kg and 120 µg/kg. Moreover, Gigantoxin I also caused the rounding of almost all treated A431 cells when examined by phase-contrast microscopy (Honma and Shiomi, 2006). Consistent with that observation, A431 cells were sensitive to killing by four of the venom extracts used in the current study. A significant reduction of A431 cell viability was found using a concentration of 40 µg/ml of *H. malu*, *H. magnifica*, *C. adhaesivum* and *E. quadricolor* venom extracts. A further study is needed to estimate the LD_{50} (IC_{50}) for the four venom extracts.

Heteractis magnifica venom extract also had a significant effect on the killing of A431 and A549 cells at 40 μg/ml when assayed in the current study by the MTT assay.In addition, two cytolysins, magnificalysins I and II purified from *H. magnifica*, caused haemolytic and lethal activities in a mouse model (Khoo et al., 1993). The LD_{50} values of magnificalysins I and II in mice were approximately 0.14 μg/ml and 0.32 μg/ml, respectively (Khoo et al., 1993). Previously, the actinoporin RTX-A isolated from *H. crispa* exerted a significant cytotoxic effect on several human cancer cell lines, including HL-60, MDAMB-231, Hela, THP-1 and SNU-C4 at 10^{-9} M (Fedorov et al., 2010). Consistent with these observations, the current results from the MTT assay showed a significant decrease in viability of A549 cells after 48h and 72h treatment using *H. crispa* venom extract.

(Malpezzi et al., 1995) reported that lipid fractions from *Bunodosoma caissarum*, when tested on T47D cells at concentrations ranging from 50–500 μg/ml, produced cell death. Consistent with this, *H. malu* and *C. adhaesivum* produced a significant killing effect on T47D at 40 μg/ml.

In conclusion, the current study, as reported in this chapter, has shown that five different sea anemone venoms have cytotoxic effects that vary depending on the origins of the venom and the different cancer cell line. Of the three cancer cell lines tested, A549 was the most sensitive to the venoms at 40 μg/ml. In 40 μg/ml, A431 was vulnerable to inhibition by venoms from *H. malu*, *H. magnifica*, *C. adhaesivum* and *E. quadricolor*, whereas T47D was susceptible to venoms from *H. malu* and *C. adhaesivum.* In the chapters that follow, further examination of how sea anemone venom kills lung and breast cancer cell lines will be

investigated with the aim being to determine the underlying mechanisms involved in these effects.

CHAPTER 3: THE EFFECT OF *HETERACTIS MAGNIFICA* VENOM ON HUMAN BREAST CANCER CELL LINES INVOLVES DEATH BY APOPTOSIS

3.1 Introduction

Some of the most potent marine toxins known are from sea anemones, and include a rich source of two classes of peptide toxins: sodium channel and potassium channel toxins (Honma and Shiomi, 2006). *In vitro* and *in vivo* studies have demonstrated that more than 32 species of sea anemones produce lethal cytolytic peptides and proteins (Anderluh and Macˇek, 2002). The cytotoxic mechanisms of sea anemone venoms work through various modes of action which are cell type dependent and venom structure related. Up-to-date cytotoxicity studies about compounds extracted from sea anemones on different cell lines are referred to in Chapters 1–4 (Mariottini and Pane, 2014a).

Some studies have been conducted on the haemolytic activity and neurotoxic activity of *H. magnifica* venom (Subramanian et al., 2011, Khoo et al., 1995, Khoo et al., 1993, Nedosyko et al., 2014b). However, the effect of the crude extract on breast cancer cell lines and the mechanisms involved in this effect have not been elucidated. The past decade has seen a dramatic increase in the number of preclinical anti-cancer lead compounds from diverse marine life entering human clinical trials (Simmons et al., 2005). Hence, the current study of the potential cytotoxicity of sea anemone venom will contribute to this important area. In particular, it will investigate the sensitivity of breast cancer cell lines. Breast cancer is the second most common cancer in the world and the most common cancer in females accounting for 23% of all cases (Saadat, 2008).

Apoptosis is a major target of anti-cancer therapeutics; therefore, it is important to discover novel therapeutics with this mechanism of action (Reed, 2003). Apoptosis is triggered through intrinsic and extrinsic signalling pathways (Elmore, 2007). The extrinsic signalling pathway leading to apoptosis involves transmembrane death receptors that are members of the tumour necrosis factor (TNF) receptor gene superfamily. Members of this receptor family bind to extrinsic ligands (FasL, TNF-alpha, Apo3L and Apo2L) and transduce intracellular signals, ultimately resulting in the destruction of the cell (Rubio-Moscardo et al., 2005, Suliman et al., 2001). The intrinsic signalling pathway for programmed cell death involves non-receptor-mediated intracellular signals (Elmore, 2007). Stimuli of the intrinsic pathway induce changes in the inner mitochondrial membrane that result in the loss of transmembrane potential, causing the release of pro-apoptotic proteins (Bcl-10, Bax, Bak, Bid, Bad, Bim, Bik and Blk) into the cytosol (Adams and Cory, 2001). Pro-apoptotic proteins activate caspases that mediate the destruction of the cell through many pathways. Caspases exist as inactive zymogens and are converted into active enzymes via cleavage of the proenzyme form into large and small subunits which together form the active caspases (Lipnick and Jacobson, 2006). Caspases have been broadly classified by their known roles in apoptosis (caspase-3, -6, -7, -8 and -9) and in inflammation (caspase-1, -4, -5 and -12) (McIlwain et al., 2013).

Binding extrinsic ligands (Fas ligand) to Fas receptors causes oligomerization of caspase-8 which activates caspase-3 through direct proteolytic processing, leading to further downstream caspase activation (Cullen and Martin, 2009). Caspase-8

can also cleave the BH3-only protein which promotes the Bax/Bak-dependent cytochrome release from mitochondria and the formation of the apoptosome, resulting in activation of caspase-9 (Baliga and Kumar, 2003). Active caspase-9 then instigates a caspase activation cascade by processing caspase-3/7 which propagate further caspase-processing events (Cullen and Martin, 2009). Caspase-3/7 is the most prevalent caspase within cells and is responsible for most apoptic effects (Rodríguez-Hernández et al., 2006). Caspase-3/7's activation induces poly(ADP-ribose) polymerase (PARP) cleavage, DNA breaks and finally leads to apoptosis (Chaitanya et al., 2010).

Mitochondrial dysfunction is another key event of apoptosis. Mitochondria play the pivotal roles in integrating and directing the death signal towards the caspase cascade (Liu et al., 2004). The permeabilization of the mitochondrial outer membrane and the release of intermembrane space proteins, such as cytochrome *c*, Smac/DIABLO and the apoptosis-inducing factor (AIF) are central events in apoptosis (Gogvadzea et al., 2006).

The purpose of this chapter is to investigate the effect of *H. magnifica* venom on human breast cancer T47D and MCF7 cell lines and on the normal human breast 184B5 cell line using MTT and crystal violet assays. Cell cycle progression using PI staining was investigated by flow cytometry. The apoptotic effect of the crude venom was investigated using annexin V-FITC and PI staining. The underlying mechanism of apoptosis induced by *H. magnifica* venom was investigated using caspase-3/7, -8 and -9 assays and the mitochondrial membrane potential assay.

In addition, the current study focused on the venom of *H. magnifica* because *H. magnifica* is a large and more easily obtained sea anemone. Hence, for the detailed studies required for the study, more venom was available.

3.2 Materials and Methods

3.2.1 Materials

All the reagents used in this chapter were from Sigma-Aldrich unless otherwise noted.

3.2.2 Sea anemone venom

Venom from *H. magnifica* were frozen immediately, freeze-dried using a bench-top lyophilizer (VirTis, USA) and ground into a fine powder. Samples were re-solvated at 100 mg/ml with distilled water. The concentration of total protein in the crude extracts of *H. magnifica* was adjusted to 400 μg/ml. All the various concentrations of crude extract were made up in distilled water.

3.2.3 Human cell culture

Human adherent breast cancer cells T47D (ductal carcinoma, an endogenously expressing mutant p53 cell line) and MCF7 (adenocarcinoma, a p53 wild type cell line) as well as 184B5 cells (human non-cancer breast cell line) were obtained from the American Type Culture Collection. For a description of the cell culture, refer to subsection 2.2.4.2.

3.2.4 Cell viability test

To assess the cytotoxicity effects of crude extracts, two bioassays (MTT and crystal violet) were used. For a description of the assays, refer to subsection 2.2.5.

3.2.5 Cell cycle analysis

Cell cycle distribution was evaluated by flow cytometry (Nicoletti et al., 1991). The MCF7 and T47D cell lines were established at 1×10^6 cells/ml in a T25 cm^2 flask (4×10^3 cells/mm^2) and incubated overnight at 37°C in 5% CO_2 to allow adherence. The cells were treated with the *H. magnifica* venom extract at working concentrations of 0, 15 and 40 µg/ml for 24h at 37°C in 5% CO_2. Following treatment, the cells were harvested by trypsinisation then fixed with 3 ml ice-cold 70% ethanol at -20°C overnight. The cell pellet was suspended in 1 ml of mixture solution (20 µg/ml of PI and 200 µg/ml of RNase in 0.1%Triton X-100 in phosphate-buffered saline [PBS]) and incubated at room temperature in the dark for 30 minutes. Samples were analysed by Accuri C6 flow cytometry.

3.2.6 Measurement of apoptotic events by flow cytometry

The treatment of cells was as for the cell cycle analysis. Cells were exposed to 0, 15 and 40 µg/ml of the treatment. Cells were then counted using trypan blue exclusion assay. After treatment, the cells were washed twice with cold 0.1% sodium azide in phosphate-buffered saline (PBS). The pellets were re-suspended in binding buffer at 10^6 cells/ml. Then, 100 µl of the solution was transferred to a culture tube: following this, 5 µl of annexin V-FITC (BD

Biosciences) and 5 µl of PI were added to double stain the cells. After 15 minutes of incubation in the dark at room temperature, 200 µl of binding buffer was added to the cells. Early and late apoptosis were analysed by Accuri C6 flow cytometry.

3.2.7 Caspase assay

Caspase activities were measured using caspase-3/7, -8 and -9 assay kits (Promega Corporation, Australia). This was conducted by seeding 1×10^4 cells/well in a luminometer plate (BD Biosciences, USA) and incubating for 24h at 37°C in 5% CO_2. Cells were treated with crude venom extract at concentrations of 0, 15, 30 and 40 mg/ml in a final volume of 0.1 ml per well for 24h: cells were washed with 1 × PBS (phosphate-buffered saline). Next, 50 µl of medium was taken out and 0.05 ml of the Caspase -3/7, -8 or -9 reagent was added separately to each well, giving a final volume per well of 0.1 ml. The plates were incubated in the dark for one hour and the luminescence was recorded every 10 minutes for one hour at 28°C in a microplate reader.

3.2.8 Mitochondrial membrane potential

Cells were seeded in a T25cm^2 flask (4×10^3 cells/mm^2) and incubated overnight at 37°C + 5% CO_2 to allow cell attachment to the flasks. Cells were treated with the *H. magnifica* venom extract at working concentrations of 0, 15 and 40 µg/ml for 24h at 37°C in 5% CO_2. After staining the cells with JC-1 dye, the numbers of cells exhibiting green and red fluorescence were quantified via flow cytometry

using Accuri C6. The data were analysed with CellQuest software (Cossarizza et al., 1993 , Tsujimoto and Shimizu, 2007).

3.2.9 Statistical analysis

Data were presented as the mean plus or minus the standard error of mean (SEM). The experiments were replicated at least three independent times. The IC_{50} calculation was determined using GraphPad Prism V. 5.02 for Windows (GraphPad Software, San Diego, California, USA). Statistical analysis of the data was carried out using ANOVA, followed by Tukey's HSD post hoc test. These tests were performed using SPSS software (Version 18). Differences were considered significant when the *p*-value was less than 0.05. Responses to treatment were compared to the untreated control for a given cell line. In addition, the response of both cancer cell lines in the assays was compared to that of the non-cancer control cell line. Area Under the Curve (AUC) can be used to compare efficacy of the treatment applied to different cell lines (Fallahi-Sichani et al., 2013). Differences in the viability-dose response curves were estimated by comparing the AUC for the test and reference cell line, using the individual replicate (n = 3) data.

3.3 Results

3.3.1 *H. magnifica* venom induces cell killing of T47D and MCF7 cells

For T47D cells, treatment reduced the numbers of viable cells in a dose-dependent manner for both assays. There was greater than 90% reduction in cell numbers after 24h treatment with 15 µg/ml of crude venom (Figures 3.1 and 3.2). Among these three cell lines, T47D showed the most marked cytotoxicity with an IC_{50} value of 5.99 µg/ml for the MTT assay and 5.67 µg/ml for the crystal violet assay.

The crude venom also significantly reduced the survival of MCF7 cells; however, the incremental changes for the four lowest doses of extract for MCF7 cells were less than for the T47D cells. The treatment of MCF7 cells with 20 µg/ml of crude venom for 24h resulted in a 65% and 90% reduction in relative cell survival in the MTT assay and in the cell number detected in the crystal violet assay, respectively.

In contrast, for the crystal violet assay, the crude venom caused less cytotoxicity on the human non-cancer breast 184B5 cell line, as evidenced by higher IC_{50} values (14.70 µg/ml) on 184B5 compared to the values on MCF7 (9.26 µg/ml) and T47D (5.67 µg/ml) cell lines. In the MTT assay, however, a significant reduction in viability was found at 15 µg/ml or higher concentration of the crud venom , showing some resistance compared to the MCF7 cell line (Figures 3.1 and 3.2). The IC_{50} values for 184B5, MCF7 and T47D cell lines were 6.74 µg/ml, 15.76 µg/ml and 5.99 µg/ml, respectively. In addition, differences in the AUC of the dose response curves (ΔAUC) between T47D and MCF7 cell lines and the reference cell line (184B5) were estimated using the R package PK (Jaki and Wolfsegge, 2011) (Table 3.1).

Table 3.1: Breast cancer (T47D and MCF7) cell lines compared to the relevant control (184B5) using Area Under Curve analysis.

Tissue	Breast cancer cell line	Breast normal cell line	CSV ΔAUC *p*-value	MTT ΔAUC *p*-value
Breast	T47D	184B5	0.044	0.45
Breast	MCF7	184B5	0.005	0.12

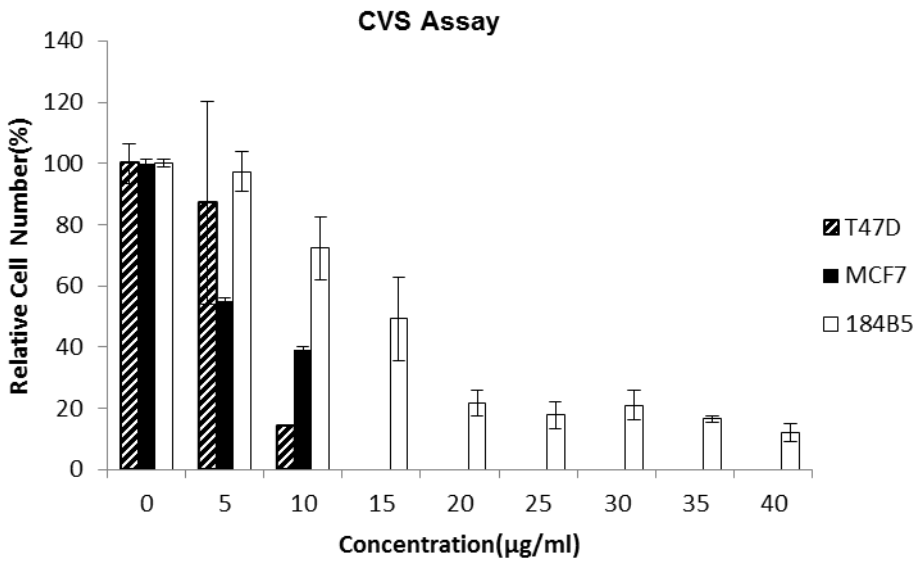

Figure 3.1: Relative cell number (%) of T47D, MCF7 and 184B5 cells estimated by crystal violet assay

Notes: In 96-well plates following 24h exposure to *Heteractis magnifica* venom. Data are shown as surviving cell numbers compared to the untreated control and are presented as the mean ± SEM of three separate trials. All doses of 10 µg/ml or greater significantly killed T47D and MCF7 cells compared to those in the 0 µg/ml control ($p < 0.05$).

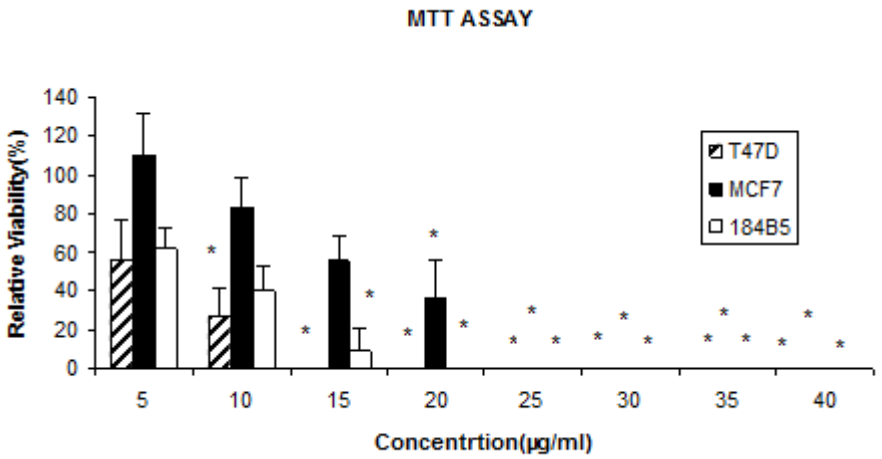

Figure 3.2: Cell viability monitored by MTT assay after 24h treatment of T47D, MCF7 and 184B5 cells with *Heteractis magnifica* venom

Notes: Data are shown as a percentage of relative survival compared to the untreated control and are presented as the mean ± SEM of three separate trials. Treatments significantly different from the untreated control at $p < 0.05$ are presented as *.

The cell survival in flasks was also estimated as part of the Trypan Blue assay. As shown in Figure 3.3, relative survival decreased in a dose-dependent manner.

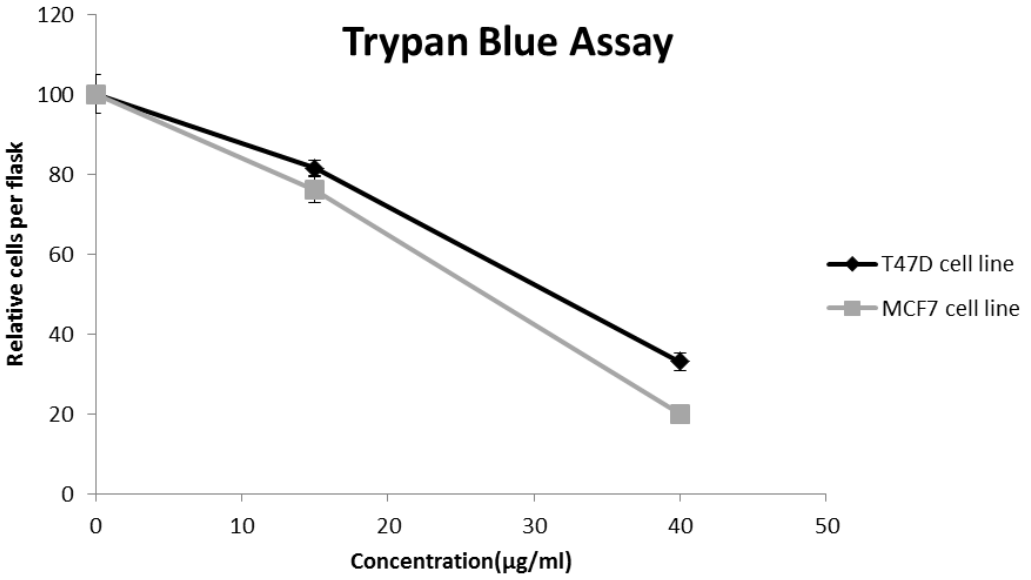

Figure 3.3: Relative cell per ml for T47D and MCF7 cell lines in flasks following treatment for analysis in apoptosis assay

Notes: This was estimated by the Trypan blue exclusion assay after 24h exposure to the treatment. Data are shown as a percentage of relative surviving cell numbers compared to the untreated control and are presented as the mean ± SEM of three separate trials.

3.3.2 *H. magnifica* venom deregulates cell cycle control

Cell cycle distribution was analysed by flow cytometry using PI staining. *Heteractis magnifica* venom treatment of the breast cancer cell lines significantly increased the sub-G1 peak with a concomitant decrease in the G1 phase, compared to the untreated control (Figures 3.4 and 3.5). The increase in the sub-G1 peak was significant at 40 µg/ml for both cell lines.

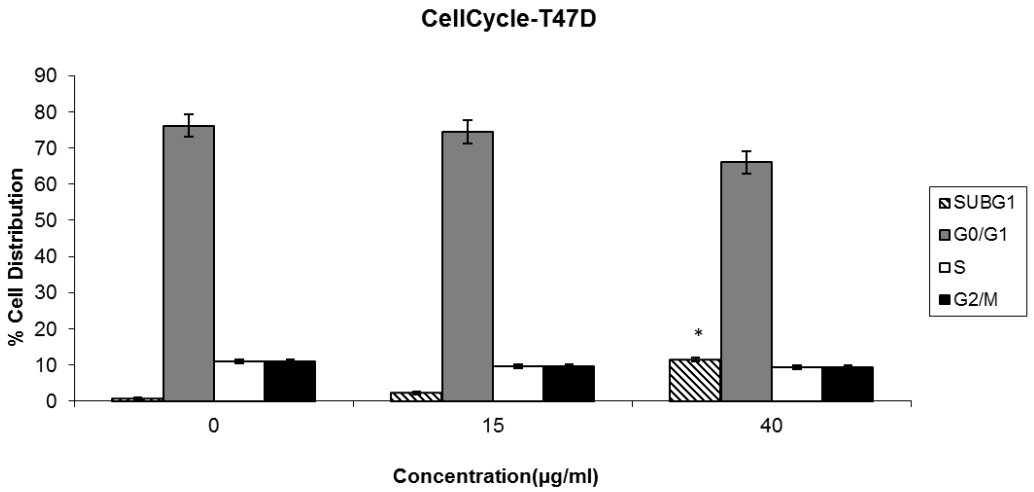

Figure 3.4: Effect of *H. magnifica* venom on cell cycle progression determined by PI staining and analysed for DNA content by flow cytometry

Notes: Data were obtained from 20,000 events and are presented as a percentage of cells in the sub-G1, G0/G1, S and G2/M phases. The values are shown as means ± SEM for n = 3. Treatments significantly different from the untreated control at $p < 0.05$ are presented as *.

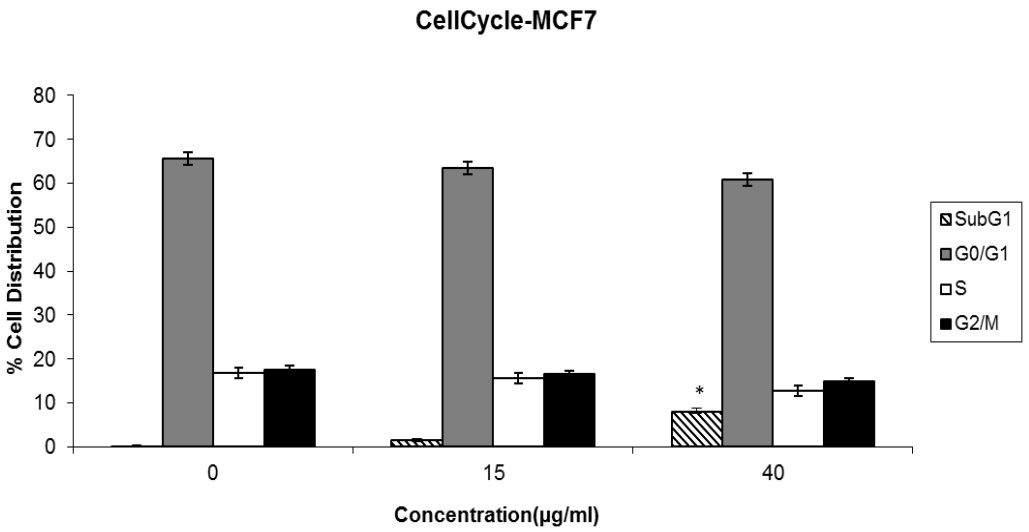

Figure 3.5: Effect of *Heteractis magnifica* on cell cycle progression determined by PI staining and analysed for DNA content by flow cytometry

Notes: Data were obtained from 20,000 events and presented as a percentage of cells in the sub-G1, G0/G1, S and G2/M phases. The values are shown as means ± SEM. Treatments significantly different from the untreated control at $p < 0.05$ are presented as *.

3.3.3 *H. magnifica* venom induces apoptosis of T47D and MCF7 cells

To determine whether the venom-induced reduction in cell viability was from the induction of apoptosis, the numbers of apoptotic cells were estimated by staining the cells with annexin V and PI, followed by flow cytometry. The increment of the response to the treatment was the largest in the MCF7 cells. The most significant increase was observed at 40 µg/ml: this included approximately 19% early apoptosis compared with 1.2% in untreated MCF7 cells (Figure 3.6). In T47D cells, the most significant increase was found to be 16% early apoptosis

compared with 5.1% in untreated cells (Figure 3.7). This is a clear indicator that *H. magnifica* induces apoptosis in both the human breast cancer cell lines tested.

Late apoptosis and necrosis are not distinguishable using the current method because cells at both stages were stained by PI and annexin V-FITC. In both of the human breast cancer cell lines, significant increases in late apoptosis or necrosis were observed at 40 µg/ml (in Figures 3.6 and 3.7).

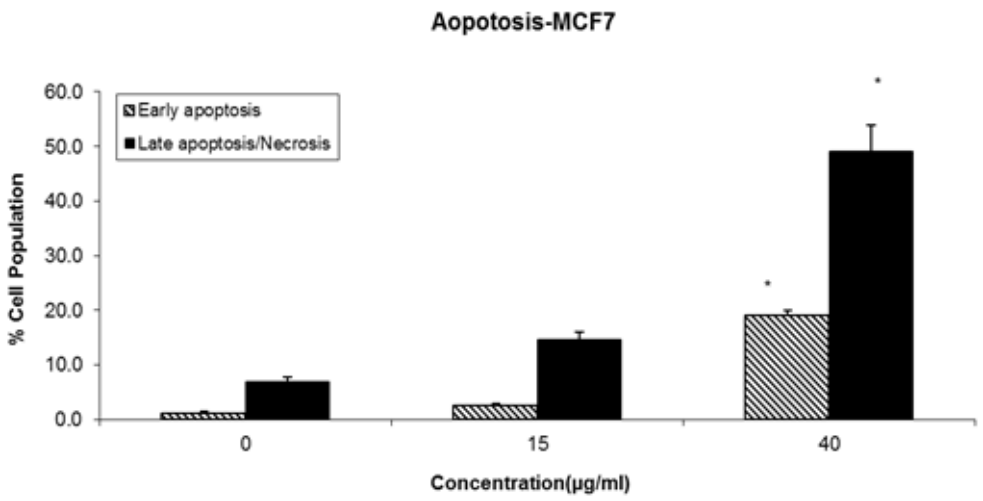

Figure 3.6: Apoptotic effect of *Heteractis magnifica* on MCF7 cells determined by annexin V-conjugated PI staining through flow cytometry

Notes: Data were obtained from 20,000 events and early apoptotic cells (annexin positive) and late apoptotic cells (annexin positive/PI positive, including necrotic cells) are presented as a percentage of total cells analysed. The values are shown as means ± SEM. Treatments significantly different from the untreated control at $p < 0.05$ are presented as *.

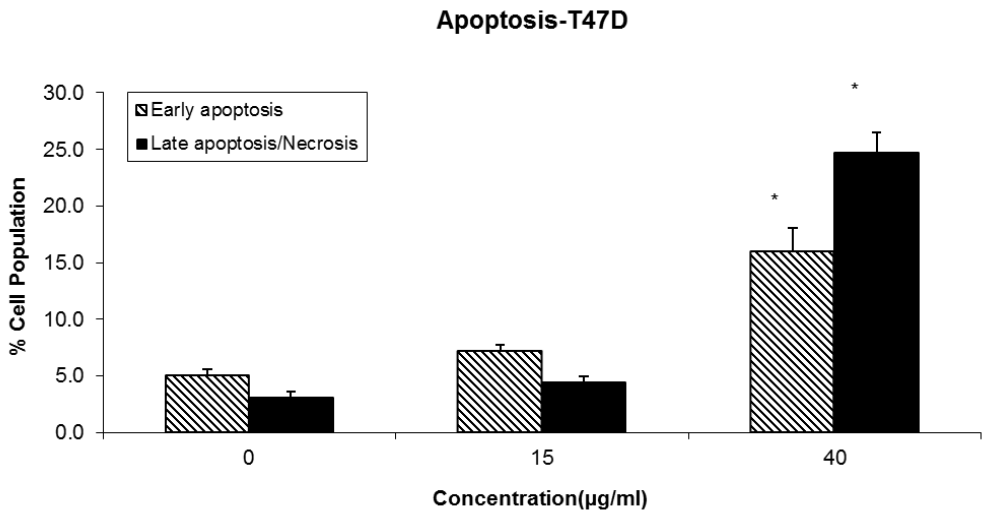

Figure 3.7: Apoptotic effect of *Heteractis magnifica* on T47D cells determined by annexin V-conjugated PI staining through flow cytometry

Notes: Data were obtained from 20,000 events and early apoptotic cells (annexin positive) and late apoptotic cells (annexin positive/PI positive, including necrotic cells) are presented as a percentage of total cells analysed. The values are shown as means ± SEM. Treatments significantly different from the untreated control at $p < 0.05$ are presented as *.

3.3.4 *H. magnifica* venom increases the activation of caspases

Treatment of T47D and MCF7 cells with venom at 30 µg/ml and 40 µg/ml for 24h significantly increased the activation of caspases, via caspases-8, -9 and -3 (see Figures 3.8 and 3.9). Caspase-3 increased significantly at 15 µg/ml of *H. magnifica*, venom; however, caspase-8 and -9 did not increase significantly until the dose reached 30 µg/ml and 40 µg/ml, respectively.

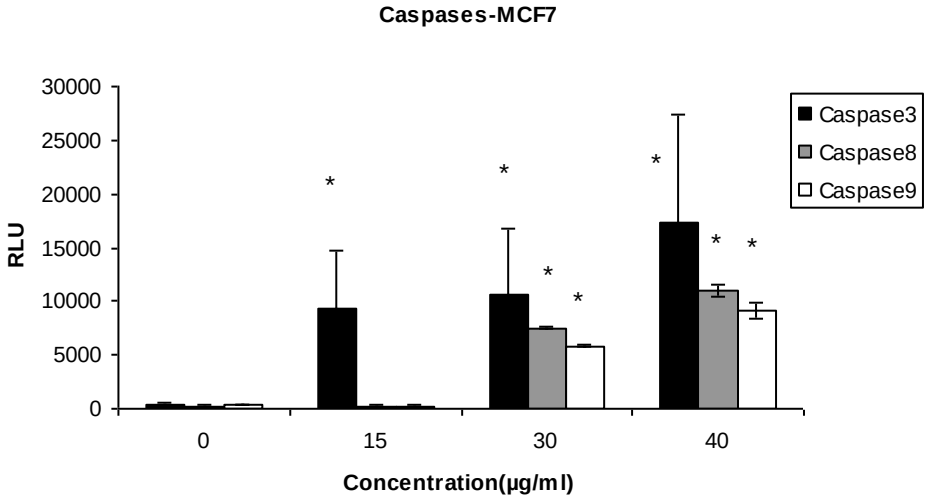

Figure 3.8: Caspase activities determined using a luminescent kit on MCF7 cells after 24h treatment with *Heteractis magnifica*

Notes: Data are presented as relative luminescence units (RLUs). The values are shown as means ± SEM of three independent experiments. Treatments significantly different from the untreated control at $p < 0.05$ are presented as *.

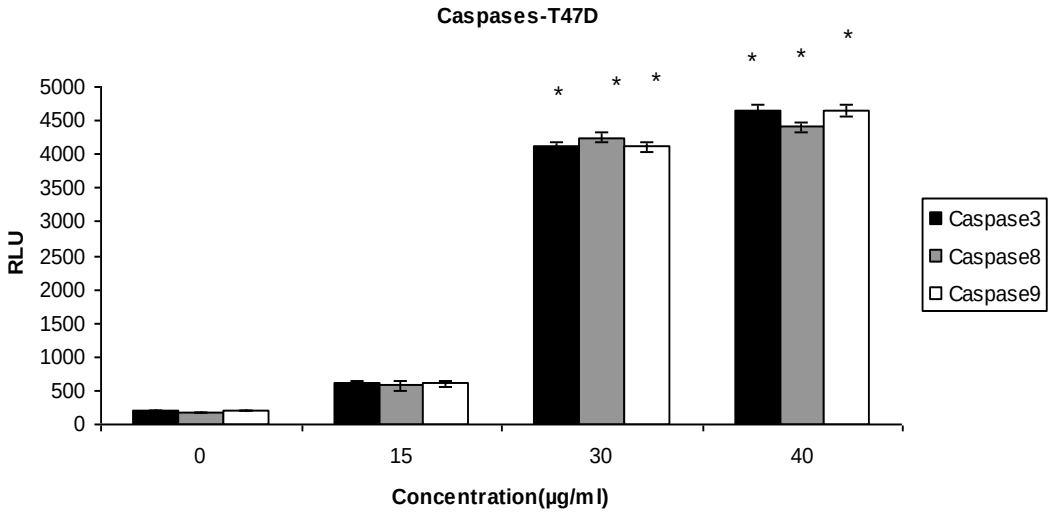

Figure 3.9: Caspase activities determined using a luminescent kit for T47D cells after 24h treatment with *Heteractis magnifica* venom

Notes: Data are presented as relative luminescence units (RLUs). The values are shown for relative luminescence units as means ± SEM for independent experiments. Treatments significantly different from the untreated control at $p < 0.05$ are presented as *.

3.3.5 *H. magnifica* venom increases mitochondrial membrane permeability

Increases in mitochondrial membrane potential (Δψ) were observed for both cell lines. Treatment of T47D and MCF7 cells with 40 µg/ml of venom significantly increased the percentage of cells positive for JC-1 monomers from 4% in untreated cells to 53% and 37.5%, respectively (Figure 3.10).

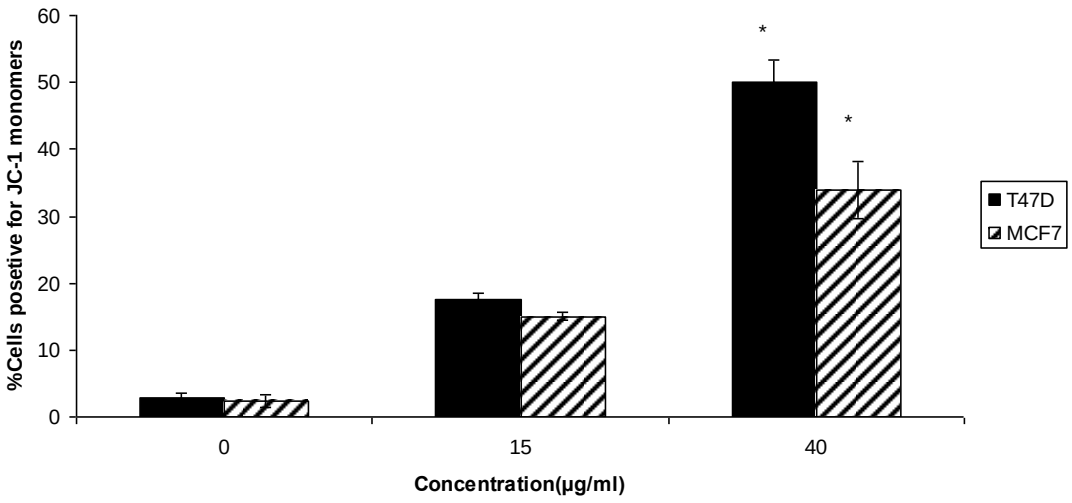

Figure 3.10: Loss of mitochondrial membrane potential indicated by JC-1 dye using flow cytometry after 24h treatment with venom from *Heteractis magnifica*

Notes: Data were obtained from 20,000 events and presented as a percentage of cells positive for JC-1 monomer. The values are shown as means ± SEM from independent experiments. Treatments significantly different from the untreated control at $p < 0.05$ are presented as *.

3.4 Discussion

One of the most ancient marine animals possessing a variety of peptide and protein toxins for chemical defence is the sea anemone. Chemical defence toxins are currently being investigated for biomedical applications including designing novel drugs for human therapeutics (Tejuca et al., 2009, Honma and Shiomi, 2006).

The potential cytotoxic effect of *H. magnifica* on human cancer cells and the underlying mechanism for this effect have not been investigated or elucidated. In this study, the venom from the sea anemone, *H. magnifica*, was highly effective in killing the breast cancer T47D and MCF7 cell lines in a dose-dependent manner.

In the crystal violet assay, the treatment of T47D and MCF7 cell lines with 15 µg/ml of venom for 24h detected more than a 90% reduction in the number of adherent cells. Interestingly, identical concentrations of venom exerted less effect on the 184B5 human non-cancer breast cells. This cell line showed only a 50% reduction in the number of viable adherent cells after treatment for 24h with 15 µg/ml of venom. The difference in sensitivity was supported by higher IC_{50} values of 14.70 µg/ml for 184B5 cell lines, compared to 9.26 µg/ml for MCF7 cell lines and 5.67 µg/ml for T47D cell lines after 24h treatment. These findings from the crystal violet assay assessment are encouraging because they support the potential for the development of therapeutics from this venom. The venom could be used at doses which had less effect on non-cancer cells than on the targeted cancer cells. However, when using the MTT assay, a significant reduction in relative viability as an endpoint based on metabolism was found at venom doses of 20 µg/ml or higher for T47D, MCF7 and 184B5 cells. Different mechanisms of the assays may underlie these differences between the MTT and crystal violet results (Mickuviene et al., 2004).

Control of the cell cycle progression of cancer cells is an effective strategy for cancer therapy because deregulated cell cycle control is a fundamental aspect of cancer for many common malignancies (Senderowicz, 2003). Analysis of the cell cycle phase distribution of treated human breast cell lines T47D and MCF7 revealed that proliferation inhibition by *H. magnifica* venom involved cell cycle arrest. The treatment with *H. magnifica* venom induced the accumulation of a sub-G1 population with a concomitant decrease in the G1 phase, indicating induction

of apoptosis. In T47D and MCF7 cells, venom treatment led to the accumulation of 11% and 8% in the sub-G1 phase, respectively, with a corresponding decrease in the percentage of the G1 phase fraction as compared with the control untreated cells.

Apoptosis plays a crucial role in defence against cancer and the induction of this process is one mechanism by which chemotherapeutic agents can kill cancer cells (Campbell et al., 2007). At least two broad pathways lead to apoptosis: the death receptor pathway (extrinsic) and the mitochondrial pathway (intrinsic). The extrinsic pathway is triggered by the binding of death-inducing ligands to cell surface receptors, which results in the activation of caspase-8 (Kettleworth, 2007). The intrinsic pathway, in contrast, is triggered by cytotoxic stresses, which converge in the mitochondria, leading to the release of several mitochondrial inter-membrane space proteins, such as cytochrome *c*, which associate with apoptosis protease-activating factor 1 (Apaf-1) and pro-caspase-9 to form an apoptosome (Elmore, 2007). Consistent with this, the investigation of the apoptotic effect of *H. magnifica* venom showed that both T47D and MCF7 cell lines underwent significant induction of apoptosis as evidenced by increases in mitochondrial potential.

Related to the current study, RTX-A toxin from the closely related anemone species, *H. crispa*, induces apoptosis in a malignant transformation model of mouse JB6P^{+}CI41 cells (Fedorov et al., 2010). The RTX-A toxin (*H. crispa*) induces P53 independent apoptosis and inhibits the activation of the oncogenic AP-1 and NF-KB nuclear transcriptional factors (Fedorov et al., 2010). The

intrinsic and extrinsic apoptosis pathways converge with the activation of caspase-3 and, subsequently, with other executioner caspases and nucleases that drive the terminal events of programmed cell death (Elmore, 2007, MacFarlane, 2003a, Crow et al., 2004, Pizon et al., 2011a, Prunell et al., 2005). Activated initiator caspases can cleave and activate effector caspases, such as caspase-3 which, in turn, cleave a variety of cellular substrates (Chandler et al., 1998). *Heteractis magnifica* venom dramatically increased the levels of caspase-8, cleaved caspase-9 and activated caspase-3 as detected by ELISA assays. This implies the induced release of cytochrome *c* from mitochondria into the cytosol. Also demonstrated was the enhanced permeability of the outer mitochondrial membranes. The breakdown of mitochondrial membrane potential ($\Delta\psi$), in turn, leads to the release of cytochrome *c* from the mitochondria and the activation of caspase cascades that result in cell death (Kroemer, 2003, Crompton, 2000, Malhi et al., 2010, Wang et al., 2005). The current study is believed to be the first of its kind for breast cancer cells that has demonstrated that *H. magnifica* venom induces apoptosis through the activation of caspases.

This could be via both death receptor-mediated and mitochondria-mediated apoptotic pathways. Another possibility is that the extrinsic pathway could activate the intrinsic pathway via caspase-8, and that caspase-8 could also be activated by caspase-9. Significant increases in the three caspases tested were observed for MCF7 and T47D cell lines, with the T47D cell line exhibiting the greater response. The difference in the magnitude of response of the two cell lines was perhaps from inherent phenotypic differences due to the different genetic

background of each cell line. Biological issues, such as the monoclonal nature, the absence of tumour stroma and technical factors, such as culture adaptation, limit direct comparison with *in vivo* tumours. Improved genetic and epigenetic characterisation of a set of cell lines from the same type of cancer will help in choosing the best research tool.

In summary, this study has found that *H. magnifica* venom significantly kills breast cancer cells in a dose-dependent manner. This was associated with induced apoptosis in T47D and MCF7 human breast cancer cell lines, with this effect mediated by the activation of caspases and increasing permeability of the outer mitochondrial membranes.

CHAPTER 4: *HETERACTIS MAGNIFICA* VENOM INDUCES APOPTOSIS IN A LUNG CANCER CELL LINE THROUGH ACTIVATION OF A MITOCHONDRIA-MEDIATED PATHWAY

4.1 Introduction

Marine animals are amongst the most venomous species on earth and the Cnidarians, in particular, are well known for the potency of their stings. Sea anemones are one of the most ancient predatory animals on the earth and the venom is known to contain a variety of active compounds that affect voltage gated Na^+ and K^+ channels, pore-forming toxins (actinoporins) and protease inhibitors (Bosmans and Tytgatb, 2007, Standkera et al., 2006). Sea anemone venom has cytolytic activities (Anderluh and Macˇek, 2002); haemolytic activities (Lanioa et al., 2001a, Uechi et al., 2005b); and immunomodulating activities (Pento et al., 2011b, Tytgat and Bosmans, 2007a). Some studies have also addressed the anti-carcinogenic effects of sea anemone venom (Chapter 3) (Marino et al., 2004, Ramezanpour et al., 2012b). However, the molecular mechanisms involved in the effect of sea anemone venom on cancer cells have not been elucidated.

Non-small cell lung cancers (NSCLC) are the major histological type of lung cancer and are divided further into adenocarcinoma, squamous cell carcinoma (SCC) and large cell carcinoma histologies. Non-small cell lung cancer (NSCLC) accounts for approximately 85% of all lung cancers (Mitsudomi et al., 2005, Ray et al., 2010). Apoptosis is a fundamental cellular event during development and is a hallmark of cancer (Figure 4.1). It is an important phenomenon in cytotoxicity induced by anti-cancer drugs (Kim et al., 2002, Hanahan and Weinberg, 2011d). Yet little work has been conducted on the role of apoptosis in lung cancer (Shivapurkar et al., 2003, Fine et al., 2000). Therefore, continued research into the

underlying mechanisms of the action of the sea anemone venom is necessary to further understand cancer treatment with this bioactive natural compound.

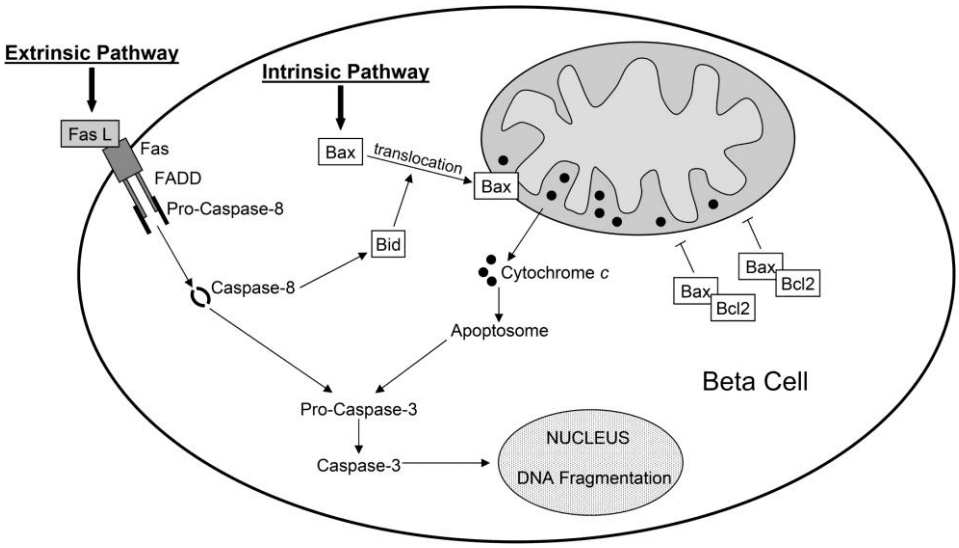

Figure 4.1: Extrinsic and intrinsic pathways of apoptosis

Note: The schematic diagram outlines key signalling molecules involved in the extrinsic (death receptor) and intrinsic (mitochondrial) apoptosis pathways (Bruin et al., 2008).

The principal aims of this study were to:

1) To investigate the cytotoxic effects of *H. magnifica* venom on the human lung A549 cancer cell line and the normal human breast 184B5 cell line by using MTT and crystal violet assays.

2) To determine how *H. magnifica* venom kills lung cancer cells and to examine the mechanisms involved in this effect.

4.2 Materials and Methods

4.2.1 Materials

All the reagents used in this chapter were from Sigma-Aldrich unless otherwise noted.

4.2.2 Sea anemone venom

The lyophylized crude extract from *H. magnifica* was disolvedat 100 mg/ml with distilled water. The concentration of total protein in the crude extracts of *H. magnifica* was adjusted to 400 μg/ml. All the various concentrations of crude extract were made up in distilled water.

4.2.3 Human cell culture

The human adherent lung cancer A549 cell line and human non-cancer lung cell line MRC5 were obtained from the American Type Culture Collection (subsection 2.2.4.2).

4.2.4 Cell proliferation assay

To assess the cytotoxicity effects of crude extracts, two colorimetric bioassays, namely, MTT and crystal violet assays were used. These methods were described in detail in subsection 2.2.5.

4.2.5 Cell cycle analysis

Cell cycle distribution was evaluated by flow cytometry. For details of this method, refer to subsection 3.2.5.

4.2.6 Apoptosis assessed by flow cytometry

Apoptosis induced by venom from *H. magnifica* in A549 cells was analysed by flow cytometry using an annexin V-FITC apoptosis detection kit. For details of this method, refer to subsection 3.2.6.

4.2.7 Caspase 3/7 assay

The activation of caspase 3/7 was analysed using a caspase Glo3/7 assay kit from Promega. For detail of this method, refer to subsection 3.2.7.

4.2.8 Mitochondrial membrane potential

Mitochondrial membrane potential ($\Delta\Psi$) was determined by JC-1, a cationic and lipophilic dye, using an Accuri C6 flow cytometer. For details of this method, refer to subsection 3.2.8.

4.2.9 Statistical analysis

Data are presented as the mean ± SEM (standard error of mean). The experiments were replicated at least three independent times. The IC_{50} calculation was determined using GraphPad Prism V. 5.02 for Windows (GraphPad Software, San Diego, California, USA). Statistical analysis of the data was carried out using ANOVA, followed by Tukey's HSD post hoc test. These tests were performed

using SPSS software (Version 18). Differences were considered significant when the *p*-value was less than 0.05. In addition, the response of the lung cancer A549 cell line in the assays was compared to that of the non-cancer control MRC5 cell line. Differences in the viability-dose response curves were estimated by comparing the area under the curve (AUC) for the test and reference cell lines, using the individual replicate (n = 3) data.

4.3 Results

4.3.1 *H. magnifica* venom reduces the survival of A549 cell line

Initially, the effect of *H. magnifica* venom on the survival of A549 and MRC5 cells cultured with different concentrations of venom (5–40 µg/ml) for 24h was determined by MTT assay. In A549 cells, venom decreased the survival of cells in a dose-dependent fashion. There was greater than 90% reduction in cell survival after 24h treatment with 25 µg/ml of crude venom (Figure 4.2). *Heteractis magnifica* venom also inhibited the growth of MRC5 cells; however, the degree of inhibition was less than was observed for the A549 cells (Figure 4.2), as evidenced by higher IC_{50} values of 18.17 µg/ml on the human lung normal MRC5 cell line compared to 11.14 µg/ml on the A549 cell line.

Cytotoxicity induced by treatment was also measured by crystal violet assay. The treatment significantly decreased cell numbers of both cell lines. A significant reduction in cell numbers was observed for doses of 20 µg/ml and higher for 24h

which decreased to approximately 40% ($p < 0.05$) (Figure 4.3). The treatment showed quite similar toxicity on both cell lines as evidenced by similar IC_{50} values on the human lung normal cell line (24.28 µg/ml) and the lung cancer cell line (22.91 µg/ml). Also, no differences in the AUC of the dose response curves (ΔAUC) between the A549 cell line and the reference cell line 184B5 were shown by either the MTT assay or the crystal violet assay, using the R package PK (Jaki and Wolfsegge, 2011) (Table 4.1).

Table 4.1: *p*-values of lung cancer (A549) cell line compared to the relevant control (MRC5)

Tissue	Lung cancer cell line	Lung normal cell line	CSV ΔAUC *p*-value	MTT ΔAUC *p*-value
Lung	A549	MRC5	0.39	0.63

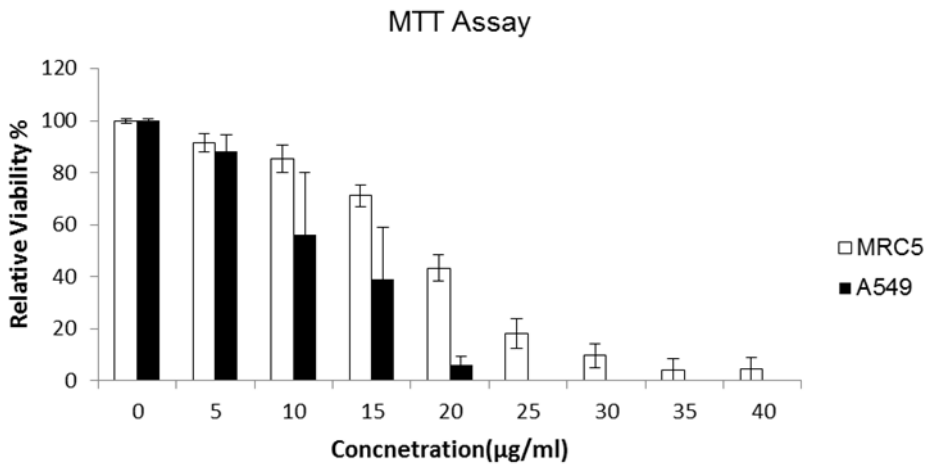

Figure 4.2: Relative viability as determined by MTT assay after 24h treatment of A549 and MRC5 cells with increasing concentrations of venom from *Heteractis magnifica*

Notes: Cell viability was calculated relative to the untreated media (0 µg/ml) control. The values are shown as means ± SEM, n = 3. Doses of 15 µg/ml or greater significantly killed the A549 cell line compared to the 0 µg/ml control ($p < 0.05$).

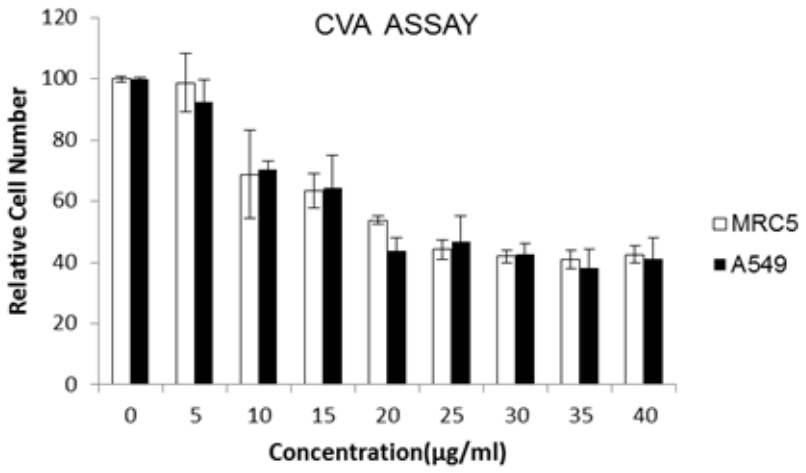

Figure 4.3: Cell viability percentage of A549 and MRC5 cells estimated by crystal violet assay

Notes: In 96-well plates following 24h exposure to *H. magnifica* venom extract. Data are shown as the relative surviving cell numbers as a percentage compared to the untreated control (0 µg/ml) and are presented as the mean ± SEM of three separate trials. Doses of 20 µg/ml or greater significantly killed the A549 cell line compared to the 0 µg/ml control ($p < 0.05$).

4.3.2 *H. magnifica* venom arrests cell cycle progression in A549 cell line

The inhibitory effect of *H. magnifica* venom on the viable number of A549 cells involves perturbation of the cell cycle progression, as indicated by changes in the cellular DNA content distribution detected by flow cytometric analysis. Significant differences ($p < 0.05$) were found in the proportions of cells in the G0/G1 and S phases between treated and untreated cells. Increasing venom concentrations in the A549 cell line increased the proportion of cells in the G0/G1 phases and decreased the proportion in the S phase. This implies that treating

cancer cells with venom would prevent them from entering the DNA synthesis phase (Figure 4.4).

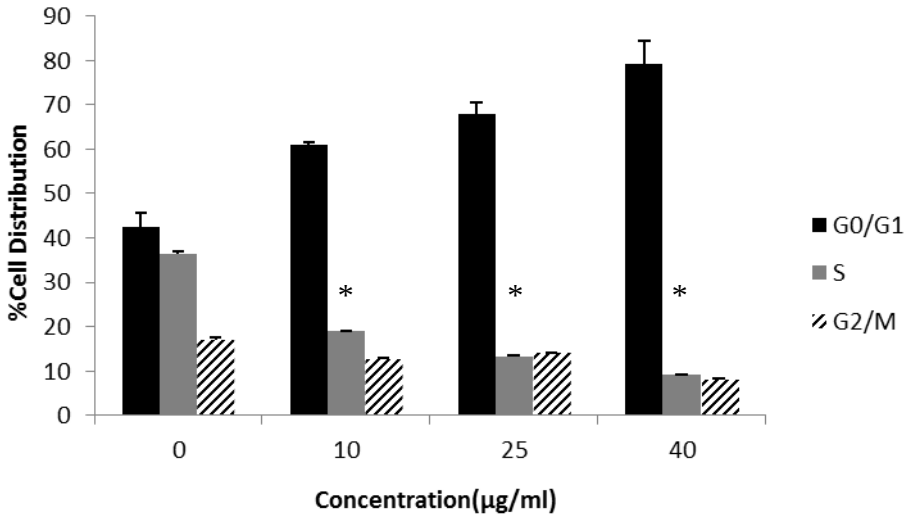

Figure 4.4: Effect of *Heteractis magnifica* venom on cell cycle progression determined by PI staining followed by analysis of DNA content by flow cytometry

Notes: Data were obtained from 20,000 events and are presented as a percentage of cells in the sub-G0/G1, S and G2/M phases. The values are shown as means ± SEM. Treatments significantly different from the untreated control at $p < 0.05$ are presented as *.

4.3.3 *H. magnifica* venom induces apoptosis of A549 cells

To determine whether the decrease in cell viability involved apoptosis, A549 and MRC5 cell lines were stained with FITC-conjugated annexin V and PI and analysed by flow cytometry. In A549 cells, the level of induction of apoptosis after 24hrs treatment with *H. magnifica* venom (40 µg/ml) was significant ($p < 0.05$). The highest concentration of venom (40 µg/ml) induced 32.2% and 32.3% of early and late apoptosis, respectively, compared to 5% early apoptosis in untreated cells ($p < 0.05$) (Figure 4.5a). In contrast to this, no increase in the

proportion of cells undergoing early apoptotic cell death was observed for MRC5 cells: instead, cells appeared to be dying by necrosis (Figure 4.5b).

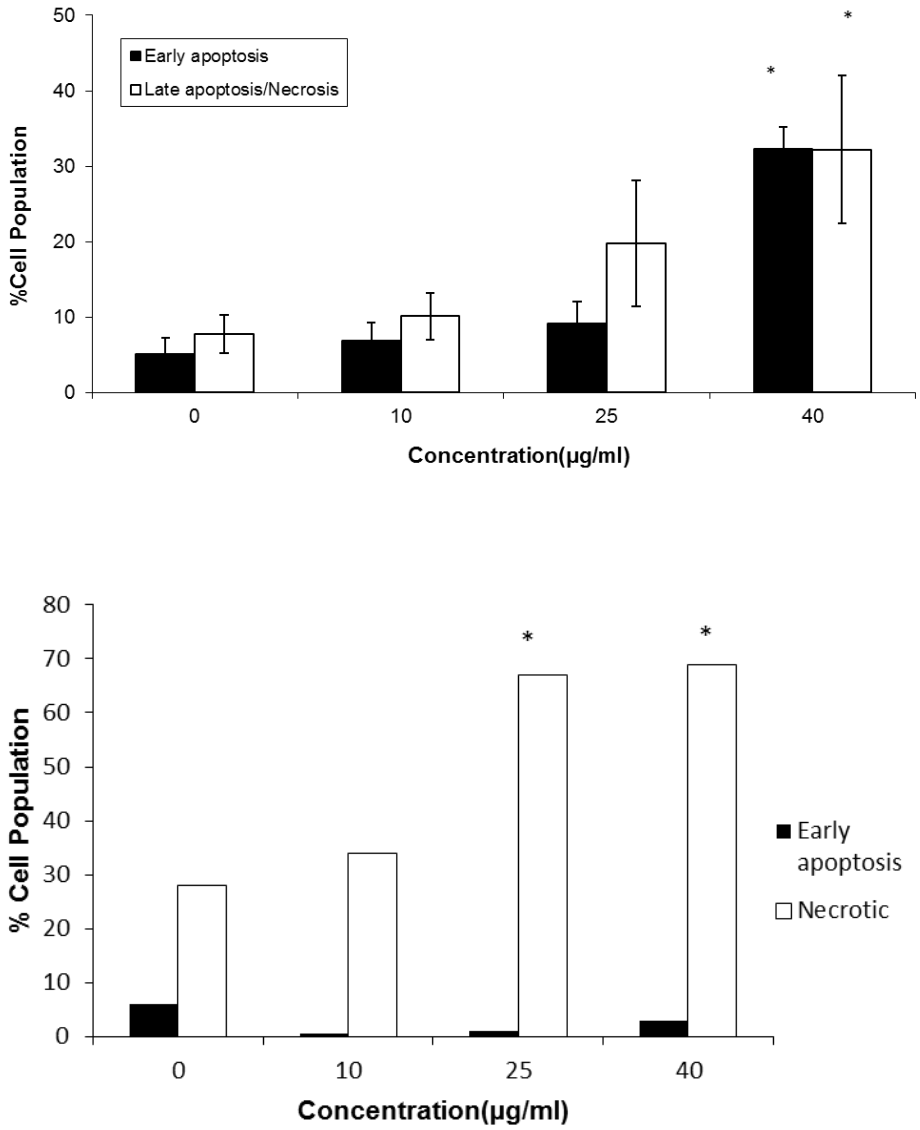

Figure 4.5: Effect of *Heteractis magnifica* venom on apoptosis in a)A549 and b)MRC5 cell lines

Notes: Data as determined by annexin V-conjugated PI staining followed by flow cytometry. Data were obtained from 10,000 events for a percentage of the cell population. Early = early apoptotic cells (annexin positive); late = necrotic and late apoptotic cells (annexin positive/PI positive). * = significantly different from the untreated control at $p < 0.05$.

4.3.4 *H. magnifica* venom increases the activation of caspases

It was found that apoptotic cell death is mediated by the activation of caspases. The involvement of caspases in the action of *H. magnifica* venom was assessed through the activity of executioner caspase 3/7. Treatment of A549 cells with venom from *H. magnifica* at 10–40 µg/ml for 24h resulted in significant increases in caspase 3/7 activities relative to that of untreated cells (Figure 4.6).

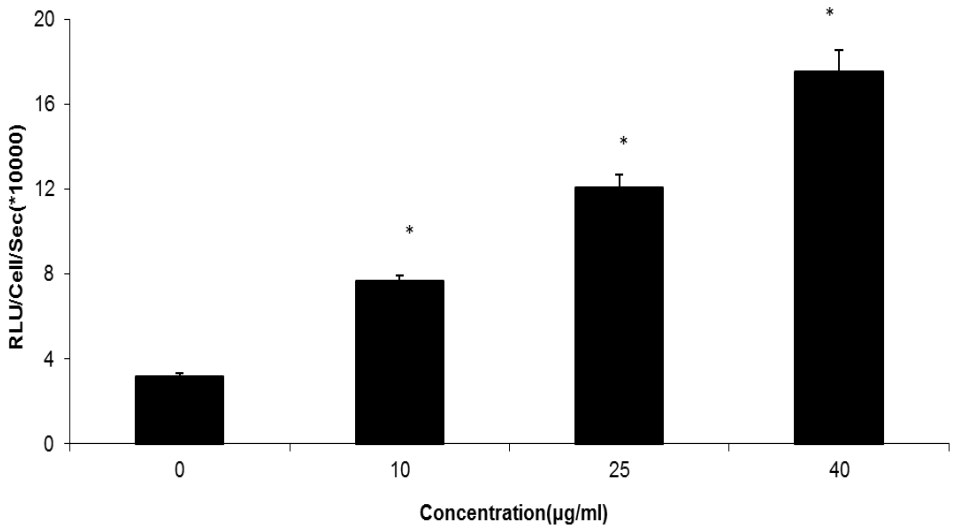

Figure 4.6: Caspase activity determined for A549 cells after 24h treatment with venom from *Heteractis magnifica* using a luminescent kit

Notes: Data are presented as relative luminescence unit (RLU) cells/s (10^4). Values are shown as means ± SEM of three independent experiments. * = significantly different from the untreated control at $p < 0.05$.

4.3.5 *H. magnifica* venom increases mitochondrial membrane potential

To further assess the effects of *H. magnifica* venom on the mitochondrial apoptotic pathway, the mitochondrial membrane potential (Δψ) in A549 cells treated with different concentrations of the venom was measured using JC-1 fluorescence. Treatment of A549 cells with 10, 25 and 40 µg/ml of *H. magnifica* venom significantly increased the percentage of cells positive for JC-1 monomers from 2.8% in untreated cells to 16.8%, 20.7% and 65.3%, respectively (Figure 4.7).

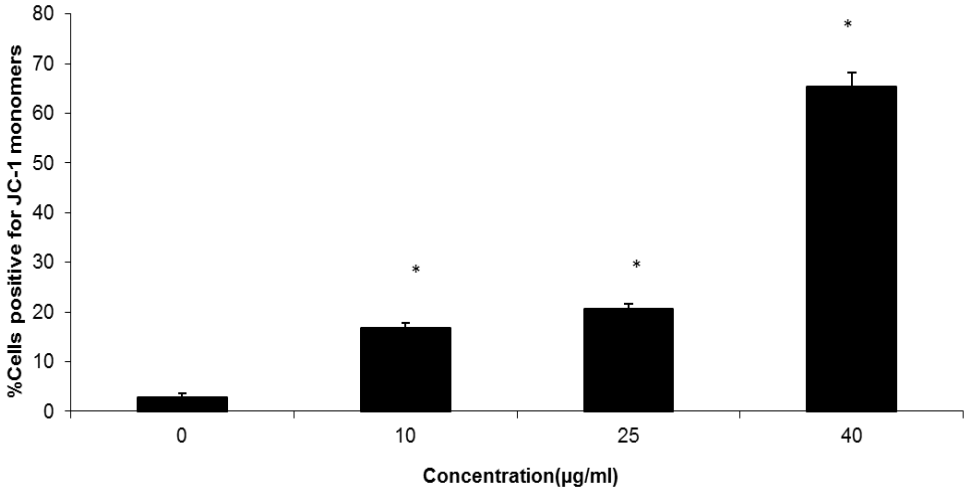

Figure 4.7: Loss of mitochondrial membrane potential examined by JC-1 dye using flow cytometry after 24h treatment with *Heteractis magnifica* venom

Notes: The values are shown as means ± SEM of three independent experiments. * = significantly different from the untreated control at $p < 0.05$.

4.4 Discussion

The current study demonstrates that toxins found in *H. magnifica* venom induce apoptosis in a human lung cancer cell line A549. In the MTT assay, the treatment of the A549 cell line with 20 µg/ml of venom for 24h resulted in a less than 10% survival rate. In contrast, an identical concentration of venom exerted less effect on the survival of MRC5 human non-cancer lung cells which exhibited 50% cell survival. However, there was no significant difference between the human cancer A549 cell line with IC_{50} values of 11.14 µg/ml and 18.17 µg/ml for the human non-cancer lung MRC5 cell line. In addition, in the crystal violet assay, the treatment showed quite similar toxicity on both cell lines. A zoanthoxanthin alkaloid from zoanthid corals, *Epizoanthus* sp., was shown to be cytotoxic *in vitro* against A549 human lung carcinoma by IC_{50} values of 2.38 µg/mL (Jiménez and Crews, 1993). The other study showed that six acetylenic compounds isolated from the stony coral, *Montipora* sp., did not show any cytotoxicity against A549 human lung cancer cells (Bae et al., 2000). The addition of *H. magnifica* venom to A549 cancer cells delayed progression through the cell cycle with a marked reduction in the number of cells in the S phase and an associated accumulation of cells in the G0/G1 phases. Control of the progression of the cell cycle of cancer cells is an effective strategy for cancer therapy because deregulated cell cycle control is a fundamental aspect of cancer for many common malignancies (Senderowicz, 2003).

Heteractis magnifica venom also induced apoptosis in a dose-dependent manner in A549 cells. The inhibition of apoptosis, a universal and efficient cellular

suicide pathway, is one of the hallmark characteristics of cancer (Elmore, 2007). At least two broad pathways lead to apoptosis (Campbell et al., 2007): firstly, the death receptor pathway initiated mainly by tumour necrosis factor receptors (TNFRs) and, secondly, the mitochondrial pathway which involves mitochondria and Bcl-2 family members (Kroemer, 2003). Although a number of manuscripts have been published on the topic of apoptosis, each year, fewer of these appear on apoptosis in the lung than on apoptosis in other major organs (Fine et al., 2000, Shivapurkar et al., 2003). Lung cancer is particularly resistant to the induction of apoptosis. This is probably due to the prevalence of elevated Bc1-2 protein expression in lung cancer which can block apoptosis. The Bcl-2 protein can block apoptosis by most chemotherapeutic agents (Shivapurkar et al., 2003). The current study's findings demonstrated that the proportion of early apoptotic (annexin V-positive/PI-negative) cells increased in A549 cells in a dose-dependent manner for cell populations treated for 24h with *H. magnifica* venom. Indeed, the proportion of early apoptotic cell numbers increased dose dependently to reach significance following treatment with 40 µg/ml of the venom in comparison to the untreated 0 µg/ml control. In contrast, for MRC5 non-cancer origin lung cells, following venom treatment, a decrease was found in the proportion of early apoptotic cells relative to the untreated control.

Effector caspases, including caspase 3/7, activate deoxyribonuclease (DNase) resulting in the fragmentation of DNA in response to various apoptotic stimuli (Pizon et al., 2011b, MacFarlane, 2003b). Caspase 3/7 is an important apoptosis protein that is activated initially in both the death receptor and the mitochondrial pathways (Kominsky et al., 2002). In the current study, activation was

investigated to identify the pathway of apoptosis in the A549 cell line in response to *H. magnifica* venom. The apoptotic effects involving caspase 3/7 were found to have increased following treatment with all doses of venom tested.

Mitochondrial dysfunction is another key event of apoptosis. An important parameter of mitochondrial dysfunction is the loss of mitochondrial membrane potential ($\Delta\psi$)(Crompton, 2000). Loss of DWm is lethal to cells because they become bioenergetically deficient (Kroemer, 2003). Breakdown of $\Delta\psi$, in turn, leads to cytochrome *c* binding to apoptosis protease-activating factor 1 (Apaf-1) and inactive pro-caspase-9 to form an apoptosome. This results in activation of caspase-9, triggering the subsequent cleavage of caspase-3 and -7 (Fan et al., 2005 , Tsujimoto and Shimizu, 2007). Treatment of A549 cells with the venom induced cleavage of caspase 3/7, and increased mitochondrial membrane permeability. The loss of $\Delta\psi$ following treatment of A549 cells was significant at all doses of venom tested.

In summary, our results revealed that *H. magnifica* venom displays potent cytotoxic activity against non-small cell lung carcinoma (NSCLC) A549 cells. In addition, the venom induced cell cycle arrest in the lung cancer cell line. Cell death induced by venom from *H. magnifica* was mediated by the activation of caspases and the mitochondrial membrane pathways.

CHAPTER 5: ISOLATION AND CHARACTERISATION OF A BIOACTIVE COMPOUND FROM *HETERACTIS MAGNIFICA*

5.1 Introduction

The world's oceans, covering more than 70% of the earth's surface, represent an enormous resource for natural products, including the discovery of potential chemotherapeutic agents (Cragg and Newman, 2013). These natural products have been produced during millions of years of evolution in response to a very competitive environment. These marine origin compounds are very promising for biomedical research in designing very specific and potent new pharmaceuticals (Aneiros and Garateix, 2004). Among marine organisms, the sea anemones are considered to be a rich source of bioactive substances (Lagos et al., 2001). In addition, compared to other Cnidarians (typically jellyfish toxins), sea anemone toxins are more stable (Honma and Shiomi, 2006).

A number of toxins have been isolated from various species of sea anemones and are characterised. The lists of peptide toxins isolated from Cnidarian organisms were presented in Chapter 1 (Table 1.6) (Botana, 2014). Toxins from sea anemones have been identified as having cytolytic activities (Anderluh and Maček, 2002); haemolytic activities (Lanioa et al., 2001; Uechi et al., 2005); and immunomodulating activities (Pentón et al., 2011; Tytgat and Bosmans, 2007).

Heteractis magnifica, belonging to the family Stichodactylidae, is the second largest in size of all sea anemones (Yamaguchi et al., 2010b). *Heteractis magnifica* is found only in the marine waters of South East Asia and northern Australia (Fautin and Allen 1994). The relatively few biological studies conducted on this sea anemone have focused on the haemolytic activity and neurotoxic activity of *H. magnifica* venom (Khoo et al., 1995, Khoo et al., 1993). The crude

extract of *H. magnifica* venom, potentially responsible for exhibiting cytotoxic activity, was first determined in Chapter 2 (Ramezanpour et al., 2012b). The mechanisms of action underlying the cytotoxicity of the venom were studied on breast cancer cells (Chapter 3) (Ramezanpour et al., 2014a) and lung cell lines (Ramezanpour et al., 2014b) (Chapter 4). These cancers were chosen for these studies because the most commonly diagnosed cancers worldwide were those of the lung (1.8 million, 13.0% of the total) and breast (1.7 million, 11.9%) (Maxwell, 2001).

The novel study summarised in this chapter focused on the isolation and purification of the bioactive compound from the venom of the sea anenome, *H. magnifica*. The peptide were analysed by mass spectrometry and identified by amino acid sequencing, then matched to the SWISS PROT database. The recombinant protein was produced in the *Escherichia coli* (*E. coli*) expression system. Investigation was undertaken of the cytotoxic anti-cancer effects of the individual bioactive compound from the purified fraction.

Therefore, the aims of this study were to isolate and purify the bioactive compound from the crude venom extract of the sea anemone, *H. magnifica*; to produce recombinant peptide; and to provide sufficient material for functional investigations. In addition, the study aimed to determine the cytotoxicity of the bioactive compound using the MTT cell viability assay on human breast cancer (T47D and MCF7) cell lines and on a non-cancer (184B5) cell line. Furthermore, the study aimed to determine the cytotoxicity of the bioactive compound using the MTT cell viability assay on a human lung cancer (A549) cell line and a non-cancer (MRC5) cell line.

5.2 Materials and Methods

5.2.1 Reagents

Sephadex G-50 (fine powder) FPLC (fast protein liquid chromatography) columns (Superdex 200, 16/60 HiLoad column) were purchased from Pharmacia Biotech (Sweden). The restriction enzymes, plasmid and vector were kindly provided by Dr Shiwani Sharma (Ophthalmology, Flinders University). The TRIzol reagent was from Invitrogen (Carlsbad, California, USA) and the HiTrap column was from GE Healthcare. The reagent isopropyl β-D-1-thiogalactopyranoside (IPTG) (I6758-1G) was purchased from Sigma.

5.2.2 Sea anemone venom

Venom from one *H. magnifica* of a large size were frozen immediately, freeze-dried using a bench-top lyophilizer (VirTis, USA) and ground into a fine powder. Samples were re-solvated at 100 mg/ml with distilled water. The concentration of total protein in the crude extracts of *H. magnifica* was adjusted to 400 μg/ml. All of the various concentrations of crude extract were made up in distilled water.

5.2.3 Human cell culture

Human adherent breast cancer cells T47D (ductal carcinoma, an endogenously expressing mutant p53 cell line) and MCF7 (adenocarcinoma, a p53 wild type cell line), as well as 184B5 cells (a human breast epithelial cell line), A549 cancer cells (a human lung adenocarcinoma epithelial cell line) and MRC5 cells (a

human lung fibroblast cell line) were obtained from the American Type Culture Collection (subsection 2.2.4).

5.2.4 Gel filtration chromatography

The dried crude extract was resuspended in Milli-Q water and filtered through a 0.2 µm syringe filter. The fractions were then chromatographed by FPLC (Amersham Pharmacia, Sweden) on a HiLoad 16/60 Superdex 200 gel filtration column equilibrated in buffer (50 millimolar [mM] ammonium acetate and 150 mM sodium chloride). The chromatography was performed at a flow rate of 0.5 ml/min and 1.5 ml fractions were collected.

5.2.5 Cell viability assays

Cytotoxicity of each fraction was monitored by MTT (subsection 2.2.5.2) and crystal violet assays (subsection 2.2.5.1).

5.2.6 Protein analysis

Protein purity of any fraction that showed cytotoxic effect was assessed using TGX Any kD Stain-Free™ precast gel (567-8123, Bio-Rad, USA). The gel was stained with silver stain to visualize the protein.

5.2.7 Mass spectrometry

The relevant band of the gel (Section 5.2.6) was cut out and identified by mass spectrometry analysis. The molecular weight of the separated fraction (Peak A) was determined using a Thermo Orbitrap XL linear ion trap mass spectrometer

fitted with a nanospray source (Thermo Electron, San Jose, California, USA) and the Dionex UltiMate® 3000 high-performance liquid chromatography (HPLC) system (Dionex). Tandem mass spectrometry (MS/MS) analysis was performed according to the target mass range. Acylation patterns were determined by the difference between the detected molecular mass and the molecular mass that was calculated from SDS-PAGE (sodium dodecyl sulphate polyacrylamide gel electrophoresis).

5.2.8 Isolation of RNA and reverse transcription

Total RNA (ribonucleic acid) was extracted from the intact tentacle of the sea anemone *H. magnifica* using the TRIzol reagent (Invitrogen, Carlsbad, California, USA) as directed by the manufacturer's protocol. After ascertaining the quality of the RNA preparation by electrophoresis in a denaturing agarose-formaldehyde gel, 1 µg of total RNA was mixed with the reverse transcription reagents in a reaction volume of 20 µl (Table 5.1). The complementary DNA (cDNA) was then amplified by the degenerate primer: 5'-CAT ATA TGG ATC CTT CTA CTT CGA TTC AGA GAC TGG A-3' and the polymerase chain reaction (PCR) anchor primer, followed by re-amplification of the primary PCR products using the degenerate primer: 5'-GGT GGT GCT CGA GTC GCC CTG CAT ATA GCT CGG CAT G-3'.The primer was designed from previously published research on *H.crispa* anemone (APHC1) peptide that matched in BLAST (Basic Local Alignment Search Tool) databases with our mass spectrometry analysis (Andreev et al., 2008a)

Table 5.1: Preparation of reverse transcription

Component	Volume/reaction	Final concentration
10 × RT buffer	2 µl	1 ×
25× dNTP mix (100 mM)	0.8 µl	4 mM
Random primers	2 µl	
Multiscribe reverse transcriptase	1 µl	
RNase inhibitor (10 U/µl)	1 µl	10 U (per 20 µl reaction)
Template RNA	Variable	1 µg (per 20 µl reaction)
RNase free water	Variable to give final volume 20 µl	
Total volume	20 µl	

5.2.9 Rapid amplification of cDNA ends (RACE)

Polymerase chain reaction (PCR) amplifications were performed in a 20 µL volume using a thermal cycler (Axygen MaxyGen, Fisher Biotech, Australia) (Table 5.2). The PCR final concentrations' reactions were 0.4 µL forward primer; 0.4 µL reserved primer; 2 µL 10 × buffer; 0.4 µL dNTPs (deoxynucleotides) (100 mM); 1.2 µL magnesium chloride ($MgCl_2$); 0.1 units Taq DNA polymerase; 11 µL H_2O and 4 µL cDNA.

Table 5.2: Program for reverse PCR amplification carried out in thermal cycler

Conditions	Step 1	Step 2	Step 3	Step 4	Step 5
Temperature (ºC)	95	94	60	72	25
Time (minutes)	100	20	30	30	∞

5.2.10 Cloning and sequencing of polymerase chain reaction (PCR) products

The forward primer 5'-CAT ATA TGG ATC CTT CTA CTT CGA TTC AGA GAC TGG A-3' and reverse primers 5'-GGT GGT GCT CGA GTC GCC CTG CAT ATA GCT CGG CAT G-3' contained *BamHI* and *XhoI* sites, respectively (as underlined), designed from the conserved regions of 56-residue-long polypeptide $APHC_1$ (Swiss-port B2G331). Once the fragment was treated using shrimp alkaline phosphatase, it was ligated with a *BamHI*- and *XhoI*-digested pET32a+ vector. The recombinant plasmid carried a His-tag in the N-terminal that facilitated its purification using a HisTrap affinity column. Recombinant plasmids were used to transform the competent *Escherichia coli* BL21(DE3) provided in the cloning kit (Novagen, 69450-3). The transformed cells were cultured at 37°C in lysogeny broth (LB) medium containing 100 µg/ml ampicillin up to a culture density OD600 ~0.6–0.8. Expression was induced by adding isopropyl β-D-1-thiogalactopyranoside (IPTG) up to 1 mM. The cells were cultured at 37 ^{o}C for 4–8h, harvested and resuspended in the lysis buffer (EDTA-free protease inhibitor cocktail tablet in 2 mL 1 × PBS). The fractions were ultrasonicated and centrifuged at 13,000 rpm for 30 minutes. The supernatant was decanted into a fresh 50 mL tube and was examined on a 1.2% agarose gel.

5.2.11 Nucleotide sequence analysis

To analyse the peptide sequence, the vector and nucleotide sequences were subjected to gene sequencing using the capillary electrophoresis 3130xL genetic analyser (Life Technologies) according to the manufacturer's protocol. The

obtained sequences were translated to amino acid sequences (GenBank: AM933240) and matched in BLAST (Basic Local Alignment Search Tool) databases.

5.2.12 Purification of recombinant

After examining the construct of recombinant protein, the supernatant was applied onto a HiTrap affinity 1 ml column (GE Healthcare, 17-5247-01), which was pre-equilibrated with starting buffer according to the protocol supplied by the manufacturer. The fusion protein was desalted on a buffer exchange column (Sephadex G-50 fine powder) and lyophilized using a bench-top lyophilizer (VirTis, USA). The purity of recombinant protein was verified using SDS–PAGE. Cells were treated with the uninduced sample (without adding IPTG [isopropyl β-D-1-thiogalactopyranoside]), negative control (pET32a+ BL21) and the recombinant protein (*H. magnifica* peptide [HMP]) (pET32a+ BL21 + insert HMP DNA) for 24 hours (24h).

5.2.13 Cell proliferation assay

The effects of the recombinant protein on the growth of human cancer cell lines (A459, MCF7 and T47D) and human non-cancer cell lines (MRC5, 184B5) were determined with the MTT assay as previously described (subsection 2.2.5.2).

5.3 Results

5.3.1 Gel filtration chromatography

The isolation and purification of the bioactive compound from the crude venom extract included several steps. Fractions from the crude venom extract from *H. magnifica* were chromatographed on a gel filtration column (Figure 5.1). Three peaks were identified and arbitrarily denoted A, B and C. Fractions from each of peak A (97–107), peak B (108–117) and peak C (118–125) were collected, pooled into three groups as indicated and lyophilized (VirTis, USA) for further study of cytotoxic activities.

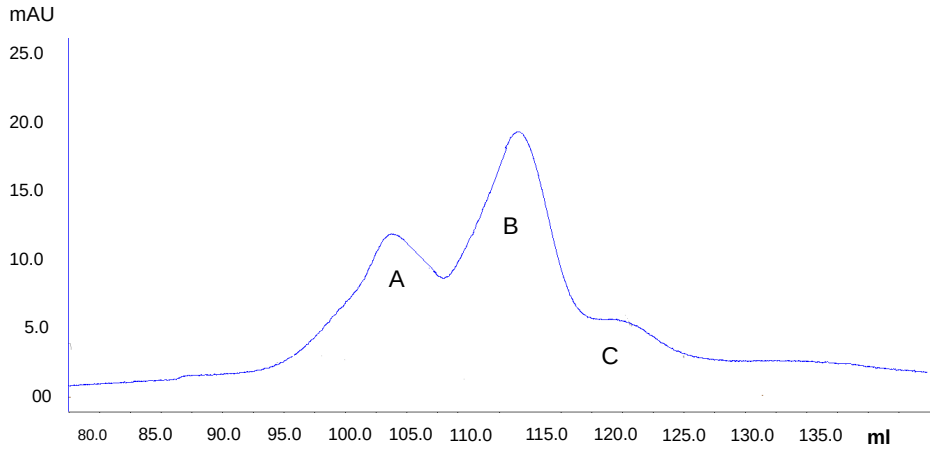

Figure 5.1: *Heteractis magnifica* venom extract analysed by gel filtration chromatography (fast protein chromatography [FPLC])

Notes: Three peaks as indicated by A, B and C were chromatographed through a HiLoad 16/60 Superdex 200 column.

5.3.2 Effect of fractions A, B and C on the A549 cells

The investigation of the cancer preventive properties of the fractions from the fast protein chromatography (FPLC) was carried out using MTT and crystal violet assays on the human lung cancer A549 cell line. The current study's experimental results showed that the fractions comprising peak A exhibited significant cytotoxic activity on the A549 cell line (Figures 5.2a and 5.2b).

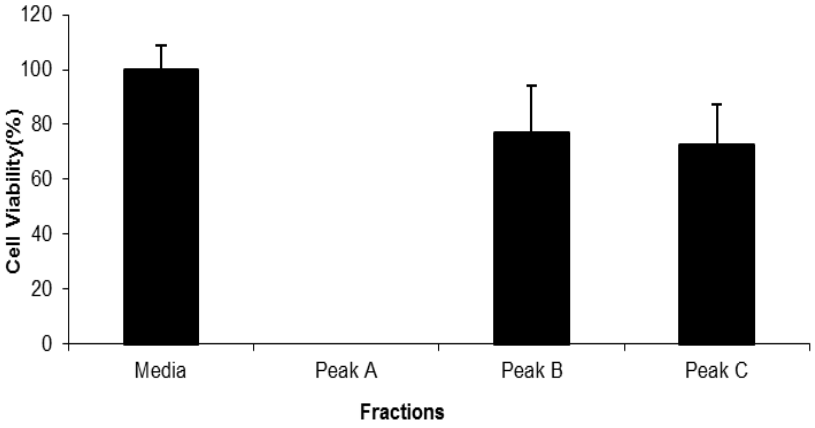

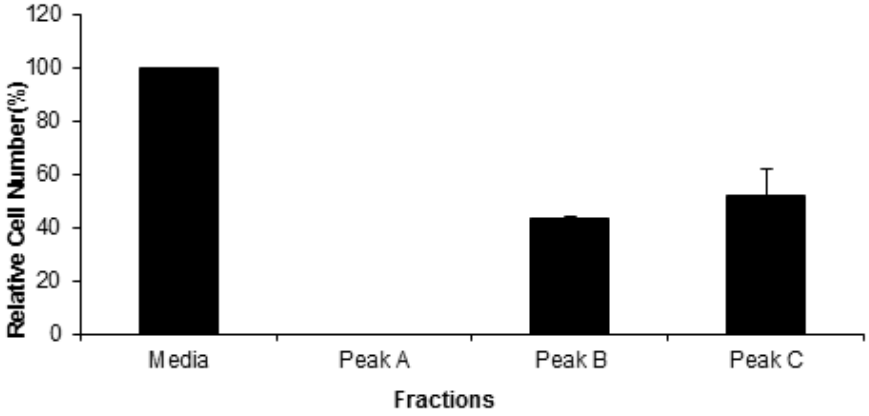

Figure 5.2: Cell viability percentage of A549 human lung cancer cell line estimated by a)MTT assay and b)crystal violet assay

Notes: After 24h exposure to the FPLC fractions. Data are shown as the mean of three replicates + SEM.

5.3.3 Sodium dodecyl sulphate polyacrylamide gel electrophoresis (SDS-PAGE)

The purified preparation of the fraction which exhibited cytotoxic activity showed only one main protein band (approximately 9 kDa) by SDS-gel electrophoresis (Figure 5.3, Figure A5.1 in Appendix V).

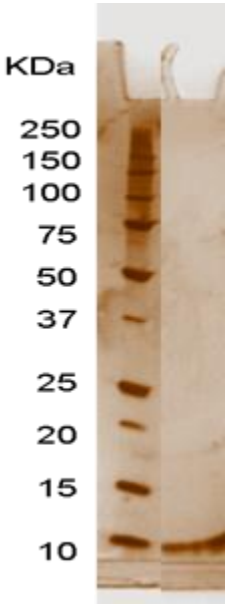

Figure 5.3: SDS-PAGE of purified fraction (peak A)

Notes: Aliquots of pooled fraction showed only one main protein band. Visualization was by silver staining. The molecular masses indicated as 9 kDa were estimated from standards electrophoresed in a parallel lane.

5.3.4 Mass spectrum

After tryptic digestion of the gel slice from the fraction (peak A), the resulting peptides were analysed by tandem mass spectrometry (MS/MS). The relative positions of the mass spectrophotometry sequenced peptide were quite similar to

that of the TRPV1 (transient receptor potential cation channel, subfamily V, member 1) analgesic peptide from *H. crispa* (Andreev et al., 2008a) (Table 5.3). The Basic Local Alignment Search Tool (BLAST) showed that the *H. magnifica* peptide shared a high degree of homology (85–90%) with protease inhibitor APHC1 (Swiss-port B2G331) from *H. crispa*. The peptide thus purified was named HMP, as an abbreviation for *H. magnifica* peptide.

Table 5.3: Peptide sequence from the fraction (peak A) determined by mass spectrometry

Accession	Coverage	#PSMs	#Peptide	#AAs	MW[KDa]	Calc.pI	Score	Description
B2G331	12.82	3	2	78	8.6	8.40	10.94	Analgesic polypeptide HC1 = *Heteractis crispa* PE=1 SV=1 [APHC1-HETCR]
	Confidence icon	Sequence	Protein accessions	#Protein	#Protein groups	Activation type	Modification	Probability
	High	RFYFDSETGK	B2G331	1	1	CID		33.8

Notes: The relative position of the mass spectrophotometry-sequenced peptide was matched to TRPV1 analgesic peptide from *H. crispa*.

5.3.5 Polymerase chain reaction (PCR) product analysis and cloning

Full-length HMP-cDNA cloned into a pET32a+ vector was used as a template. The recombinant plasmid pET32a-HMP was amplified by the primers. To confirm the transformation of pET32a-HMP into *E. coli* BL21 (DE3) component cells, PCR reaction and enzymatic digestion with *BamHI* and *XhoI* were performed and showed that the target gene was inserted correctly (Figure 5.5).

SSGLVPRGSGMKETAAAKFERQHMDSPDLGTDDDDKAMADIGSGSFYFD

SETGKCTPFIYGGCGGNGNNFETLHACRAICRATRAITSITPWGLTGLEGFF

AERRNYIRIGEWDAPCSGALSAAGVVVTRSVTATLASALAPAPFAFFPSFL

ATFAGFP.

Figure 5.4: Protein sequence alignment of HMP determined against a known protein (APHC1) after transformation of pET32a-HMP into *E. coli* BL21(DE3) component cells

5.3.6 Expression and purification of recombinant protein

The expression and secretion of the HMP fusion protein in *E. coli* were followed by the induction of IPTG (isopropyl β-D-1-thiogalactopyranoside). The optimal growth temperature was determined to be 37ºC and the culture was induced with 1 Mm IPTG for 4h before purification of the HMP (Figure 5.6). Positive clones expressed a recombinant protein of molecular mass ~25 KDa identified by Coomassie blue staining. The size of the protein fragment observed from SDS-PAGE was in accordance with that expected from 6 × His-tag-HMP fusion protein (Figure A5.2 in Appendix V).

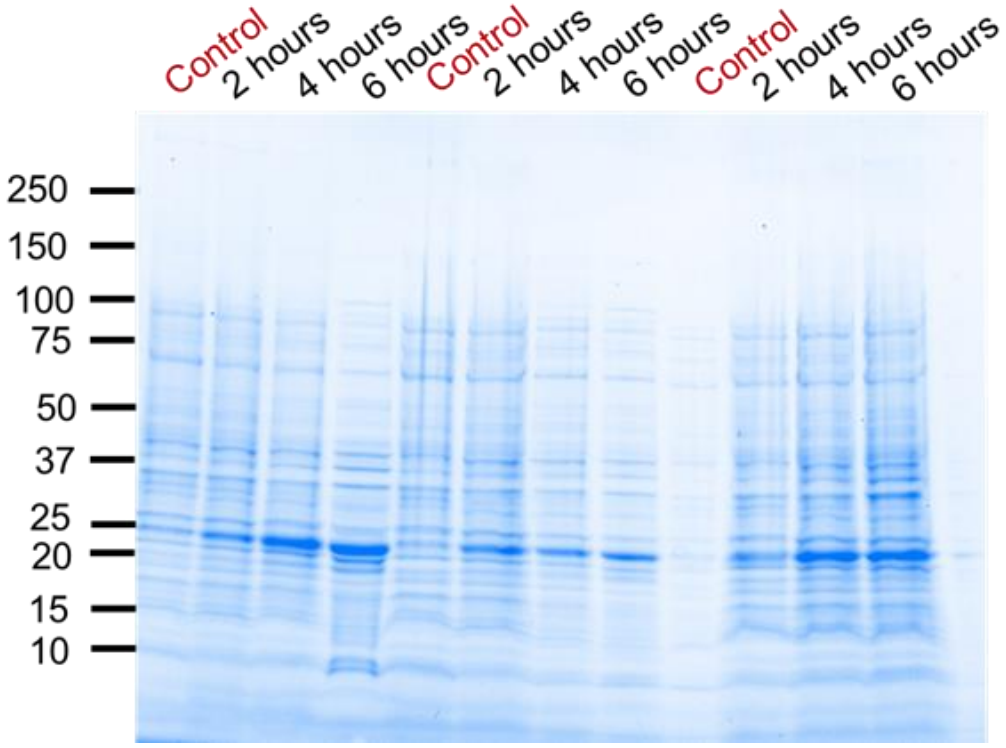

Figure 5.5: Expression of *Heteractis magnifica* recombinant protein

Note: For 2h, 4h and 6h after adding 1 mM isopropyl β-D-1-thiogalactopyranoside (IPTG)

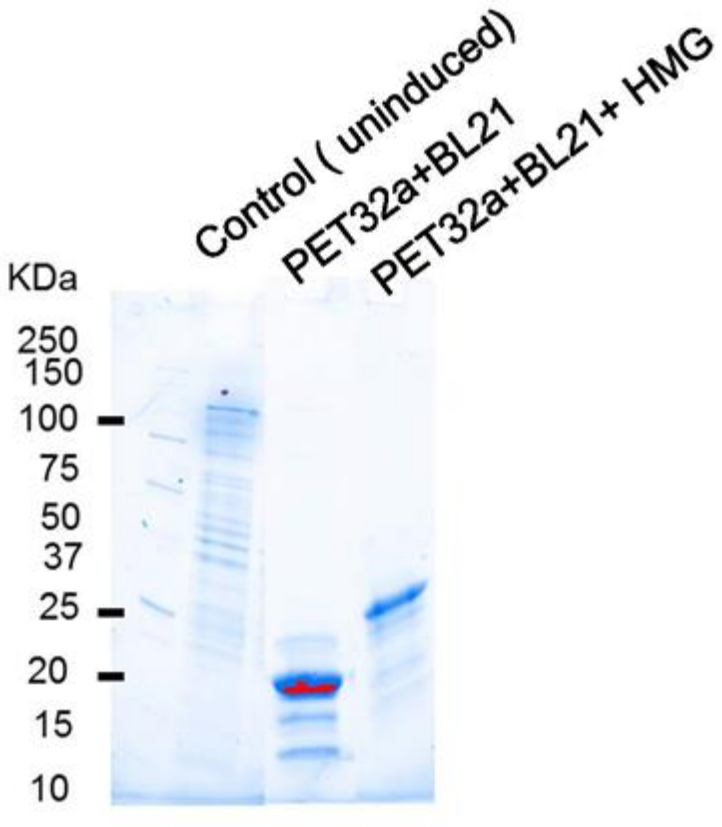

Figure 5.6: SDS-PAGE analysis of HMP expression

Notes: KDa, molecular mass standards; Lane 1, supernatant from control (uninduced) cells; Lane 2, supernatant from induced cells vector = pET32a+ BL21; Lane 3, supernatant from induced cells vector = pET32a+ BL21 + HMP DNA

5.3.7 Biological activity

H. magnifica peptide (HMP) significantly inhibited the proliferation of the human lung cancer cell line (A549) in a dose-dependent manner (Figure 5.7a). There was a significant reduction in cell numbers of the lung cancer cell line after treatment with 7.5 µg/ml or more of the purified recombinant fusion peptide. The IC_{50} value

was 6.6 µg/ml after treatment for 24 h. The IC_{50} values are summarised in Table 5.4. In addition, significant decreases in cell viability were observed after treatment with HMP on MCF7 and T47D cell lines (Figure 5.7c and d). In contrast, HMP caused less cytotoxicity on the normal breast cell line 184B5 (Figure 5.7b). A significant reduction in cell numbers of T47D and MCF7 cell lines was observed for a dose of 7.5 µg/ml; however, when the same concentration was applied to 1845B cells, there was no significant effect on cell numbers. The only significant reduction was at 10 µg/ml for the 1845B cell line; this was evident from lower IC_{50} values of 5.2 µg/ml on MCF7 cells and 6.9 µg/ml on T47D cells, respectively, compared to 10.28 µg/ml on 184B5 cells after treatment for 24h (Table 5.4).

Table 5.4: IC_{50} values of purified peptide from *H. magnifica in vitro*

Purified Peptide	**Cell Type**	**IC_{50} (µg/ml)**
		MTT
H. magnifica	T47D	6.97
	MCF7	5.28
	184B5	10.28
	A549	6.60
	MRC5	n/t

Note: n/t = not tested

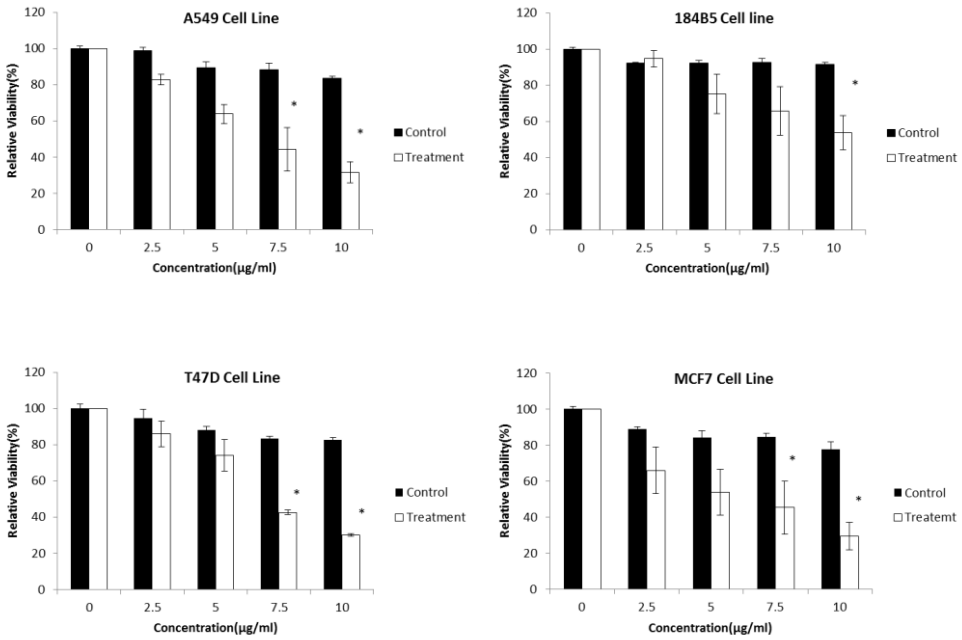

Figure 5.7: Relative viability as determined by MTT assay after 24h treatment of a)A549, b)18B5, c)T47D and d)MCF7 cell lines with increasing concentrations of control pET32a+ BL21; and treatment = pET32a+ BL21 + insert HMP DNA

Notes: Cell viability was calculated relative to the untreated media (zero) control. The values are shown as mean ± SEM, n = 3; * significantly different from the untreated control (0 µg/ml) at $p \leq 0.05$.

5.4 Discussion

The existence of a bioactive component from sea anemone venom that could influence human lung and breast cancers, the two most common cancers in the world, however, has not been previously reported. The present work described the comprehensive screening, purification and characterisation of a bioactive compound from the venom of *H. magnifica*. The sequence of *H. magnifica* peptide (HMP) exhibited a high degree of identity (90%) with the 56-residue-long polypeptide $APHC_1$ from *H. crispa*. The analgesic peptide ($APHC_1$) acted as a modulation of TRPV1 activity that could significantly reduce capsaicin-induced

acute pain (Andreev et al., 2008a). Two new polypeptide compounds, $APHC_2$ and $APHC_3$, that were also found in *H. crispa* exhibited an analgesic activity (Kozlov et al., 2009). However, the anti-carcinogenic effects of the isolated peptides ($APHC_1$, $APHC_2$ and $APHC_3$) have not been reported.

Two cytolysins were purified from *H. magnifica* which showed haemolytic and lethal activities. The relative molecular weight of magnificalysins I and II was 19 KDa and they were highly homologous to cytolysin from the sea anenome *Stichodactyla helianthus* (Khoo et al., 1993, Wang et al., 2000). However, the molecular weight of HMP was approximately 9 KDa and, based on the BLAST search, the HMP shared a high degree of homology with $APHC_1$ from *H. crispa*.

In A549, MCF7 and T47D cell lines, the levels of cytotoxic biological activity obtained with the recombinant protein (pET32a+ BL21 + insert HMP DNA) were significantly higher than those of the vector without the insert (pET32a+ BL21). The IC_{50} values of HMP on MCF7 and T47D cell lines were 5.28 µg/ml and 6.97 µg/ml, respectively, which were comparable to that of the normal breast 184B5 cell line (IC_{50} value 10.28 µg/ml), making HMP a candidate for breast cancer chemotherapy; however, more studies need to be considered.

In addition, in a comparison between commercial drugs for breast and lung cancer treatment and HMP, the IC_{50} value of HMP (6.6 µg/ml) for the A549 cell line was similar to that of paclitaxel (8 µg/ml) (Georgiadis et al., 1977). However, the IC_{50} values of paclitaxel treatment for T47D and MCF7 cell lines were 41.1 µg/ml and 3.7 µg/ml, respectively, which showed that the T47D cancer cell line was more resistant to paclitaxel than the MCF7 cell line (Lv et al., 2012): the current

study's results showed that the IC_{50} values of HMP treatment for T47D and MCF7 cell lines were 5.28 µg/ml and 6.97 µg/ml, respectively. This is an important finding because the T47D cell line is resistant to paclitaxel (Lv et al., 2012).

CHAPTER 6: GENERAL DISCUSSION

6.1 General Discussion

The overall aim of this study was to characterise the anti-cancer properties of bioactive compounds in sea anemone venom and to investigate the underlying mechanisms of their effects. Initially, the anti-cancer activities of the venom from five sea anemones were investigated on three cancer cell lines. The anti-cancer activities of the crude extracts were found to be cancer cell type-dependent because different susceptibilities were observed after treatment of different cell lines with each of the different venom extracts. Venoms from *C. adhaesivum*, *H. malu* and *H. magnifica* showed a range of positive cytotoxicity on human cancer cell lines, although *H. crispa* and *E. quadricolor* were not very effective anti-cancer agents *in vitro* (Ramezanpour et al., 2012a). Appendix III presents a summary of the statistically significant reductions in cell numbers (*p*-values).

Due to these differences, questions regarding the effectof each of the crude extracts on cancer cell lines and their potential underlying mechanism could not be answered based on the currently available literature nor on the initial data (Chapter 2), highlighting the need for additional knowledge in the area of the mechanism of cytotoxicity. *Heteractis magnifica* venom was chosen for further studies because it is the second largest in size of all sea anemones and is easily obtainable. The extract of *H. magnifica* was highly effective at killing cancer cell lines. The IC_{50} value of A549 cells showed more selective cytotoxic activity against human lung cancer cell line compared with human lung non-cancer MRC5 cell line. The IC_{50} values are summarised in Table 6.1.

Table 6.1: IC_{50} values of *H. magnifica* venom extract *in vitro*

Extract Compound	Cell Type	IC_{50} (µg/ml) MTT	Crystal Violet
H. magnifica	T47D	5.99	5.67
	MCF7	15.76	9.26
	1845B	6.74	14.70
	A549	11.14	22.91
	MRC5	18.17	24.28

Notes: IC_{50} calculation was determined using GraphPad Prism V. 5.02 Windows (GraphPad Software, San Diego, California, USA).

In addition, differences in the AUC of the dose response curves (ΔAUC) between the test and reference cell line were estimated using the R package PK (Jaki and Wolfsegge, 2011). The relative cell number was lower in T47D and MCF7 cell lines compared with the 184B5 cell line in the crystal violet assay. However, no difference in viability was found between A549 and MRC5 cell lines.The *p*-values are summarised in Table 6.2.

Table 6.2: *p*-values estimated by comparing area under the curve (AUC) for the test and reference cell line

Tissue	Cancer Cell Line	Normal Cell Line	CSV ΔAUC *p*-value	MTT ΔAUC *p*-value
Lung	A549	MRC5	0.39	0.63
Breast	T47D	184B5	0.044	0.45
Breast	MCF7	184B5	0.005	0.12

Note: Using the individual replicate (n = 3) data (Chaper 5).

Further research showed that *H. magnifica* crude venom extract acted to inhibit both cancer cell lines through several assays: (a) the cell cycle was arrested in G1 phase with a concomitant increase in the sub-G1 population in breast cell lines; (b) however, in A549 cells, the cell cycle was arrested in S phase with an associated accumulation of cells in the G0/G1 phases; (c) in addition, *H. magnifica* up-regulated apoptosis through activation of the caspases and mitochondrial membrane pathways in T47D, MCF7 and A549 cell lines.

Although there were some common mechanisms of action, the magnitude of the response was different for each cell line. For example, significant activation of the three caspases was observed for MCF7 and T47D cell lines, with T47D exhibiting the greater response. However, MCF7 and T47D cell lines are different in many ways, including molecular profiles, culture doubling times *in vitro* and tumorigenicity *in vivo* (National Cancer Institute, 2012). The MCF7 cells are reportedly P53 wild type, while T47D cells are P53 mutant. Inhibition of endogenous mutant p53 by RNAi led to massive apoptosis in two mutant p53-expressing in T47D cell line (Yamada et al., 2009, Lim et al., 2009). However, both cell lines are molecularly classified as Luminal A (oestrogen receptor-

positive, oestrogen receptor-positive and human epidermal growth factor receptor 2-negative) (Holliday and Speirs, 2011). In the future, other upstream and downstream of Phosphatidylinostil 3-Kinase (PI3K) pathway could be tested via reverse transcription polymerase chain reaction (RT-PCR) to confirm the current results in order to further clarify the underlying mechanisms of action (e.g. other Bcl-2 family members and the c-Kit gene).

Given that the crude venom extract had significant anti-cancer activity, the next step was to find the source of the bioactivity which involved purification and characterisation of individual compounds from the crude venom extract. The purified peptide analysed by tandem mass spectrometry (MS/MS) revealed that the *Heteractis magnifica* peptide (HMP) was homologous to the protease inhibitor $APHC_1$ (85–90% identity) from the sea anemone, *H. crispa*. The $APHC_1$ is known to be an analgesic agent that can modulate the activity of TRPV1 (transient receptor potential cation channel, subfamily V, member 1) . Further research has provided intriguing evidence that the blocking the TRPV1receptors can be a useful therapeutic approach for inflammation and possibly neuropathic pain (Andreev et al., 2008a). There appears to be the same evolutionary origin between the $APHC_1$ of the sea anemone *H. crispa* and HMP from the sea anenome *H. magnifica*. However, the anti-carcinogenic effect of the $APHC_1$ has not been reported and more data are needed to ascertain whether or not an anti-cancer property applies to $APHC_1$ peptide.

The deduced sequence when expressed and purified as a peptide with a His-tag (HMP-His) was found to be effective in inhibiting breast ductal tumour (T47D), breast adenomacarcinoma (MCF7) and lung adenomacarcinoma (A549), while, at

the same dose, the compound showed less effect on the survival of 184B5 human non-cancer breast cell lines. The IC_{50} value of A549 cells was 6.6 µg/ml after treatment for 24h and the IC_{50} values of the commercial drug paclitaxel for NSCLC cell lines were 27.3 µg/ml, 8 µg/ml and 0.023 µg/ml at exposure durations of 3h, 24h and 120h, respectively (Georgiadis et al., 1977). Thus, the IC_{50} values for 24h are of the same order of magnitude in this comparison. The IC_{50} values are summarised in Table 6.3.

In addition, the higher cytotoxic activity of HMP-His fusion protein on human cancer cell lines was evident from the lower IC_{50} values of 5.2 µg/ml for the MCF7 cell line and 6.9 µg/ml for the T47D cell line, compared to 10.9 µg/ml for the 184B5 cell line after treatment for 24h. In contrast, the IC_{50} values of 41.1 µg/ml for the T47D cell line and 3.7 µg/ml for the MCF7 cell line were reported after treatment with paclitaxel which showed that the T47D cancer cell line was more resistant to paclitaxel than was the case for the MCF7 cell line (Lv et al., 2012).

Table 6.3: IC_{50} values of purified peptide from *H. magnifica in vitro*

Purified peptide	Cell Type	IC_{50} (µg/ml) MTT
H. magnifica	T47D	6.97
	MCF7	5.28
	1845B	10.28
	A549	6.60
	MRC5	Not tested

Note: The IC_{50} calculation was determined using GraphPad Prism V. 5.02 Windows (GraphPad Software, San Diego, California, USA).

Although paclitaxel has shown significant anti-neoplastic activity against various human cancers, a major difficulty in the clinical use of paclitaxel has been its poor water solubility (Li et al., 1998). On the other hand, HMP is totally water soluble and it might be possible to improve the efficiency of the delivery of HMP by adding a nanoparticle to this molecule to direct it to tumour sites. Also, urokinase and antibodies that binds to specific receptors upregulated on cancer cells may can help the drug delivery. However, an understanding of the type of hazards introduced by using nanoparticles for drug delivery and of the biological responses to nanomaterials is needed to develop the conjugates in the future (Jong and Borm, 2008). In addition, previous studies showed paclitaxel has a cytotoxic effect on both prostate and ovarian carcinoma cell lines (Cameron et al., 1995, Röyttä et al., 1987). Further research to test the effects of HMP on these cancer cell lines would be of interest.

Furthermore, removing the affinity tag (His-tag) can improve the potency of the cytotoxicity. It would be interesting to study the selectivity and determine the IC_{50} values of HMP without a tag. Further study may also facilitate an understanding of the active sites of the *H. magnifica* peptide (HMP). However, the development of a peptide as a clinically useful drug is limited by the inherent instability of peptides towards metabolic degradation (Svenson et al., 2008). Strategies are available for transforming a peptide into a drug candidate which would increase stability, bioavailability and biological activity. Most peptides that have been successfully stabilized against proteolysis have undergone several types of chemical modifications, such as mask protease recognition or cleavage sites

(Adessi and Soto, 2002). Therefore, more research is required to convert HMP into a stable drug candidate.

On the other hand, it is important to produce the novel peptide on a large scale in optimized and inexpensive media for the process to be commercially viable. In theory, large-scale production of bioactive compounds can be achieved by chemical synthesis or through extraction from marine animals. Chemical synthesis has not yet been developed to synthesize complex molecules at the kilogram scale and, in cases where this may already be technically possible, most of the compounds may not be complex to synthesize but the price may still not be affordable for commercial applications (Rocha et al., 2011c). In addition, the amount of crude peptide extract from each sea anemone would require large-scale cultivation of this sea animal. As this is also prohibitive, a feasible alternative is by recombinant protein production as a scale-up in fermentation and purification. Large quantities of recombinant protein have been successfully produced in microbial hosts for therapeutic purposes (Demain and Vaishnav, 2009). Thus, further studies based on the optimization and scale-up of peptide in fermentation are required in the future.Furthermore, additional studies need to be carried out to investigate the quality of the product, its safety, efficacy and tolerance doses.

REFERENCES

ADAMS, J. & CORY, S. 2001. Life-or-death decisions by the Bcl-2 protein family. *Trends Biochem Sci,* 26**,** 61-66.

ADESSI, C. & SOTO, C. 2002. Converting a peptide into a drug: strategies to improve stability and bioavailability. *Curr Med Chem,* 9**,** 963-978.

ALBERT, B. 2008. cancer as a microevolutionary process. *In:* 5 (ed.) *Mol Biol Cell.* Garland Science.

ALBINI, A., IWAMOTO, Y., KLEINMAN, H., MARTIN, R., AARONSON, A., KOZLOWSKI, J. & MCEWAN, R. 1987. A Rapid in Vitro Assay for Quantitating the Invasive Potential of Tumor Cells. *Cancer Res,* 47**,** 3239-3245.

ANDERLUH, G. & MACˇEK, P. 2002. Cytolytic peptide and protein toxins from sea anemones (Anthozoa :Actiniaria). *Toxicon,* 40**,** 111-124.

ANDREEV, Y. A., KOZLOV, S. A., KOSHELEV, S. G., IVANOVA, E. A., MONASTYRNAYA, M. M., KOZLOVSKAYA, E. P. & GRISHIN, E. V. 2008a. Analgesic compound from sea anemone Heteractis crispa is the first polypeptide inhibitor of vanilloid receptor 1 (TRPV1). *J. Biol. Chem.,* 283**,** 23914-23921.

ANDREEV, Y. A., KOZLOV, S. A., KOSHELEV, S. G., IVANOVA, E. A., MONASTYRNAYA, M. M., KOZLOVSKAYA, E. P. & GRISHIN, E. V. 2008f. Analgesic compound from sea anemone Heteractis crispa is the first polypeptide inhibitor of vanilloid receptor 1 (TRPV1). *J. Biol. Chem,* 283**,** 23914-23921.

ANEIROS, A. & GARATEIX, A. 2004. Bioactive peptides from marine sources: pharmacological properties and isolation procedures. *J Chromatogr B Analyt Technol Biomed Life Sci,* 803**,** 41-53.

ANTONIOU, A. C. & EASTON, D. F. 2006. Models of genetic susceptibility to breast cancer. *Oncogene,* 25**,** 5898–5905.

ATTOUB, S., ARAFAT, K., GÉLAUDE, A., SULTAN, M., BRACKE, M., COLLIN, P., TAKAHASHI, T., ADRIAN, T. & DE WEVER, O. 2013. Frondoside A Suppressive Effects on Lung Cancer Survival, Tumor Growth, Angiogenesis, Invasion, and Metastasis. *PLoS One,* 8.

BAE, B., IM, K., CHOI, W., HONG, J., LEE, C., CHOI, J., SON, B., SONG, J. & JUNG, J. 2000. New acetylenic compounds from the stony coral Montipora sp. *J Nat Prod,* 63**,** 1511-1514.

BALIGA, B. & KUMAR, S. 2003. Apaf-1/cytochrome c apoptosome: an essential initiator of caspase activation or just a sideshow? *Cell Death Differ,* 10**,** 16-18.

BARRETT, J. C. & WISEMAN, R. W. 1987. Cellular and molecular mechanisms of multistep carcinogenesis: relevance to carcinogen risk assessment. *Environ Health Perspect,* 76**,** 65-70.

BAUM, M. & SCHIPPER, H. 2005. *Fast Facts-Breast Cancer,* Health Press Limited.

BEDARD, P. L. & CARDOSO, F. 2008. Recent advances in adjuvant systemic therapy for early-stage breast cancer. *Ann Oncol,* 19**,** 122-1227.

BERGOT, E., LEVALLET, G., CAMPBELL, K., DUBOIS, F., LECHAPT, E. & ZALCMAN, G. 2013a. Predictive biomarkers in patients with resected non-small cell lung cancer treated with perioperative chemotherapy. *Eur Respir Rev,* 22**,** 565-576.

BERGOT, E., LEVALLET, G., CAMPBELL, K., DUBOIS, F., LECHAPT, E. & ZALCMAN, G. 2013b. Predictive biomarkers in patients with resected non-small cell lung cancer treated with perioperative chemotherapy. *Eur Respir Rev,* 22**,** 565-76.

BOFFETTA, P. 2004. Epidemiology of environmental and occupational cancer. *Oncogene,* 23**,** 6392–6403.

BONADONNA, G., BRUSAMOLINO, E., VALAGUSSA, P., ROSSI, A., BRUGNATELLI, L., BRAMBILLA, C., DE LENA, M., TANCINI, G., BAJETTA, E., MUSUMECI, R. & VERONESI, U. 1976a. Combination chemotherapy as an adjuvant treatment in operable breast cancer. *N Engl J Med,* 294**,** 405-410.

BONADONNA, G., BRUSAMOLINO, E., VALAGUSSA, P., ROSSI, A., BRUGNATELLI, L., BRAMBILLA, C., DE LENA, M., TANCINI, G., BAJETTA, E., MUSUMECI, R. & VERONESI, U. 1976d. Combination chemotherapy as an adjuvant treatment in operable breast cancer. *N Engl J Med,* 294**,** 405-10.

BONADONNA, G., VALAGUSSA, P., MOLITERNI, A., ZAMBETTI, M. & BRAMBILLA, C. 1995. Adjuvant cyclophosphamide, methotrexate, and fluorouracil in node-positive breast cancer: the results of 20 years of follow-up. *N Engl J Med,* 332**,** 901-906.

BOSMANS, F. & TYTGATB, J. 2007. Sea anemone venom as a source of insecticidal peptides acting on voltage-gated Na+ channels. *Toxicon,* 49**,** 550–560.

BOTANA, L. M. 2014. *Seafood and Freshwater Toxins: Pharmacology, Physiology, and Detection,* CRC Press.

BOWER, M. & WAXMAN, J. 2010. *Oncology* Wiley-Blackwell

BRANDBERG, Y., SANDELIN, K., ERIKSON, S., JURELL, G., LILJEGREN, A., LINDBLOM, A., LINDÉN, A., VON WACHENFELDT, A., WICKMAN, M. & ARVER, B. 2008. Psychological reactions, quality of life, and body image after bilateral prophylactic mastectomy in women at high risk for breast cancer: A prospective 1-year follow-up study. *J Clin Oncol.,* 26**,** 3943-3949.

BRASH, D. E., RUDOLPH, J. A., SIMON, J. A., LIN, A., MCKENNA, G. J., BADEN, H. P., HALPERIN, A. J. & PONTÉN, J. 1991. A role for sunlight in skin cancer: UV-induced p53 mutations in squamous cell carcinoma. *Proc Natl Acad Sci U S A,* 88**,** 10124–10128.

BRUCE, A., ALEXANDER, J., JULIAN, L., MARTIN, R., KEITH, R. & PETER, W. 2007. *Molecular Biology of the Cell,* New York, Garland Science.

BRUHN, T., SCHALLER, C., SCHULZE, C., SANCHEZ-RODRIGUEZ, J., DANNMEIER, C., RAVENS, U., HEUBACH, J., ECKHARDT, K., SCHMIDTMAYER, J., SCHMIDT, H., ANEIROS, A., WACHTER, E. & BÉRESS, L. 2011. Isolation and characterisation of five neurotoxic and

cardiotoxic polypeptides from the sea anemone Anthopleura elegantissima. *Toxicon,* 93**,** 693-702.

BRUIN, J. E., GERSTEIN, H. C., MORRISON, K. M. & HOLLOWAY, A. C. 2008. Increased Pancreatic Beta-Cell Apoptosis following Fetal and Neonatal Exposure to Nicotine Is Mediated via the Mitochondria. *Toxicol Sci,* 103**,** 362-370.

BURKE, W. A. 2002. cnidarians and human skin. *Dermatol Ther,* 15**,** 18-25.

CAMERON, M., CAUDLE, M., SULLIVAN, W., PELUSO, J. & WIMALASENA, J. 1995. The steroidogenic and morphological effects of paclitaxel on cultured ovarian cancer cells. *Oncol Res,* 7**,** 145-156.

CAMPBELL, C. T., PRINCE, M., LANDRY, G. M., KHA, V. & KLEINER, H. E. 2007. Pro-apoptotic effects of 1'-acetoxychavicol acetate in human breast carcinoma cells. *Toxicol. Lett,* 173**,** 151-160.

CANCER COUNCIL. 2004. *Assessment and Management of Lung Cancer* [Online]. Australia.

CANCER COUNCIL. 2010. *Breast cancer Incidence and mortality* [Online].

CANCER COUNCIL. 2012. *Radiotherapy* [Online].

CANCER COUNCIL. 2014a. *Chemotherapy* [Online]. Australia.

CANCER COUNCIL. 2014c. *Skin Cancer in Australia* [Online].

CANCER COUNSIL. 2014. *skin cancer chemotherapy* [Online].

CARLGREN, O. 1949. *A survey of the Ptychodactiaria, Corallimorpharia and Actiniaria,* Kungliga Svenska Vetenskapsakadamiens Handlingar, .

CHAITANYA, G. V., ALEXANDER, J. S. & BABU, P. P. 2010. PARP-1 cleavage fragments: signatures of cell-death proteases in neurodegeneration. *Cell Commun Signal,* 8.

CHANDLER, J. M., COHEN, G. M. & MACFARLANE, M. 1998. Different Subcellular Distribution of Caspase-3 and Caspase-7 following Fas-induced Apoptosis in Mouse Liver. *J. Biol. Chem,* 273**,** 10815-10818.

CHANGA, S., RODRIGUEZ-LANETTYB, M., YANAGIC, K., NOJIMAD, S. & SONGE, J. 2011. Two anthozoans, Entacmaea quadricolor (order Actiniaria) and Alveopora japonica (order Scleractinia), host consistent genotypes of Symbiodinium spp. across geographic ranges in the northwestern Pacific Ocean. *Animal Cells and Systems,* 15**,** 315 324.

CHIBA, K., KAWAKAMI, K. & TOHYAMA, K. 1998. Simultaneous evaluation of cell viability by neutral red, MTT and crystal violet staining assays of the same cells. *Toxicol In Vitro,* 12**,** 251-258.

CHILLER, J. S., HARRINGTON, D., BELANI, C., P. & LANGER, G. 2002. Comparison of four chemotherapy regimens for advanced non-small-cell lung cancer. *N Engl J Med,* 346.

CLAMP, A., DANSON, S. & CLEMONS, M. 2003. Hormonal and genetic risk factors for breast cancer. *Surgeon,* 1**,** 23-31.

CLEMONS, M. & GOSS, P. 2001. Estrogen and the risk of breast cancer. *N Engl J Med,* 344**,** 276-285.

CLIVE, W. 1991. *The metastatic cell: behaviour and biochemistry,* Chapman and Hall.

COOPER, G. 2000. *The Cell,* Sinauer Associates.

COSSARIZZA, A., BACCARANI-CONTRI, M., KALASHNIKOVA, G. & FRANCESCHI, C. 1993 A new method for the cytofluorimetric analysis

of mitochondrial membrane potential using the J-aggregate forming lipophilic cation 5,5',6,6'-tetrachloro-1,1',3,3'-tetraethylbenzimidazolcarbocyanine iodide (JC-1). *Biochem Biophys Res Commun,* 197**,** 40-45.

CRAGG, G. M. & NEWMAN, D. J. 2013. Natutal products: A continuing source of novel drug leads. *Biochim Biophys Acta,* 1830**,** 3670–3695.

CROMPTON, M. 2000. Bax, Bid and the permeabilization of the mitochondrial outer membrane in apoptosis. *Curr Opin Cell Biol,* 12**,** 414-419.

CROW, M. T., MANI, K., NAM, Y. J. & KITSIS, R. N. 2004. The Mitochondrial Death Pathway and Cardiac Myocyte Apoptosis. *Circ Res,* 95**,** 957-970.

CULLEN, S. & MARTIN, S. 2009. Caspase activation pathways: some recent progress. *Cell Death Differ,* 16**,** 935-938.

CURTIN, J., BUSAM, K., PINKEL, D. & BASTIAN, B. 2006. Somatic Activation of KIT in Distinct Subtypes of Melanoma. *J Clin Oncol* 24**,** 4340-4346.

DALAY, M., MERCER, R., BRUGLER, M. R., CARTWRIGHT, P., COLLINS, A. G., DAWSON, M. N., FAUTIN, D., FRANCE, S. C., MCFADDEN, C. S., OPRESKO, D. M., RODRIGUEZ, E., ROMANO, S. L. & STAKE, J. L. 2008. The phylum Cnidaria: A review of phylogenetic patterns and diversity 300 years after Linnaeus. *Zootaxa,* 1668**,** 127–182.

DALY, M., MERCER, R., BRUGLER, M. R., CARTWRIGHT, P., COLLINS, A. G., DAWSON, M. N., FAUTIN, D., FRANCE, S. C., MCFADDEN, C. S., OPRESKO, D. M., RODRIGUEZ, E., ROMANO, S. L. & STAKE, J. L. 2008. The Phylum Cnidaria: A Review of Phylogenetic Patterns and Diversity 300 Years After Linnaeus. *Zootaxa***,** 127-182.

DALY, M. D., FAUTIN, D. G. & CAPPOLA, V. A. 2003. Systematics of the Hexacorallia (Cnidaria: Anthozoa). *Zool J Linnean Soc,* 139**,** 419-473.

DARBY, S., MCGALE, P., CORREA, C., TAYLOR, C., ARRIAGADA, R., CLARKE, M., CUTTER, D., DAVIES, C., EWERTZ, M., GODWIN, J., GRAY, R., PIERCE, L., WHELAN, T., WANG, Y. & PETO, R. 2011. Effect of radiotherapy after breast-conserving surgery on 10-year recurrence and 15-year breast cancer death: meta-analysis of individual patient data for 10,801 women in 17 randomised trials. *Lancet,* 378**,** 1707-1716.

DEMAIN, A. & VAISHNAV, P. 2009. Production of recombinant proteins by microbes and higher organisms. *Biotechnol Adv,* 27**,** 297-306.

DOMCHEK, S., FRIEBEL, T., SINGER, C., EVANS, D., LYNCH, H., ISAACS, C., GARBER, J., NEUHAUSEN, S., MATLOFF, E., EELES, R., PICHERT, G., VAN T'VEER, L., TUNG, N., WEITZEL, J., COUCH, F., RUBINSTEIN, W., GANZ, P., DALY, M., OLOPADE, O., TOMLINSON, G., SCHILDKRAUT, J., BLUM, J. & REBBECK, T. 2010a. Association of risk-reducing surgery in BRCA1 or BRCA2 mutation carriers with cancer risk and mortality. *JAMA,* 304**,** 967-75.

DOMCHEK, S., FRIEBEL, T., SINGER, C., EVANS, D., LYNCH, H., ISAACS, C., GARBER, J., NEUHAUSEN, S., MATLOFF, E., EELES, R., PICHERT, G., VAN T'VEER, L., TUNG, N., WEITZEL, J., COUCH, F., RUBINSTEIN, W., PA., G., DALY, M., OLOPADE, O., TOMLINSON,

G., SCHILDKRAUT, J., BLUM, J. & REBBECK, T. 2010b. Association of risk-reducing surgery in BRCA1 or BRCA2 mutation carriers with cancer risk and mortality. *JAMA,* 304**,** 967-675.

ELMORE, S. 2007. Apoptosis: A Review of Programmed Cell Death. *Toxicol Pathol,* 35**,** 495–516.

FALLAHI-SICHANI, M., SAMAN HONARNEJAD, S., HEISER, L. M., GRAY, J. W. & SORGER, P. 2013. Metrics other than potency reveal systematic variation in responses to cancer drugs. *Nat Chem Biol,* 9**,** 708-714.

FAN, T., HAN, L., CONG, R. & LIANG, J. 2005 Caspase Family Proteases and Apoptosis. *Acta Biochim Biophys Sin (Shanghai),* 37**,** 719-27.

FAUTIN, D. 1981. *The Clownfish Sea Anemones: Stichodactylidae (Coelenterata: Actiniaria) and Other Sea Anemones Symbiotic with Pomacentrid Fishes,* American Philosophical Society.

FAUTIN, D. 2009. Structural diversity, systematics, and evolution of cnidae. *Toxicon,* 54**,** 1054-64.

FAUTIN, D., G. & ALLEN, G., R. 1994. *Anemone Fishes and Their Host Sea Anemones* Tetra-Press.

FAUTIN, D. G. & ALLEN , G. R. 1994. *Anemone Fishes and Their Host Sea Anemones* Tetra-Press.

FEDOROV, S., DYSHLOVOY, S., MONASTYRNAYA, M., SHUBINA, L., LEYCHENKO, E., KOZLOVSKAYA, E., JIN, J. O., KWAK, J. Y., BODE, A. M., DONG, Z. & STONIK, V. 2010. The anticancer effects of actinoporin RTX-A from the sea anemone Heteractis crispa (=Radianthus macrodactylus). *Toxicon,* 55**,** 811-817.

FINE, A., JANSSEN-HEININGER, Y., SOULTANAKIS, R., SWISHER, S. & UHAL, B. 2000. Apoptosis in lung pathophysiology. *Am J Physiol Lung Cell Mol Physio* 279**,** 423-427.

FISHER, B., CONSTANTINO, J. P., REDMOND, C. K., FISHER, E., WICKERHAM, D. & CRONIN, W. 1994. Endometrial Cancer in Tamoxifen-Treated Breast Cancer Patients: Findings from NSABP B-14. *J. Natl. Cancer Inst,* 86**,** 527–537.

FLAHERTY, K. T., INFANTE, J. R., DAUD, A., GONZALEZ, R., KEFFORD, R. F., SOSMAN, J., HAMID, O., SCHUCHTER, L., CEBON, J., IBRAHIM, N., KUDCHADKAR, R., BURRIS, H. A., FALCHOOK, G., ALGAZI, A., LEWIS, K., LONG, G. V., PUZANOV, I., LEBOWITZ, P., SINGH, A., LITTLE, S., SUN, P., ALLRED, A., OUELLET, D., KIM, K. B., PATEL, K. & WEBER, J. 2012a. Combined BRAF and MEK Inhibition in Melanoma with BRAF V600 Mutations. *N Engl J Med,* 367**,** 1694-1703.

FLAHERTY, K. T., INFANTE, J. R., DAUD, A., GONZALEZ, R., KEFFORD, R. F., SOSMAN, J., OMID HAMID, O., SCHUCHTER, L., CEBON, J., IBRAHIM, N., KUDCHADKAR, R., BURRIS, H. A., FALCHOOK, G., ALGAZI, A., LEWIS, K., LONG, G. V., PUZANOV, I., LEBOWITZ, P., SINGH, A., LITTLE, S., SUN, P., ALLRED, A., OUELLET, D., KIM, K. B., KIRAN PATEL, K. & WEBER, J. 2012b. Combined BRAF and MEK Inhibition in Melanoma with BRAF V600 Mutations. *N Engl J Med* 367**,** 1694-1703.

FRAZÃO, B., VASCONCELOS, V. & ANTUNES, A. 2012. Sea Anemone (Cnidaria, Anthozoa, Actiniaria) Toxins: An Overview. *Mar Drugs,* 10**,** 1812–1851.

FRIEDBERG, E., WALKER, G., SIEDE, W. & WOOD, R. 2006. *DNA Repair and Mutagenesis,* Washington, ASM.

GEORGIADIS, M., RUSSELL, E., GAZDAR, A. & JOHNSON, B. 1977. Paclitaxel cytotoxicity against human lung cancer cell lines increases with prolonged exposure durations. *Clin Cancer Res,* 3**,** 449-454.

GEYER, C., FORSTER, J., LINDQUIST, D., CHAN, S., ROMIEU, C., PIENKOWSKI, T., JAGIELLO-GRUSZFELD, A., CROWN, J., CHAN, A., KAUFMAN, B., SKARLOS, D., CAMPONE, M., DAVIDSON, N., BERGER, M., OLIVA, C., RUBIN, S., STEIN, S. & CAMERON, D. 2006a. Lapatinib plus Capecitabine for HER2-Positive Advanced Breast Cancer. *N Engl J Med,* 355**,** 2733-2743.

GEYER, C. E., FORSTER, J., LINDQUIST, D., CHAN, S., ROMIEU, C. G., PIENKOWSKI, T., JAGIELLO-GRUSZFELD, A., CROWN, J., CHAN, A., KAUFMAN, B., SKARLOS, D., CAMPONE, M., DAVIDSON, N., BERGER, M., OLIVA, C., STEPHEN D. RUBIN, S. D., STEIN, S. & CAMERON, D. 2006b. Lapatinib plus Capecitabine for HER2-Positive Advanced Breast Cancer. *N Engl J Med* 355**,** 2733-2743.

GOGVADZEA, V., ORRENIUSA, S. & ZHIVOTOVSKYA, B. 2006. Multiple pathways of cytochrome c release from mitochondria in apoptosis. *Biochim Biophys Acta,* 1757**,** 639-647.

GONDRAN, M., ECKELI, A., MIGUES, P., GABILAN, N. & RODRIGUES, A. 2002. The crude extract from the sea anemone, Bunodosoma caissarum elicits convulsions in mice: possible involvement of the glutamatergic system. *Toxicon,* 40**,** 1667-1674.

GORDON, D., EAUCLAIRE, M., CESTE, S., KOPEYAN, C., CARLIERI, E., KHALIFA, R., PELHATE, M. & ROCHAT, H. 1996. Scorpion toxins affecting sodium current inactivation bind to distinct homologous receptor sites on rat brain and insect sodium channels. *J Biol Chem,* 271**,** 8034-8045.

GRAY-SCHOPFER, V., DA ROCHA DIAS, S. & MARAIS, R. 2005. The role of B-RAF in melanoma. *Cancer Metastasis Rev,* 24**,** 165-183.

GUNDUZ, E. & GUNDUZ, M. (eds.) 2011. *Breast Cancer - Current and Alternative Therapeutic Modalities*: InTech.

GUO, J., SI, L., KONG, Y., FLAHERTY, K., XU, X., ZHU, Y., CORLESS, C., LI, L., LI, H., SHENG, X., CUI, C., CHI, Z., LI, S., HAN, M., MAO, L., LIN, X., DU, N., ZHANG, X., LI, J., WANG, B. & QIN, S. 2011. Phase II, Open-Label, Single-Arm Trial of Imatinib Mesylate in Patients With Metastatic Melanoma Harboring c-Kit Mutation or Amplification. *J Clin Oncol* 29**,** 2904-2909.

HANAHAN, D. & WEINBERG, R. A. 2011a. Hallmarks of Cancer: The Next Generation. *Cell,* 144**,** 646–674.

HANAHAN, D. & WEINBERG, R. A. 2011d. Hallmarks of Cancer: The Next Generation. *Cell,* 144**,** 646–74.

HARNETT, P. R., CARTMILL, J. & GLARE, P. 1999. *Oncology A Case Based Manual,* Oxford University Press.

HERCEG, Z. & HAINAUT, P. 2007. Genetic and epigenetic alterations as biomarkers for cancer detection, diagnosis and prognosis. *Mol Oncol,* 1**,** 26-41.

HOLLIDAY, D. & SPEIRS, V. 2011. Choosing the right cell line for breast cancer research. *Breast Cancer Res,* 13**,** 215.

HONMA , T. & SHIOMI, K. 2006. Peptide Toxins in Sea Anemones: Structural and Functional Aspects. *Mar Biotechnol* 8**,** 1-10.

HONMA, T. & SHIOMI, K. 2006. Peptide toxins in sea anemones: structural and functional aspects. *Mar Biotechnol (NY),* 8**,** 1-10.

HTTP://ATJ.NET.AU/DIVE20079229ANEMONE_BAY.HTML 2014.

HTTP://WWW.ANEMONE-CLOWN.FR/PHOTOS/G/AMPHIPRION-AKALLOPISOS-HETERACTIS-MAGNIFICA.JPG. 2006.

HTTP://WWW.BREASTLIFT4YOU.COM/BREAST_ANATOMY.HTM. 2014.

HTTP://WWW.FISHCHANNEL.COM/SALTWATER-AQUARIUMS/REEFKEEPING/KEEPING-MARINE-ANEMONES.ASPX. 2013.

HTTP://WWW.INTERHOMEOPATHY.ORG/SEA_ANEMONE_MUST_PROTECT_BY_WITHDRAWAL_INWARDLY 2009. Heteractis malu.

HTTPS://WWW.MEERWASSER-LEXIKON.DE/TIERE/882_ENTACMAEA_QUADRICOLOR.HTM 2009.

HUTTON , D. M. C. & SMITH , V. J. 1996. Antibacterial Properties of Isolated Amoebocytes From the Sea Anemone Actinia equina. *Bid. Bull* 441-451.

JAKI, T. & WOLFSEGGE, M. J. 2011. Estimation of pharmacokinetic parameters with the R package PK. *Pharmaceutical Statistics,* 10**,** 284–288.

JIMÉNEZ, C. & CREWS, P. 1993. 13C-NMR assignments and cytotoxicity assessment of zoanthoxanthin alkaloids from zoanthid corals. *J Nat Prod,* 56**,** 9-14.

JONG, W. H. D. & BORM, P. J. A. 2008. Drug delivery and nanoparticles: Applications and hazards. *Int J Nanomedicine,* 3**,** 133–149.

KARTHIKAYALU, S., RAMA, V., KIRUBAGARAN, R. & VENKATESAN, R. 2010. Characterization, purification and phylogenetic analysis of a cytolysin from the sea anemone Heteractis magnifica of the Indian Ocean. *J Venom Anim Toxins*

16**,** 223-240.

KEM, W. R., PENNINGTON, M. W. & NORTON, R. S. 1999. Sea anemone toxins as templates for the design of immunosuppressant drugs. *Perspect. Drug Discovery Des,* 15-16**,** 111-129.

KETTLEWORTH, C. R. 2007. *Cell Apoptosis Research Advances,* Nova Science.

KHOO, H., LIM, J. & TAN, C. 1995. Effects of sea anemone (Heteractis magnifica and Actinia equina) cytolysins on synaptosomal uptake of GABA and choline. *Toxicon,* 33**,** 1365-1371.

KHOO, K., KAM, W., KHOO, H., GOPALAKRISHNAKONE, P. & CHUNG, M. 1993. Purification and partual characterization of 2 cytolysisns from a tropical sea-anemone, Heteractis-magnifica *Toxicon,* 31**,** 1567-1579.

KHUDER, S. A. 2001. Effect of cigarette smoking on major histological types of lung cancer: a meta-analysis. *Lung Cancer,* 31**,** 139-148.

KIM, R., TANABE, K., UCHIDA, Y., EMI, M., INOUE, H. & TOGE, T. 2002. Current status of the molecular mechanisms of anticancer drug-induced apoptosis. The contribution of molecular-level analysis to cancer chemotherapy. *Cancer Chemother Pharmacol,* 50**,** 343-352.

KLAUNIG, J. & KAMENDULIS, L. 2004. The role of oxidative stress in carcinogenesis. *Annu Rev Pharmacol Toxicol,* 44**,** 239-267.

KOMINSKY, D., BICKEL, R. & TYLER, K. 2002. Reovirus-induced apoptosis requires both death receptorand mitochondrial-mediated caspase-dependent pathways of cell death. *Cell Death Differ,* 9**,** 926-933.

KOZLOV, S., ANDREEV, I., MURASHEV, A., SKOBTSOV, D., D'IACHENKO, I. & GRISHIN, E. 2009. New polypeptide components from the Heteractis crispa sea anemone with analgesic activity. *Bioorg Khim,* 35**,** 789-798.

KROEMER, G. 2003. Mitochondrial control of apoptosis: an introduction. *Biochem Biophys Res Commun,* 304**,** 433-435.

KUENG, W., SILBER, E. & EPPENBERGER, U. 1989. Quantification of cells cultured on 96-well plates. *Anal. Biochem.,* 182**,** 16-19.

LAGOS, P., DURAN, R., CERVEÑANSKY, C., FREITAS, J. & SILVEIRA, R. 2001. Identification of hemolytic and neuroactive fractions in the venom of the sea anemone Bunodosoma cangicum. *Braz J Med Biol Res,* 34**,** 895-902.

LANIOA, M., MORERAB, V., ALVAREZA, C., TEJUCA, M., GOÂ MEZA, M., PAZOSA, F., BESADAB, V. & MARTÕÂNEZ, D. 2001a. Purifcation and characterization of two hemolysins from Stichodactyla helianthus. *Toxicon,* 39**,** 187-194.

LANIOA, M., MORERAB, V., ALVAREZA, C., TEJUCA, M., GOÂ MEZA, M., PAZOSA, F., BESADAB, V. & MARTÕÂNEZ, D. 2001b. Purifcation and characterization of two hemolysins from Stichodactyla helianthus. *Toxicon,* 39**,** 187-194.

LEE, Y., KIM, J., KIM, S., HA, S., MOK, T., MITSUDOMI, T. & CHO, B. 2011. Lung cancer in never smokers: Change of a mindset in the molecular era. *Lung Cancer,* 72**,** 9-15.

LI, C., URIBE, D. & DALING, J. 2005. Clinical characteristics of different histologic types of breast cancer. *Br J Cancer,* 93**,** 1046-1052.

LI, C., YU, D., NEWMAN, R., CABRAL, F., STEPHENS, L., HUNTER, N., MILAS, L. & WALLACE, S. 1998. Complete regression of well-established tumors using a novel water-soluble poly(L-glutamic acid)-paclitaxel conjugate. *Cancer Res,* 58**,** 2404-2409.

LIM, L. Y., VIDNOVIC, N., ELLISEN, L. W. & LEONG, C. 2009. Mutant p53 mediates survival of breast cancer cells. *Br J Cancer. 2009 Nov 3; 101(9): 1606–1612.,* 101**,** 1606-1612.

LIPNICK, S. & JACOBSON, M. 2006. *Developmental Neurobiology,* Kluwer Academic/Plenum Publishers.

LIU, M., WANG, Z., LI, H., WU, R., LIU, Y. & WU, Q. 2004. The permeabilization of the mitochondrial outer membrane and release of intermembrane space proteins such as cytochrome c, Smac/DIABLO, and

AIF, are unequivocally one of the central events in apoptosis. *Toxicol Appl Pharmacol,* 194**,** 141-155.

LOUIS, C. J. 1978. *Tumors Basic Principles and Clinical Aspects,* Churchill livingstone.

LV, K., LIU, L., WANG, L., YU, J., LIU, X., YONGXIA, C., MINJUN, D., RONGYUE, T., LINJIAO, W., PEIFEN, F., WUGUO, D. M., WENXIAN, H. M. & LISONG, T. M. 2012. Lin28 Mediates Paclitaxel Resistance by Modulating p21, Rb and Let-7a miRNA in Breast Cancer Cells. *PLOS ONE,* 7.

MACFARLANE, M. 2003a. TRAIL-induced signalling and apoptosis. *Toxicol Lett,* 139**,** 89-97.

MACFARLANE, M. 2003b. TRAIL-induced signalling and apoptosis. *Toxicol Lett,* 139**,** 89-97.

MADHU, R. & MADHU, K. 2007. Occurrence of anemonefishes and host sea anemones in Andaman and Nicobar Islands. *J. Mar. Biol. Ass. India,* 49**,** 118 - 126.

MALHI, H., GUICCIARDI, M. E. & GORES, G. J. 2010. Hepatocyte Death: A Clear and Present Danger. *Physiological Reviews,* 90**,** 1165–1194.

MALPEZZI, E. L. A., MATSUI, D. H., GROOTE, S. C. T. S., FREITAS, J. C., SANTELLI, G. M. & FERNANDES, J. B. 1995. Antitumoral activity in an organic extract of the sea anemone Bunodosoma caissarum. *Toxicon,* 33**,** 291-299.

MARINO, A., VALVERI, V., MUIÀ, C., CRUPI, R., RIZZO, G., MUSCI, G. & GIUSEPPA, L. S. 2004. Cytotoxicity of the nematocyst venom from the sea anemone Aiptasia mutabilis. *Comp Biochem Physiol C.,* 139**,** 295-301.

MARIOTTINI, G. & PANE, L. 2014a. Cytotoxic and Cytolytic Cnidarian Venoms. A Review on Health Implications and Possible Therapeutic Applications. *Toxins,* 6**,** 108–151.

MARIOTTINI, G. L. & PANE, L. 2014c. Cytotoxic and Cytolytic Cnidarian Venoms. A Review on Healt Implications and Possible Therapeutic Applications. *Toxins,* 6**,** 108-151.

MARTIN, A. & WEBER, B. 2000a. Genetic and Hormonal Risk Factors in Breast Cancer. *J Natl Cancer Inst,* 92**,** 1126-35.

MARTIN, A. & WEBER, B. 2000b. Genetic and hormonal risk factors in breast cancer. *J Natl Cancer Inst,* 92**,** 1126-1135.

MAXWELL, P. 2001. Global cancer statistics in the year 2000. *Lancet Oncol,* 2**,** 533–543.

MAYER, A., GLASER, K., CUEVAS, C., JACOBS, R., KEM, W., LITTLE, R., MCINTOSH, J., NEWMAN, D., POTTS, B. & SHUSTER, D. 2010. The odyssey of marine pharmaceuticals: a current pipeline perspective. *Trends Pharmacol Sci,* 31**,** 255-265.

MCILWAIN, D. R., BERGER, T. & MAK, T. W. 2013. Caspase Functions in Cell Death and Disease. *Cold Spring Harb Perspect Biol,* 5.

MEIJERS-HEIJBOER, H., VAN GEEL, B., VAN PUTTEN, W., HENZEN-LOGMANS, S., SEYNAEVE, C., MENKE-PLUYMERS, M., BARTELS, C., VERHOOG, L., VAN DEN OUWELAND, A., NIERMEIJER, M., BREKELMANS, C. & KLIJN, J. 2001. Breast cancer after prophylactic

bilateral mastectomy in women with a BRCA1 or BRCA2 mutation. *N Engl J Med,* 345**,** 159-164.

MICKUVIENE, I., KIRVELIENE, V. & JUODKA, B. 2004. Experimental survey of non-clonogenic viability assays for adherent cells in vitro. *Toxicol In Vitro,* 18**,** 639-648.

MILLER, K., WANG, M., GRALOW, J., DICKLER, M., COBLEIGH, M., PEREZ, E., SHENKIER, T., DAVID CELLA, D. & NANCY E. DAVIDSON, N. E. 2007. Paclitaxel plus Bevacizumab versus Paclitaxel Alone for Metastatic Breast Cancer. *N Engl J Med,* 357**,** 2666-2676.

MITSUDOMI, T., KOSAKA, T., ENDOH, H., HORIO, Y. & HIDA, T. 2005. Mutations of the Epidermal Growth Factor Receptor Gene Predict Prolonged Survival After Gefitinib Treatment in Patients With Non–Small-Cell Lung Cancer With Postoperative Recurrence. *J Clin Oncol,* 23.

MOSMANN, T. 1983. Rapid colorimetric assay for cellular growth and survival: application to proliferation and cytotoxicity assays. *J Immunol Methods,* 65**,** 55-63.

NAKAMURA, T., MATSUMOTO, K., KIRITOSHI, A., TANO, Y. & NAKAMURA, T. 1997. Induction of Hepatocyte Growth Factor in Fibroblasts by Tumor-derived Factors Affects Invasive Growth of Tumor Cells: In Vitro Analysis of Tumor-Stromal Interactions. *Cancer Res,* 57**,** 3305-3313.

NATIONAL BREAST AND OVARIAN CANCER CENTRE. 2010. *Chemotherapy for the treatment of advanced breast cancer* [Online].

NATIONAL CANCER INSTITUTE. 2012. *Background information and SOPs | Physical Sciences in Oncology* [Online].

NEDOSYKO, A., YOUNG, J., EDWARDS, J. & BURKE DA SILVA, K. 2014a. Searching for a toxic key to unlock the mystery of anemonefish and anemone symbiosis. *PLoS One,* 9.

NEDOSYKO, A. M., YOUNG, J. E., EDWARDS, J. W. & BURKE DA SILVA, K. 2014b. Searching for a Toxic Key to Unlock the Mystery of Anemonefish and Anemone Symbiosis. *PLOS ONE*.

NEWMAN, D. J. & CRAGG, G. M. 2014. marine sourced anticancer drug and cancer pain control agant in clinical and late preclinical development. *Mar Drugs,* 12**,** 255-278.

NICKELS, S., TRUONG, T., HEIN, R., STEVENS, K., BUCK, K., BEHRENS, S., EILBER, U., SCHMIDT, M., HÄBERLE, L., VRIELING, A., GAUDET, M., FIGUEROA, J., SCHOOF, N., SPURDLE, A. & RUDOLPH, A. 2013. Evidence of gene-environment interactions between common breast cancer susceptibility loci and established environmental risk factors. *PLoS Genet,* 9.

NICOLETTI, I., MIGLIORATI , G., PAGLIACCI, M. C., GRIGNANI, F. & C., R. 1991 A rapid and simple method for measuring thymocyte apoptosis by propidium iodide staining and flow cytometry. *J Immunol Methods,* 139**,** 271-279.

PEGRAM, M., PIENKOWSKI, T., NORTHFELT, D., EIERMANN, W., PATEL, R., FUMOLEAU, P., QUAN, E., CROWN, J., TOPPMEYER, D., SMYLIE, M., RIVA, A., BLITZ, S., PRESS, M., REESE, D., LINDSAY, M. & SLAMON, D. 2004. Results of two open-label, multicenter phase II

studies of docetaxel, platinum salts, and trastuzumab in HER2-positive advanced breast cancer. *J Natl Cancer Inst,* 19**,** 759-769.

PENTO, D., PE´REZ-BARZAGA, V., Dı´AZ, I., REYTOR, M., CAMPOS, J., FANDO, R., CALVO, L., CILLI, E., MORERA, V., CASTELLANOS, L., PAZOS, F., LANIO, M., LVAREZ, C., PONS, T. & TEJUCA, M. 2011a. Validation of a mutant of the pore-forming toxin sticholysin-I for the construction of proteinase-activated immunotoxins. *Protein Eng Des Sel,* 24**,** 485–493.

PENTO, D., PE´REZ-BARZAGA, V., Dı´AZ, I., REYTOR, M., CAMPOS, J., FANDO, R., CALVO, L., CILLI, E., MORERA, V., CASTELLANOS, L., PAZOS, F., LANIO, M., LVAREZ, C., PONS, T. & TEJUCA, M. 2011b. Validation of a mutant of the pore-forming toxin sticholysin-I for the construction of proteinase-activated immunotoxins. *Protein Eng Des Sel,* 24**,** 485–493.

PEREZ, E., SUMAN, V., ROWLAND, K., INGLE, J., SALIM, M., LOPRINZI, C., FLYNN, P., MAILLIARD, J., KARDINAL, C., KROOK, J., THROWER, A., VISSCHER, D. & JENKINS, R. 2005. Two concurrent phase II trials of paclitaxel/carboplatin/trastuzumab (weekly or every-3-week schedule) as first-line therapy in women with HER2-overexpressing metastatic breast cancer. *Clin Breast Cancer,* 6**,** 425-432.

PETIT, J., AVRIL, M., MARGULIS, A., CHASSAGNE, D., GERBAULET, A., DUVILLARD, P., AUPERIN, A. & RIETJENS, M. 2000. Evaluation of cosmetic results of a randomized trial comparing surgery and radiotherapy in the treatment of basal cell carcinoma of the face. *Plast Reconstr Surg,* 105**,** 2544-2551.

PIZON, M., RAMPANARIVO, H., TAUZIN, S., CHAIGNE-DELALANDE, B., DABURON, S., CASTROVIEJO, M., MOREAU, P., MOREAU, J. F. & LEGEMBRE, P. 2011a. Actin-independent exclusion of CD95 by PI3K/AKT signalling: implications for apoptosis. *Eur J Immunol,* 41**,** 2368-2378.

PIZON, M., RAMPANARIVO, H., TAUZIN, S., CHAIGNE-DELALANDE, B., DABURON, S., CASTROVIEJO, M., MOREAU, P., MOREAU, J. F. & LEGEMBRE, P. 2011b. Actin-independent exclusion of CD95 by PI3K/AKT signalling: implications for apoptosis. *Eur J Immunol. ,* 41**,** 2368-2378.

PRITCHARD, K. 2003. Endocrine therapy of advanced disease: analysis and implications of the existing data. *Clin Cancer Res,* 9**,** 460-467.

PRUNELL, G. F., ARBOLEDA, V. A. & TROY, C. M. 2005. Caspase Function in Neuronal Death: Delineation of the Role of Caspases in Ischemia. *Curr Drug Targets CNS Neurol Disord,* 4**,** 51-61.

RAMEZANPOUR, M., BURK DA SILVA, K. & SANDERSON, B. 2014a. The effect of sea anemone (H. magnifica) venom on two human breast cancer lines: death by apoptosis. *Cytotechnology,* 66**,** 845-852.

RAMEZANPOUR, M., BURK DA SILVA, K. & SANDERSON, B. 2014b. Venom present in sea anemone (Heteractis magnifica) induces apoptosis in non-small-cell lung cancer A549 cells through activation of mitochondria-mediated pathway. *Biotechnol Lett,* 36**,** 489-495.

RAMEZANPOUR, M., BURKE DA SILVA, K. & SANDERSON, B. 2012a. Differential susceptibilities of human lung, breast and skin cancer cell lines to killing by five sea anemone venoms. *JVAT,* 18**,** 157-163.

RAMEZANPOUR, M., BURKE DA SILVA, K. & SANDERSON, B. J. 2012b. Differential susceptibilities of human lung, breast and skin cancer cell lines to killing by five sea anemone venoms. *JVAT,* 18**,** 157-163.

RAY, M. R., JABLONS, D. & HE, B. 2010. Lung cancer therapeutics that target signaling pathways: an update. *Expert Rev Respir Med,* 4**,** 631–645.

REED, J. 2003. Apoptosis-targeted therapies for cancer. *Cancer Cell,* 3**,** 17-22.

ROBERT, N., LEYLAND-JONES, B., ASMAR, L., BELT, R., ILEGBODU, D., LOESCH, D., RAJU, R., VALENTINE, E., SAYRE, R., COBLEIGH, M., ALBAIN, K., MCCULLOUGH, C., FUCHS, L. & SLAMON, D. 2006. Randomized phase III study of trastuzumab, paclitaxel, and carboplatin compared with trastuzumab and paclitaxel in women with HER-2-overexpressing metastatic breast cancer. *J Clin Oncol,* 24**,** 2786-2792.

ROCHA, J., PEIXE, L., GOMES, N. & CALADO, R. 2011a. Cnidarians as a Source of New Marine Bioactive Compounds—An Overview of the Last Decade and Future Steps for Bioprospecting. *Mar Drugs,* 9**,** 1860–188.

ROCHA, J., PEIXE, L., GOMES, N. C. M. & CALADO, R. 2011c. Cnidarians as a Source of New Marine Bioactive Compounds—An Overview of the Last Decade and Future Steps for Bioprospecting. *Mar. Drugs,* 9**,** 1860-1886.

RODRÍGUEZ-HERNÁNDEZ, A., BREA-CALVO, G., FERNÁNDEZ-AYALA, D., CORDERO, M., NAVAS, P. & SÁNCHEZ-ALCÁZAR, J. 2006. Nuclear caspase-3 and caspase-7 activation, and poly(ADP-ribose) polymerase cleavage are early events in camptothecin-induced apoptosis. *Apoptosis,* 11**,** 131-139.

RODRÍGUEZ, E., BARBEITOS, M., BRUGLER, M., CROWLEY, L., GRAJALES, A., GUSMÃO, L., HÄUSSERMANN, V., REFT, A. & DALY, M. 2014. Hidden among Sea Anemones: The First Comprehensive Phylogenetic Reconstruction of the Order Actiniaria (Cnidaria, Anthozoa, Hexacorallia) Reveals a Novel Group of Hexacorals. *PLoS One,* 9.

RÖYTTÄ, M., LAINE, K. & HÄRKÖNEN, P. 1987. Morphological studies on the effect of taxol on cultured human prostatic cancer cells. *Prostate,* 11**,** 95-106.

RUBIO-MOSCARDO, F., BLESA, D., MESTRE, C., SIEBERT, R., BALASAS, T., BENITO, A., ROSENWALD, A., CLIMENT, J., MARTINEZ, J., SCHILHABEL, M., KARRAN, E., GESK, S., ESTELLER, M., DELEEUW, R., STAUDT, L., FERNANDEZ-LUNA, J., PINKEL, D., DYER, M. & MARTINEZ-CLIMENT, J. 2005. Characterization of 8p21.3 chromosomal deletions in B-cell lymphoma: TRAIL-R1 and TRAIL-R2 as candidate dosage-dependent tumor suppressor genes. *Blood,* 106**,** 3214-3222.

SAADAT, S. 2008. Can We Prevent Breast Cancer? *Int J Health Sci,* 2**,** 167-170.

SANTOS, Y., MARTÍNEZ, M., SANDOVAL, A., RODRÍGUEZ, A., FALCÓN, A., HEIMER DE LA COTERA, E., AGUILAR, M., FLORES, P., FELIX, R. & ARREGUÍN, R. 2013. Arrhythmogenic effect of a crude extract from sea anemone Condylactis gigantea: possible involvement of rErg1 channels. *Toxicon,* 1**,** 47-54.

SAOTOME, K., MORITA, H. & UMEDA, M. 1989. Cytotoxicity test with simplified crystal violet staining method using microtitre plates and its application to injection drugs. *Toxicol In Vitro,* 3**,** 317-321.

SARKAR, A. 2009. *Biology of Cancer*, Discovery Publishing House.

SEIPEL, K. & SCHMID, V. 2006. Mesodermal anatomies in cnidarian polyps and medusae. *Int J Dev Biol,* 50**,** 589-99.

SENAN, S., DE RUYSSCHER, D., GIRAUD, P., MIRIMANOFF, R., BUDACH, V. & CANCER., R. G. O. E. O. F. R. A. T. O. 2004. Literature-based recommendations for treatment planning and execution in high-dose radiotherapy for lung cancer. *Radiother Oncol,* 71**,** 139-46.

SENCIC, L. & MACEK, P. 1990. New method for isolation of venom from the sea-anemone Actinia-cari - purification and characterization of cytolytic toxins. *Comp Biochem Phys B,* 97**,** 687-693.

SENDEROWICZ, A. M. 2003 Novel Small Molecule Cyclin-Dependent Kinases Modulators in Human Clinical Trials. *Cancer Biol Ther,* 2**,** 84-95.

SHAW, A., KIM, D., NAKAGAWA, K., SETO, T., CRINÓ, L., AHN, M., DE PAS, T., BESSE, B., SOLOMON, B., BLACKHALL, F., WU, Y., THOMAS, M., O'BYRNE, K., MORO-SIBILOT, D., CAMIDGE, D., MOK, T., HIRSH, V., RIELY, G., IYER, S., TASSELL, V., POLLI, A., WILNER, K. & JÄNNE, P. 2013a. Crizotinib versus Chemotherapy in Advanced ALK-Positive Lung Cancer. *N Engl J Med,* 368**,** 2385-94.

SHAW, A., KIM, D., NAKAGAWA, K., SETO, T., CRINÓ, L., AHN, M., DE, P. T., BESSE, B., SOLOMON, B., BLACKHALL, F., WU, Y., THOMAS, M., O'BYRNE, K., MORO-SIBILOT, D., CAMIDGE, D., MOK, T., HIRSH, V., RIELY, G., IYER, S., TASSELL, V., POLLI, A., WILNER, K. & JÄNNE, P. 2013c. Crizotinib versus Chemotherapy in Advanced ALK-Positive Lung Cancer. *N Engl J Med,* 368**,** 2385-2394.

SHEPHERD, F., DANCEY, J., RAMLAU, R., MATTSON, K., GRALLA, R., O'ROURKE, M., LEVITAN, N., GRESSOT, L., VINCENT, M., BURKES, R., COUGHLIN, S., KIM, Y. & J., B. 2000. Prospective Randomized Trial of Docetaxel Versus Best Supportive Care in Patients With Non–Small-Cell Lung Cancer Previously Treated With Platinum-Based Chemotherapy. *J Clin Oncol,* 18**,** 2095-2103.

SHIVAPURKAR, N., REDDY, J., CHAUDHARY, P. & GAZDAR, A. 2003. Apoptosis and lung cancer: a review. *J Cell Biochem,* 88**,** 885-898.

SIMMONS, T. L., ANDRIANASOLO, E., MCPHAIL, K., FLATT, P. & GERWICK , W. 2005. Marine natural products as anticancer drugs. *Mol Cancer Ther,* 4**,** 333-342.

SITHRANGA, N. & KATHIRESAN, K. 2010. Anticancer Drugs from Marine Flora: An Overview. *J Onco*.

SMITH, P. K., KROHN, R. I., HERMANSON, G. T., MALLIA, A. K., GARTNER, F. H., PROVENZANO, M. D., FUJIMOTO, E. K., GOEKE, N. M., OLSON, B. J. & KLENK, D. C. 1985. Measurement of protein using bicinchoninic acid. *Anal. Biochem.* , 150**,** 76-85.

STANDKERA, L., BERESSA, L., GARATEIXC, A., CHRISTD, T., RAVENSD, U., SALCEDAE, E., SOTOE, E., JOHNA, H., FORSSMANNA, W. & ANEIROSC, A. 2006. A new toxin from the sea anemone Condylactis gigantea with effect on sodium channel inactivation. *Toxicon,* 48**,** 211-220.

SUAREZ-JIMENEZ, G. M., HERNANDEZ, A. B. & EZQUERRA-BRAUER, J. M. 2012. Bioactive Peptides and Depsipeptides with Anticancer Potential: Sources from Marine Animals. *Mar Drugs,* 10**,** 963–986.

SUBRAMANIAN, B., SANGAPPELLAI, T., RAJAK, R. & DIRAVIAM, B. 2011. Pharmacological and biomedical properties of sea anemones Paracondactylis indicus, Paracondactylis sinensis, Heteractis magnifica and Stichodactyla haddoni from East coast of India. *Asian Pac J Trop Med,* 4**,** 722-726.

SULIMAN, A., LAM, A., DATTA, R. & SRIVASTAVA, R. 2001. Intracellular mechanisms of TRAIL: apoptosis through mitochondrial-dependent and -independent pathways. *Oncogene,* 20**,** 2122-2133.

SVENSON, J., STENSEN, W., BRANDSDAL, B., HAUG, B., MONRAD, J. & SVENDSEN, J. 2008. Antimicrobial peptides with stability toward tryptic degradation. *Biochemistry,* 47**,** 3777-3788.

TARRUELLA, S. & MARTÍN, M. 2009. Recent advances in systemic therapy. Advances in adjuvant systemic chemotherapy of early breast cancer. *Breast Cancer Res,* 11**,** 204.

TEJUCA, M., PÉREZ-BARZAGA, V., PAZOS , F., ÁLVAREZ, C. & LANIOM.E. 2009. Construction of sea anemone cytolysin-based immunotoxins for selective killing of cancer cells. *Rev. Cub. Física,* 26**,** 15-22.

THAKUR, N. L., THAKUR, A. N. & MULLER, W. E. 2005. Marine natural products in drug discovery. *Nat. prod. radiance* 4.

TOYOOKA, S., TOYOOKA, K., MARUYAMA, R., VIRMANI, A., GIRARD, L., MIYAJIMA, K., HARADA, K., ARIYOSHI, Y., TAKAHASHI, T., SUGIO, K., BRAMBILLA, E., GILCREASE, M., MINNA, J. & GAZDAR, A. 2001. DNA Methylation Profiles of Lung Tumors. *Mol Cancer Ther,* 1**,** 61-67.

TSUJIMOTO, Y. & SHIMIZU, S. 2007 Role of the mitochondrial membrane permeability transition in cell death. *Apoptosis,* 12**,** 835-840.

TYTGAT, J. & BOSMANS, F. 2007a. Sea anemone venom as a source of insecticidal peptides acting on voltage-gated Na+ channels. *Toxicon,* 49**,** 550-560.

TYTGAT, J. & BOSMANS, F. 2007b. Sea anemone venom as a source of insecticidal peptides acting on voltage-gated Na+ channels. *Toxicon,* 49**,** 550-560.

UECHI, G., TOMAA, H., ARAKAWAB, T. & SATO, Y. 2005a. Molecular cloning and functional expression of hemolysin from the sea anemone Actineria villosa. *Protein Expr Purif,* 40**,** 379–384.

UECHI, G., TOMAA, H., ARAKAWAB, T. & SATO, Y. 2005b. Molecular cloning and functional expression of hemolysin from the sea anemone Actineria villosa. *Protein Expr Purif,* 40**,** 379–384.

VANDER MOLEN, M. A., RUBIN, C. T., MCLEOD, K. J., MCCAULEY, K. L. & DONAHUE, H. J. 1996. Gap Junctional Intercellular Communication Contributes to Hormonal Responsiveness in Osteoblastic Networks. *J. Biol. Chem,* 271**,** 12165-12171.

WALKER, J. M. 1996. The Bicinchoninic Acid (BCA) assay for protein quantitation. *In:* WALKER, J. M. (ed.) *The Protein Protocols Handbook.* Humana Press.

WANG, Y., CHUA, K. & KHOO, H. 2000. A new cytolysin from the sea anemone, Heteractis magnifica: isolation, cDNA cloning and functional expression

Biochim Biophys Acta, 1478**,** 9-18.

WANG, Y., HE, Q. Y., SUN, R. W., CHE, C. M. & CHIU, J. F. 2005 GoldIII porphyrin 1a induced apoptosis by mitochondrial death pathways related to reactive oxygen species. *Cancer Res,* 65**,** 11553-11564.

WEINBERG, R. A. 2007. *The biology of cancer,* Garland Science.

WEINBERG, R. A. 2013. *The Biology of Cancer,* Garland Science.

WEINSTEIN, I. 2000. Disorders in cell circuitry during multistage carcinogenesis: the role of homeostasis. *Carcinogenesis,* 21**,** 857-864.

WYKOSKY, J., FENTON, T., FURNARI, F. & CAVENEE, W. 2011. Therapeutic targeting of epidermal growth factor receptor in human cancer: successes and limitations. *Chin J Cancer,* 30**,** 5-12.

YAMADA, T., MEHTA, R., LEKMINE, F., CHRISTOV, K., KING, M., MAJUMDAR, D., SHILKAITIS, A., GREEN, A., BRATESCU, L., BEATTIE, C. & DAS GUPTA, T. 2009. A peptide fragment of azurin induces a p53-mediated cell cycle arrest in human breast cancer cells. *Mol Cancer Ther,* 8**,** 2947-58.

YAMAGUCHI, Y., HASEGAWA, Y., HONMA, T., NAGASHIMA, Y. & K., S. 2010a. Screening and cDNA Cloning of Kv1 Potassium Channel Toxins in Sea Anemones. *Mar Drugs,* 8**,** 2893-905.

YAMAGUCHI, Y., HASEGAWA, Y., HONMA, T., NAGASHIMA, Y. & SHIOMI, K. 2010b. Screening and cDNA Cloning of Kv1 Potassium Channel Toxins in Sea Anemones. *Mar Drugs,* 8**,** 2893-2905.

YAMASAKI-MIYAMOTO, Y., YAMASAKI, M., TACHIBANA, H. & YAMADA, K. 2009. Fucoidan induces apoptosis through activation of caspase-8 on human breast cancer MCF-7 cells. *J Agric Food Chem,* 57**,** 8677-82.

YOULDEN, D., CRAMB, S. & BAADE, P. 2008. The International Epidemiology of Lung Cancer: Geographical Distribution and Secular Trends. *J Thorac Oncol,* 3**,** 819-831.

YOUNG, F. M., PHUNGTAMDET, W. & SANDERSON, B. J. 2005. Modification of MTT assay conditions to examine the cytotoxic effects of amitraz on the human lymphoblastoid cell line, WIL2NS. *Toxicol In Vitro,* 19**,** 1051-9.

YOUNG, O., RENSHAW, L., MACASKILL, E., WHITE, S., FARATIAN, D., THOMAS, J. & DIXON, J. 2008. Effects of fulvestrant 750 mg in premenopausal women with oestrogen-receptor-positive primary breast cancer. *Eur J Cancer,* 44**,** 391-399.

APPENDICES

Appendix I

Diagnostic features of Actiniaria taxa are included with voucher location and accession numbers. All the taxonomic changes are indicated by asterisks (taxa whose placement has changed) or underlined (taxa are included in molecular analyses) (Rodríguez et al., 2014).

Higher Taxon	Family	Genus	Species	Voucher	12S	16S	18S	28S	Cox3
Actiniaria									
Actinernoidea	Actinernidae	*Actinernus*	*antarcticus*	AMNH	KJ482930	KJ482966	KJ483023	KJ483126	----------
		Isactinernus	*quadrolobatus*	AMNH	KJ482932	KJ482968	KJ483024	KJ483105	KJ482998
		Synhalcurias	*laevis*	NA	KJ482942	----------	KJ483021	KJ483120	----------
	Halcuriidae	*Halcurias*	*pilatus*	AMNH	KJ482931	KJ482967	KJ483020	KJ483109	KJ482997
Actinoidea	Actiniidae	*Actinia*	*fragacea*	CAS	EU190714	EU190756	EU190845	KJ483085	GU473334
		Anemonia	*viridis*	CAS	EU190718	EU190760	EU190849	KJ483095	GU473335
		Anthopleura	*elegantissima*	KUNHM	EU190713	EU190755	EU190844	KJ483104	GU473333
		Anthostella	*stephensoni*	AMNH	JQ810719	JQ810721	JQ810723	KJ483132	JQ810726
		Bolocera	*kerguelensis*	AMNH	KJ482925	KJ482965	KJ483029	KJ483133	KJ482985
		Bunodactis	*verrucosa*	KUNHM	EU190723	EU190766	EU190854	KJ483084	----------
		Bunodosoma	*grandis*	KUNHM	EU190722	EU190765	EU190853	KJ483083	GU473336
		Epiactis	*lisbethae*	KUNHM	EU190727	EU190771	EU190858	EU190816	GU473360
		Glyphoperidium	*bursa*	AMNH	KJ482923	KJ482961	KJ483033	KJ483136	KJ482982
		Isotealia	*antarctica*	AMNH	JQ810720	JQ810722	----------	----------	JQ810727
		Isosicyonis	*alba*	AMNH	----------	KJ482959	KJ483030	KJ483134	KJ482981
		Isosicyonis	*striata*	AMNH	EU190736	EU190781	EU190864	KJ483137	FJ489493
		Korsaranthus	*natalinesis*	AMNH	KJ482920	KJ482958	KJ483017	KJ483117	KJ482987
		Macrodactyla	*doreenensis*	KUNHM	EU190739	EU190785	EU190867	KJ483049	GU473342
		Urticina	*coriacea*	KUNHM	GU473282	EU190797	EU190877	KJ483094	GU473351
	Actinodendridae	*Actinostephanus*	*haeckeli*	KUNHM	KJ482936	EU190762	KJ483034	----------	GU473353
	Capneidae	*Capnea*	*georgiana*	AMNH	----------	KJ482951	KJ483022	KJ483050	KJ482990
	Haloclavidae	*Haloclava*	*producta*	KUNHM	EU190734	EU190779	AF254370	KJ483097	JF833008
		Haloclava	sp.	AMNH	KJ482924	KJ482963	KJ483031	KJ483138	KJ482989
		Harenactis	*argentina*	AMNH	KJ482926	KJ482964	KJ483026	KJ483047	KJ482984
		Peachia	*cylindrica*	KUNHM	EU190743	EU190789	KJ483015	EU190732	----------
		Stephanthus	*antarcticus*	AMNH	KJ482927	KJ482960	KJ483019	KJ483092	KJ482983
	Liponematidae	*Liponema*	*brevicornis*	KUNHM	EU190738	EU190784	EU190866	KJ483139	KJ483001
		Liponema	*multiporum*	AMNH	KJ482922	KJ482962	----------	----------	----------
	Phymanthidae	*Phymanthus*	*loligo*	KUNHM	EU190745	EU190791	EU190871	----------	GU473345
	Preactiidae	*Dactylanthus*	*antarcticus*	AMNH	GU473272	AY345877	AF052896	KJ483086	GU473358
		Preactis	*milliardae*	AMNH	KJ482921	KJ482957	KJ483018	KJ483118	KJ482986
	Stichodactidae	*Heteractis*	*magnifica*	KUNHM	EU190732	EU190777	EU190862	KJ483093	KJ482988
Actinostoloidea	Actinostolidae	*Actinostola*	*crassicornis*	AMNH	----------	EU190753	EU190843	KJ483098	GU473332
		Actinostola	*chilensis*	AMNH	----------	GU473285	GU473302	KJ483110	GU473357
		Actinostola	*georgiana*	AMNH	KJ482928	KJ482952	KJ483032	KJ483099	KJ482991
		Antholoba	*achates*	AMNH	GU473269	GU473284	GU473301	KJ483128	GU473356
		Anthosactis	*janmayeni*	AMNH	KJ482938	GU473292	GU473308	KJ483091	GU473363
		Hormosoma	*scotti*	AMNH	EU190733	EU190778	EU190863	KJ483090	GU473366
		Paranthus	*niveus*	AMNH	GU473277	GU473295	GU473311	KJ483072	GU473344

		Stomphia	*didemon*	KUNHM	KJ482929	EU190795	EU190875	KJ483127	GU473348
		Stomphia	*selaginella*	AMNH	GU473280	GU473298	GU473314	GU473331	GU473349
Edwardsioidea	Edwardsiidae	*Edwardsia*	*elegans*	AMNH	EU190726	EU190770	EU190857	KJ483087	GU473338
		Edwardsia	*japonica*	KUNHM	GU473274	GU473288	GU473304	KJ483048	GU473359
		Edwardsia	*timida*	KUNHM	GU473281	----------	GU473315	KJ483088	KJ482996
		Edwardsianthus	*gilbertensis*	AMNH	EU190728	EU190772	EU190859	EU190817	----------
		Nematostella	*vectensis*	KUNHM	EU190750	AY169370	AF254382	KJ483089	FJ489501
Metridioidea	Actinoscyphiidae	*Actinoscyphia*	*plebeia*	AMNH	EU190712	EU190754	FJ489437	KJ483067	FJ489476
	Aiptasiidae	*Aiptasia*	*mutabilis*	KUNHM	JF832963	FJ489418	FJ489438	KJ483115	FJ489505
		Aiptasia	*pallida*	KUNHM	EU190715	EU190757	EU190846	EU190803	KJ482979
		Bartholomea	*annulata*	AMNH	EU190721	EU190763	EU190851	KJ483068	FJ489483
		Neoaiptasia	*morbilla*	KUNHM	EU190742	EU190788	EU190869	KJ483075	JF833010
	Aliciidae	*Alicia*	*sansibarensis*	AMNH	KJ482933	KJ482953	KJ483016	KJ483116	KJ483000
		Triactis	*producta*	KUNHM	EU490525	----------	EU190876	KJ483125	GU473350
	Amphianthidae	*Amphianthus*	sp.	USNM	FJ489413	FJ489432	FJ489450	FJ489467	FJ489502
		Peronanthus	sp.	AMNH	KJ482917	KJ482956	KJ483014	KJ483066	KJ482976
	Andvakiidae	*Andvakia*	*boninensis*	KUNHM	EU190717	EU190759	EU190848	KJ483053	FJ489479
		Andvakia	*discipulorum*	KUNHM	GU473273	GU473287	GU473316	KJ483051	----------
		Telmatactis	sp.	AMNH	JF832968	JF832979	KJ483013	KJ483135	----------
	Antipodactinidae	*Antipodactis*	*awii*	AMNH	GU473271	GU473286	GU473303	KJ483074	GU473337
	Bathyphelliidae	*Bathyphellia*	*australis*	KUNHM	FJ489402	FJ489422	EF589063	EF589086	FJ489482
	Boloceroididae	*Boloceroides*	*mcmurrichi*	KUNHM	GU473270	----------	EU190852	KJ483103	KJ483002
		Bunodeopsis	*globulifera*	AMNH	KJ482940	KJ482949	KJ483025	KJ483122	KJ482992
	Diadumenidae	*Diadumene*	*cincta*	KUNHM	EU190725	EU190769	EU190856	KJ483106	FJ489490
		Diadumene	*leucolena*	KUNHM	JF832957	JF832977	JF832986	KJ483123	JF833006
		Diadumene	sp.	KUNHM	JF832960	JF832976	JF832980	KJ483130	JF833005
	Galantheanthemidae	*Galatheanthemum*	sp. nov.	NA	KJ482918	KJ482955	KJ483012	KJ483065	KJ482977
		Galatheanthemum	*profundus*	AMNH	KJ482919	KJ482954	KJ483011	KJ483119	KJ482978
	Gonatiniidae	*Gonactinia*	*prolifera (Chile)*	AMNH	KJ482935	----------	KJ483008	KJ483112	KJ482994
		Gonactinia	*prolifera (USA)*	AMNH	KJ482937	KJ482969	KJ483009	KJ483077	KJ482995
		Protantea	*simplex*	AMNH	KJ482939	KJ482970	KJ483010	KJ483078	KJ482993
	Halcampidae	*Cactosoma*	sp. nov.	AMNH	GU473279	GU473297	GU473313	GU473329	GU473346
		Halcampa	*duodecimcirrata*	KUNHM	JF832966	EU190776	AF254375	EU190820	----------
		Halcampoides	*purpurea*	AMNH	EU190735	EU190780	AF254380	KJ483100	----------
	Haliplanellidae	*Haliplanella*	*lineata (USA)*	KUNHM	EU190730	EU190774	EU190860	KJ483108	FJ489506
		Haliplanella	*lineata (Japan)*	KUNHM	JF832965	JF832973	JF832987	KJ483107	JF833007
	Hormathiidae	*Actinauge*	*richardi*	KUNHM	EU190719	EU190761	EU190850	KJ483055	FJ489480
		Adamsia	*palliata*	KUNHM	FJ489398	FJ489419	FJ489436	KJ483101	FJ489474
		Allantactis	*parasitica*	KUNHM	FJ489399	FJ489420	FJ489439	KJ483056	FJ489478
		Calliactis	*japonica*	KUNHM	FJ489403	FJ489423	FJ489441	KJ483057	FJ489486

		Calliactis	*parasitica*	KUNHM	EU190711	EU190752	EU190842	KJ483102	FJ489475
		Calliactis	*polypus*	KUNHM	FJ489407	FJ489427	FJ489445	KJ483058	FJ489485
		Calliactis	*tricolor*	KUNHM	FJ489405	FJ489425	FJ489443	KJ483059	FJ489488
		Chondrophellia	*orangina*	USNM	FJ489406	FJ489426	FJ489444	KJ483060	FJ489489
		Hormathia	*armata*	AMNH	EU190731	EU190775	EU190861	KJ483062	FJ489491
		Hormathia	*lacunifera*	AMNH	FJ489409	FJ489428	FJ489446	KJ483063	FJ489492
		Hormathia	*pectinata*	AMNH	FJ489415	FJ489430	FJ489448	FJ489465	FJ489497
		Paracalliactis	*japonica*	CMHN	FJ489411	FJ489429	FJ489447	KJ483061	FJ489496
		Paraphelliactis	sp.	KUNHM	FJ489412	FJ489431	FJ489449	FJ489466	FJ489498
	Isanthidae	*Isanthus*	*capensis*	AMNH	JF832967	GU473291	GU473307	KJ483096	GU473362
		Isoparactis	*fabiani*	AMNH	JF832964	GU473283	GU473300	KJ483124	GU473355
	Kadosactinidae	*Alvinactis*	*chessi*	USNM	GU473278	GU473296	GU473312	KJ483052	GU473352
		Cyananthea	*hourdezi*	USMN	GU473275	GU473293	GU473309	KJ483081	GU473364
		Jasonactis	*erythraios*	USNM	----------	GU473289	GU473305	KJ483079	GU473339
		Kadosactis	*antarctica*	AMNH	FJ489410	EU190782	EU190865	KJ483080	FJ489504
	Metridiidae	*Metridium*	*s. lobatum*	KUNHM	JF832962	JF832971	JF832981	KJ483114	JF833002
		Metridium	*senile (WA)*	KUNHM	EU190740	EU190786	AF052889	KJ483076	FJ489494
		Metridium	*senile (ME)*	AMNH	KJ482916	KJ482950	KJ483035	KJ483113	KJ482975
	Nemathidae	*Nemanthus*	*nitidus*	KUNHM	EU190741	EU190787	EU190868	KJ483064	FJ489495
	Ostiactinidae	*Ostiactis*	*pearseae*	CAS	EU190751	EU190798	EU190878	KJ483082	GU473365
	Phelliidae	*Phellia*	*gausapata*	ZSM	EU190744	EU190790	EU190870	KJ483054	FJ489473
		Phellia	*exlex*	KUNHM	JF832958	JF832978	JF832984	KJ483121	JF833004
	Sagartiidae	*Actinothoe*	*sphyrodeta*	ZSM	FJ489401	FJ489421	FJ489440	KJ483111	FJ489481
		Anthothoe	*chilensis*	ZSM	FJ489397	FJ489416	FJ489434	FJ489453	FJ489470
		Cereus	*pedunculatus*	KUNHM	EU190724	EU190767	EU190855	EU190813	FJ489471
		Cereus	*herpetodes*	KUNHM	JF832956	JF832969	JF832983	JF832992	----------
		Sagartia	*elegans*	KUNHM	----------	----------	JF832989	JF832994	JF833012
		Sagartia	*troglodytes*	KUNHM	EU190746	EU190792	EU190872	KJ483073	FJ489499
		Sagartia	*ornata*	AMNH	JF832959	JF832975	JF832985	KJ483069	JF833011
		Sagartiogeton	*laceratus*	KUNHM	EU190748	EU190794	EU190874	KJ483071	FJ489500
		Sagartiogeton	*undatus*	KUNHM	FJ489400	FJ489417	FJ489435	KJ483070	FJ489472
		Verrillactis	*paguri*	KUNHM	FJ489414	FJ489433	FJ489440	KJ483046	FJ489503
Antipatharia									
	Aphanipathidae	*Acanthopathes*	*thyoides*	USMNH	----------	FJ376986	FJ389896	FJ626238	FJ381654
		Elatopathes	*abietina*	USMNH	----------	FJ376989	FJ389894	FJ626233	KF054437
		Phanopathes	*expansa*	USMNH	----------	FJ376987	FJ389897	FJ626242	FJ381655
		Aphanipathes	*verticillata mauiensis*	NA	----------	----------	KF054359	KF054361	KF054458
	Antipathidae	*Antipathes*	*griggi*	NA	----------	FJ376997	FJ389904	FJ429304	GU296504
		Antipathes	*atlantica*	USMNH	----------	FJ376985	FJ389895	FJ626239	HM060616
		Cirrhipathes	*anguina*	NA	----------	KJ482973	FJ389905	FJ626243	HM060614

		Stichopathes	*cf. dissimilis*	NA	----------	FJ376996	FJ626245	FJ626234	KF054420
		Stichopathes	*cf. flagellum*	NA	----------	FJ376995	FJ389903	FJ626232	FJ381660
	Cladopathidae	*Chrysopathes*	*formosa*	NA	DQ304771	DQ304771	----------	----------	DQ304771
		Trissopathes	*pseudotristicha*	USMNH	----------	FJ376991	FJ389899	FJ429305	KF054409
	Leiopathidae	*Leiopathes*	*glaberrima*	NA	FJ597644	FJ597644	FJ389898	FJ626241	FJ597644
	Myriopathidae	*Tanacetipathes*	*barbadensis*	USMNH	----------	FJ376988	FJ626244	FJ626240	FJ381650
	Schizopathidae	*Dendrobathypathes*	*boutillieri*	NA	----------	FJ376992	FJ389900	FJ626236	FJ381651
		Parantipathes	*cf. hirondelle*	NA	----------	FJ376994	FJ389902	FJ626235	----------
		Stauropathes	*cf. punctata*	NA	----------	FJ376993	FJ389901	FJ626237	FJ381657
Ceriantharia									
	Arachnactinidae	*Isarachnanthus*	*nocturnus*	NA	----------	JX125669	AB859826	AB859832	KJ482980
	Cerianthidae	*Ceriantheomorphe*	*brasiliensis*	NA	KJ482914	JF915193	AB859823	AB859831	KJ482974
		Pachycerianthus	sp.	NA	KJ482915	----------	AB859829	AB859833	----------
Corallimorpharia									
	Corallimorphidae	*Corallimorphus*	*profundus*	AMNH	KJ482941	KJ482972	KJ483027	KJ483129	----------
	Corynactinidae	*Corynactis*	*viridis*	NA	EF597099	EF589058	EF589065	KJ483041	----------
	Ricordeidae	*Ricordea*	*florida*	NA	KJ482913	EF589057	EF589067	KJ483045	DQ640648
Octocorallia									
	Briareidae	*Briareum*	*asbestinum*	RMNH	DQ640649	DQ640649	KF992837	KF992839	DQ640649
	Gorgoniidae	*Antillogorgia*	*bipinnata*	RMNH	DQ640646	NC008157	KJ411642	KJ411643	DQ640646
	Nephtheidae	*Dendronephthya*	*sinaiensis*	RMNH	FJ372991	FJ372991	KF992836	KF992838	FJ372991
Scleractinia									
	Agariciidae	*Pavona*	*varians*	NA	EF597083	KJ482943	AF052883	EU262847	NC008165.1
	Caryophylliidae	*Phyllangia*	*mouchezii*	GB	EF597022	AF265605	AF052887	EU262798	----------
		Thalamophyllia	*riisei*	GB	EF597087	AF265590	----------	EU262868	----------
	Dendrophylliidae	*Tubastraea*	*coccinea*	NA	EF597045	KJ482948	AJ133556	EU262864	----------
	Faviidae	*Montastraea*	*franksi*	NA	EF597010	KJ482947	AY026382	AY026375	NC007225.1
	Fungiacyathidae	*Fungiacyathus*	*marenzelleri*	NA	EF597074	XXXXXXX	EF589074	EU262862	----------
	Pocilloporidae	*Madracis*	*mirabilis*	GB	NC011160	NC011160	AY950684	EU262845	----------
		Meandrina	*meandrites*	NA	EF597032	----------	KJ483005	EU262815	----------
		Pocillopora	*meandrina*	NA	EF596977	KJ482945	KJ483006	EU262803	NC009798.1
	Siderastreidae	*Siderastrea*	*siderea*	NA	EF597067	KJ482944	KJ483007	EU262848	NC008167
Zoanthidea									
	Epizoanthidae	*Epizoanthus*	*illoricatus*	NA	AY995901	EU591597	KC218424	KJ483036	----------
			paguricola	NA	AY995902	AY995928	KC218427	KJ483042	----------
			scotinus	NA	GQ464967	----------	KC218425	KJ483043	----------
		Hydrozoanthus	*gracilis*	NA	GQ464953	AY995942	KJ483003	KJ483038	----------
			tunicans	MNHG	GQ464955	EU828760	KJ483004	KJ483039	----------
	Parazoanthidae	*Parazoanthus*	*axinellae*	NA	GQ464940	EU828754	KC218416	KJ483044	----------
			puertoricense	NA	AY995916	EU828758	KC218418	KJ483037	----------

			swiftii	NA	GQ464945	EU828755	KC218417	KJ483040	----------
		Savalia	*savaglia*	GB	AY995905	DQ825686	HM044299	HM044298	DQ825686
Hexacorallia incertis ordinis	Relicanthidae	*Relicanthus*	*daphneae*	FMNH	KJ482934	KJ482971	KJ483028	KJ483131	KJ482999

Appendix II: Recipes for Media

RPMI Medium

RPMI 1640 medium (10.44 g/L, with L-Glu and Phenol Red); 17.8 ml/L sodium bicarbonate (Pfizer, WA, Australia); HEPES (2.38 g); D-Glucose (2.5 g); 10 ml penicillin/streptomycin (Gibco®, Hyclone, Utah, USA) and 10% heat inactivated foetal bovine serum (FBS) Hyclon, Victoria, Australia) were added to 0.5 L of sterile Milli-Q water (Baxter) and mixed with stirring. The medium solution was adjusted to pH 7.4 and the volume increased to 1 L. The complete medium was sterilised by 0.22 µm filter under aseptic conditions and stored in 200–400 ml aliquots in sterile 500 ml glass Pyrex bottles at 4°C. The medium was equilibrated to 37°C when required for use.

DMEM Medium

Dulbecco's minimal essential medium powder (13.5 g/L); 17.8 ml/L sodium bicarbonate (Pfizer, WA, Australia); L-Glutamine (0.592 g/L); 10 ml penicillin/streptomycin (Gibco®, Hyclone, Utah, USA) and 10% heat inactivated foetal bovine serum (FBS) (Hyclon, Victoria, Australia) were added to 0.5 L of sterile Milli-Q water (Baxter). The medium was adjusted to pH 7.4 and sterilised by 0.22 µm filter before storage at 4°C. The temperature and PH of media were equilibrated for 30 minutes in a 37°C incubator immediately before use.

Appendix III

Statistical analyses of venom extracts (*H. magnifica*, *H. crispa*, *H. malu*, *E. quadricolor* and *C. adhaesivum*) on A549 human lung cancer, T47D human breast cancer and A431human skin cancer cell lines using MTT assay and crystal violet assay.

Venom (40 µg/ml)	A549 (MTT assay)	T47D (MTT assay)	A431 (MTT assay)	A549 (CVA assay)	T47D (CVA assay)	A431 (CVA assay)
H. magnifica (24h)	$p < 0.05$	$p > 0.05$	$p < 0.05$	$p < 0.05$	$p > 0.05$	$p > 0.05$
H. magnifica (48h)	$p < 0.05$	$p > 0.05$	$p > 0.05$	$p > 0.05$	$p > 0.05$	$p > 0.05$
H. magnifica (72h)	$p < 0.05$	$p > 0.05$	$p < 0.05$	$p > 0.05$	$p > 0.05$	$p > 0.05$
H. malu (24h)	$p < 0.05$	$p < 0.05$	$p < 0.05$	$p < 0.05$	$p < 0.05$	$p < 0.05$
H. malu (48h)	$p < 0.05$	$p > 0.05$	$p < 0.05$	$p < 0.05$	$p < 0.05$	$p < 0.05$
H. malu (72h)	$p < 0.05$	$p < 0.05$	$p < 0.05$	$p < 0.05$	$p > 0.05$	$p < 0.05$
H. crispa (24h)	$p > 0.05$	$p > 0.05$	$p > 0.05$	$p > 0.05$	$p > 0.05$	$p > 0.05$
H. crispa (48h)	$p < 0.05$	$p > 0.05$	$p > 0.05$	$p > 0.05$	$p > 0.05$	$p > 0.05$
H. crispa (72h)	$p < 0.05$	$p > 0.05$	$p > 0.05$	$p > 0.05$	$p > 0.05$	$p > 0.05$
E. quadricolor (24h)	$p < 0.05$	$p > 0.05$	$p < 0.05$	$p < 0.05$	$p > 0.05$	$p < 0.05$
E. quadricolor (48h)	$p < 0.05$	$p > 0.05$	$p < 0.05$	$p < 0.05$	$p > 0.05$	$p < 0.05$
E. quadricolor (72h)	$p < 0.05$	$p > 0.05$	$p < 0.05$	$p < 0.05$	$p > 0.05$	$p < 0.05$

C. adhaesivum (24h)	$p < 0.05$	$p > 0.05$	$p < 0.05$	$p < 0.05$	$p < 0.05$	$p < 0.05$
C. adhaesivum (48h)	$p < 0.05$	$p > 0.05$	$p < 0.05$	$p < 0.05$	$p < 0.05$	$p < 0.05$
C. adhaesivum (72h)	$p < 0.05$	$p < 0.05$	$p < 0.05$	$p < 0.05$	$p < 0.05$	$p < 0.05$

Appendix IV

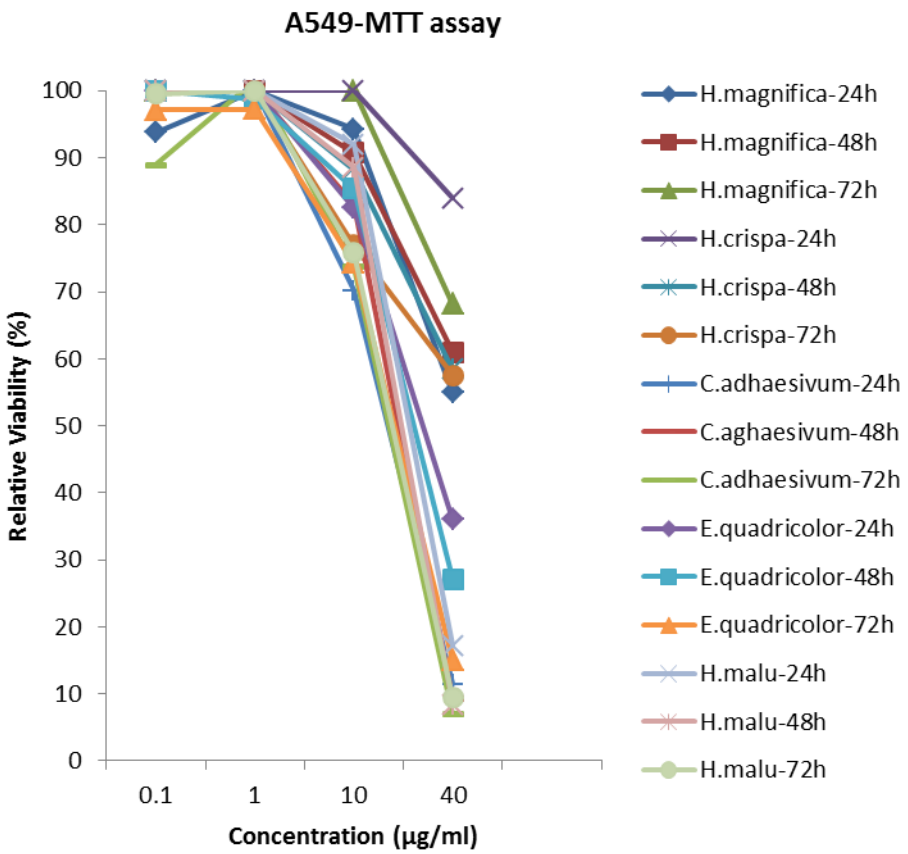

Figure A4.1: Relative cell viability (%) of A549 cells estimated by MTT assay

Notes: In 96-well plates after 24h, 48h and 72h of exposure to *H. magnifica*, *H. crispa*, *C. adhaesivum*, *E. quadricolor* and *H. malu* venom extract. Data shown as mean ± SEM, n = 3. * = treatments significantly different from the 0 µg/ml untreated control at $p < 0.05$.

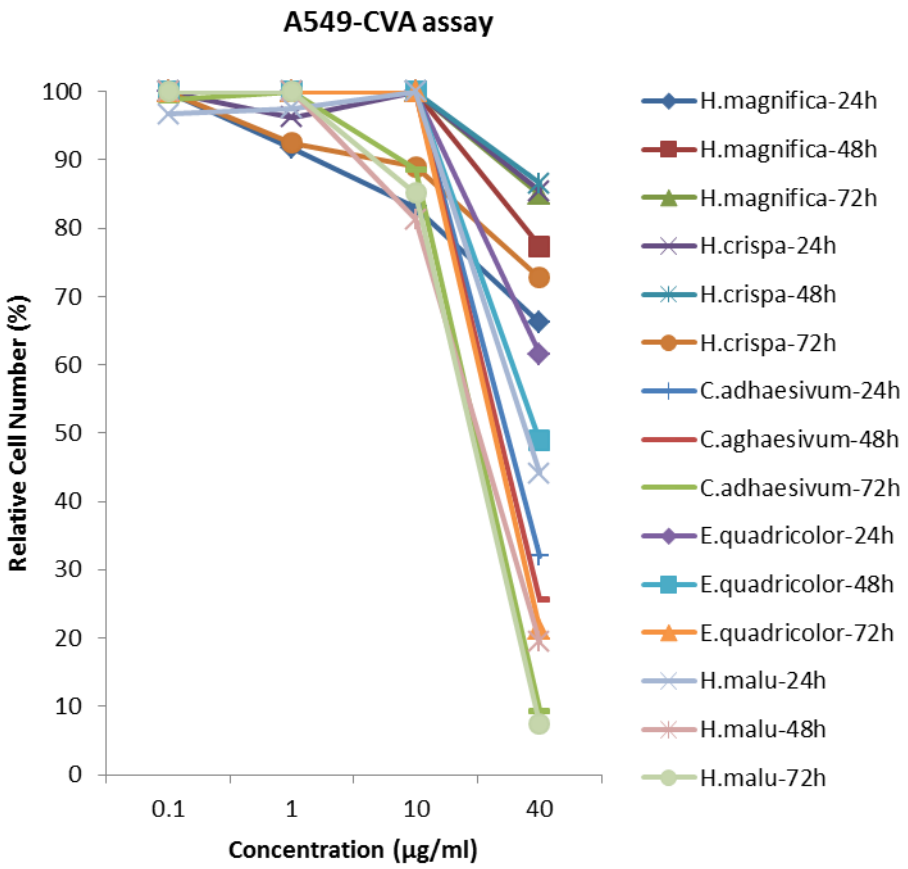

Figure A4.2: Cell number (%) of A549 cells estimated by crystal violet assay

Notes: In 96-well plates following 24h, 48h and 72h exposure to *H. magnifica*, *H. crispa*, *C. adhaesivum*, *E. quadricolor* and *H. malu* venom extract. Data shown as mean ± SEM, n = 3. * = treatments significantly different from the 0 µg/ml untreated control at $p < 0.05$.

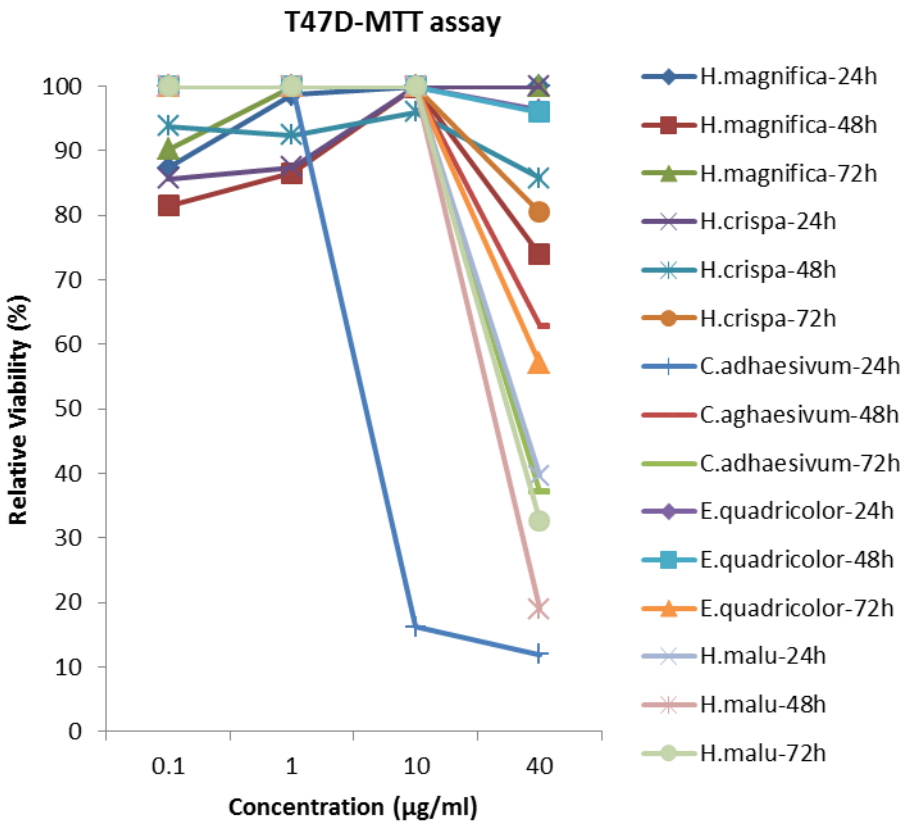

Figure A4.3: Effect of *H. magnifica, H. crispa, C. adhaesivum, E. quadricolor* and *H. malu* venom extract on growth of T47D cells measured by MTT assay at 24h, 48h and 72h

Notes: Data shown as mean ± SEM, n = 3. * = treatments significantly different from the 0 µg/ml untreated control at $p < 0.05$.

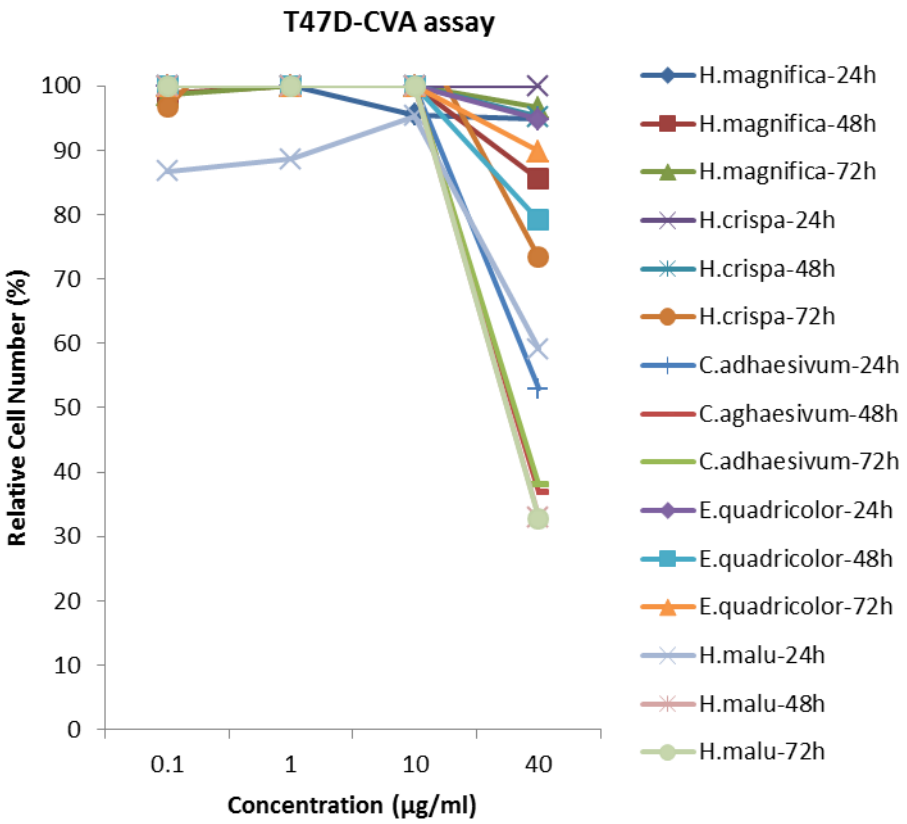

Figure A4.4: Effect of *H. magnifica*, *H. crispa*, *C. adhaesivum*, *E. quadricolor* and *H. malu* venom extract on growth of T47D cells measured by crystal violet assay at 24h, 48h and 72h

Notes: Data shown as mean ± SEM, n = 3. * = treatments significantly different from the 0 µg/ml untreated control at $p < 0.05$.

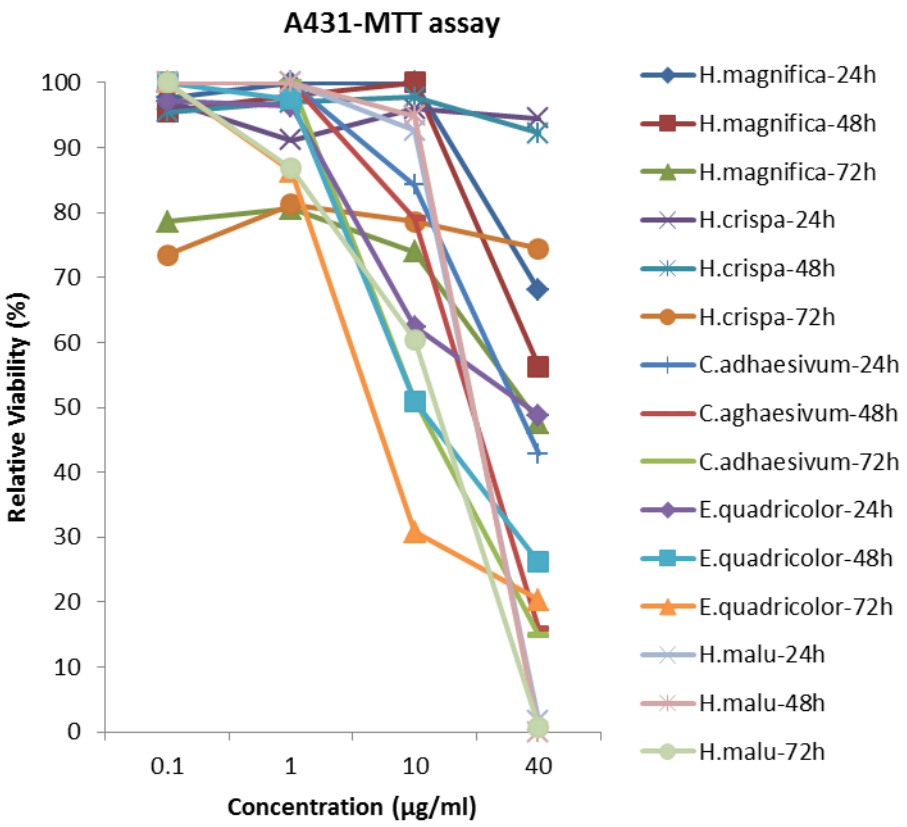

Figure A4.5: Cytotoxic effect of *H. magnifica*, *H. crispa*, *C. adhaesivum*, *E. quadricolor* and *H. malu* venom extract on A431 cell line measured by MTT assay at 24h, 48h and 72h

Notes: Data shown as mean ± SEM, n = 3. * = treatments significantly different from the 0 µg/ml untreated control at $p < 0.05$.

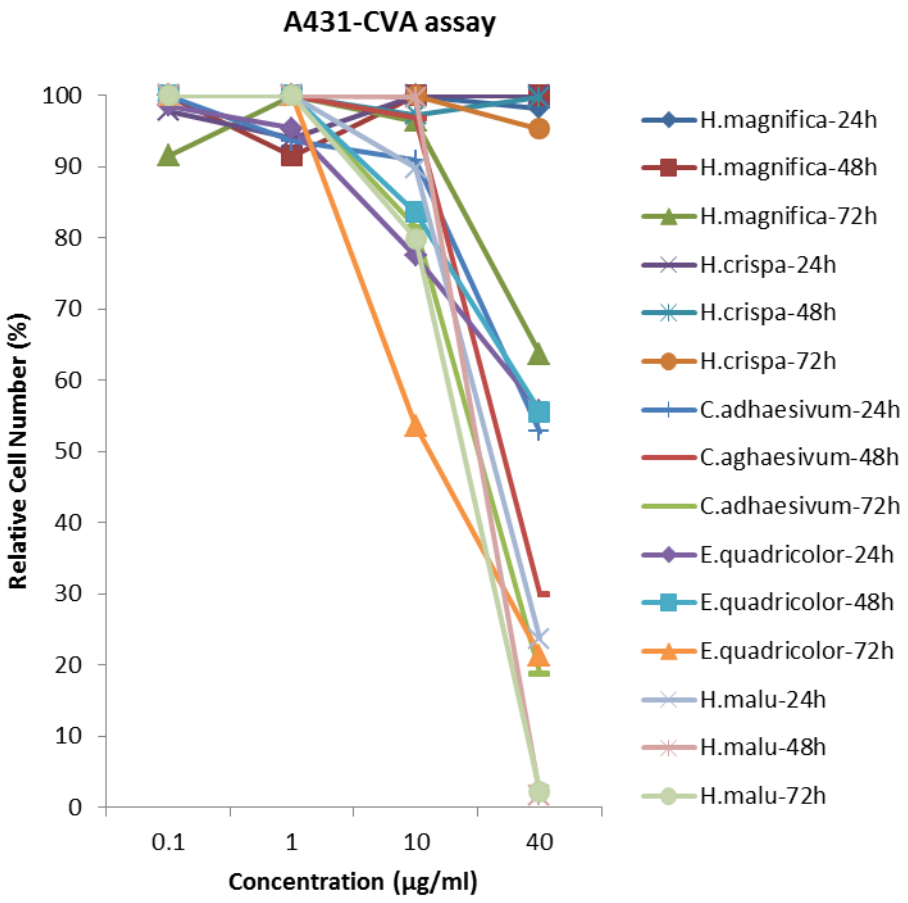

Figure A4.6: Cytotoxic effect of *H. magnifica*, *H. crispa*, *C. adhaesivum*, *E. quadricolor* and *H. malu* venom extract on A431 cell line measured by crystal violet assay at 24h, 48h and 72h

Notes: Data shown as mean ± SEM, n = 3. * = treatments significantly different from the 0 µg/ml untreated control at $p < 0.05$.

Appendix V

Figure A5.1: SDS-PAGE of purified fraction (peak A, see Figure 5.1)

Notes: Aliquots of pooled fraction showed only one main protein band. Visualization was by silver staining. The molecular masses indicated as 9 kDa were estimated from standards electrophoresed in a parallel lane.

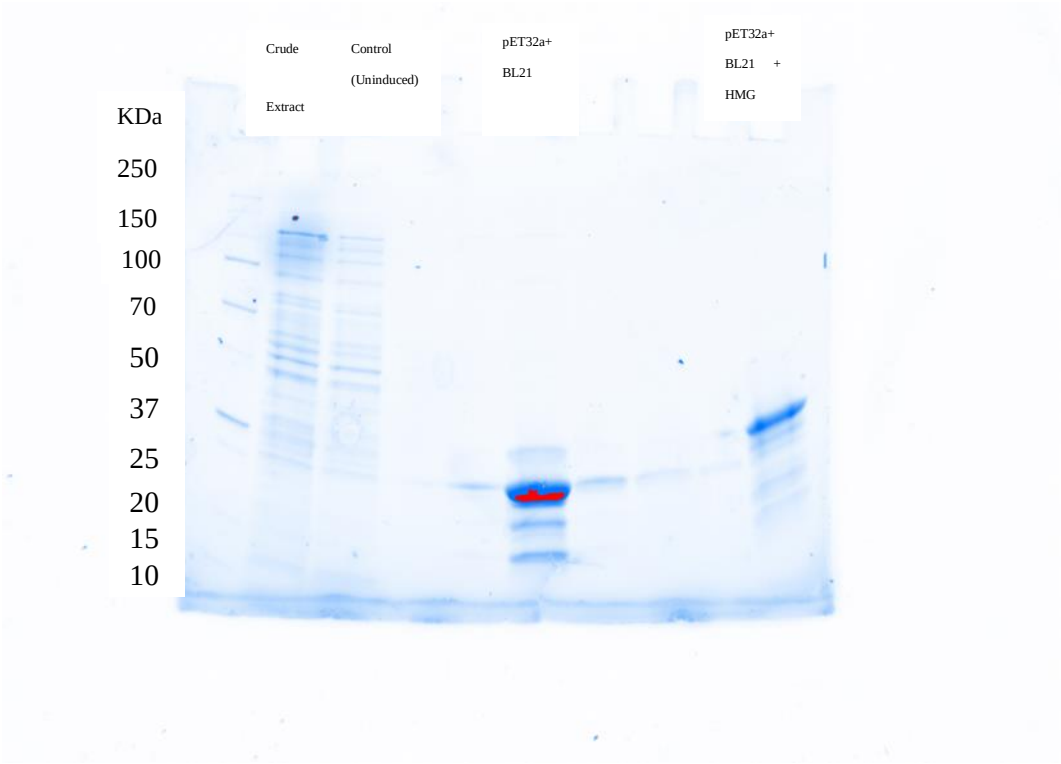

Figure A5.2: SDS-PAGE analysis of HMP expression

Notes: KDa, molecular mass standards; Lane 1, supernatant from control (uninduced) cells; Lane 2, supernatant from induced cells vector = pET32a+ BL21; Lane 3, supernatant from induced cells vector = pET32a+ BL21 + HMP DNA.

Appendix VI: Manufacturers

Reagent	Company	Address	Catalogue No	Lot No.
Acetic acid	AJAX Chemicals	Melbourne Victoria	2789	802479
Acetonitrile	Merck	Kilsyth, Victoria	100029	1000291000
Albumin from bovine serum (BSA)	Sigma-Aldrich	Missouri, USA	P0914	074K0567
Ammonium acetate	Sigma-Aldrich	Missouri, USA	A1542	631618
Ammonium bicarbonate	Merck	Kilsyth, Victoria	101136	1011361000
Bicinchoninic acid solution	Sigma-Aldrich	Missouri, USA	B9643	095K5301
Boric acid	Sigma-Aldrich	Missouri, USA	B7901	10043353
Bromophenol blue	Sigma-Aldrich	Missouri, USA	B0126	115399
Calcium chloride ($CaCl_2$)	Sigma-Aldrich	Missouri, USA	C-3881	118H2075
Caspase-Glo 3/7 assay kit	Promega	Madison, USA	G8091	32230701
Caspase-Glo 8 assay kit	Promega	Madison, USA	G8200	7966
Caspase-Glo 9 assay kit	Promega	Madison, USA	G8210	320671
Copper (II) sulphate pentahydrate	Sigma-Aldrich	Missouri, USA	C2284	095K5305
Crystal violet	Aldrich	Sydney NSW	548-62-9	DN00129MG
Dimethyl disulphide 99%	Aldrich	Sydney, NSW	471569-250ML	06709ME
Dulbecco's modified Eagle medium	Sigma-Aldrich	CA, USA	D7777	021M8309

Ethanol	Merck	Kilsyth, Victoria	4.10230.9010	42542
Ethylenediaminetetraacetic acid	Sigma-Aldrich	CA, USA	431788	60004
Foetal bovine serum (FBS)	Thermo Scientific	Melbourne, Australia	1501002	GVD0074
FITC annexin V apoptosis detection kit	BD Pharmingen	San Diego,CA	556547	40238
Formaldehyde solution	Merck	Kilsyth, Victoria	103999	1039991000
Glucose	Sigma-Aldrich	Missouri, USA	G-7021	87H13255
L-Glutamine	Sigma-Aldrich	Missouri, USA	G-8540	096K0115
Glycine	Sigma-Aldrich	Missouri, USA	G8898	56406
Glycerol	APS Chemicals	Sydney NSW	242-500ml	KNAI
HEPES. 99.5% cell culture tested	Sigma-Aldrich	Missouri, USA	H4034	104K5419
Hydrochloric acid (HCl)	Ajax Fine Chemicals	Sydney NSW	1789	A1367
Imidazole	Sigma-Aldrich	Missouri, USA	15513	288324
Isopropyle β-D-1 thiogalactopyranoside 99%	Sigma-Aldrich	Missouri, USA	16758	092M4001V
Methanol	Merck	Kilsyth, Victoria	113153	1131532500
Minisart sterile 0.2 µm filters	Sartorius Stedim	Dandenong South, Victoria	16534	90750103 exp 2012-08
Mitochondria staining kit	Sigma-Aldrich	Missouri, USA	CS0390	101M4052
Penicillin/streptomycin solution	Invitrogen Corporation	Utah, USA	15140122	1308291
Potassium chloride (KCl)	APS Chemicals	Sydney, NSW	383	F9A224

Potassium carbonate	Sigma-Aldrich	Missouri, USA	P5833	584087
Ribonuclease A from bovine pancreas	Sigma-Aldrich	Missouri, USA	R-5503	9001-99-4
Propidium iodide (PI)	Sigma-Aldrich	Missouri, USA	P4170	120M1218V
RPMI-1640 medium	Sigma-Aldrich	Missouri, USA	R1383	017K8316
Silver nitrate	Sigma-Aldrich	Missouri, USA	209139	7761888
Sodium azide	Sigma-Aldrich	Missouri, USA	S8032	2478521
Sodium acetate	Sigma-Aldrich	Missouri, USA	E302406	127093
Sodium bicarbonate $NaHCO_3$	Pfizer	West Ryde, NSW	S084PA	CE63
Sodium bicarbonate $NaHCO_3$	Sigma-Aldrich	Missouri, USA	S8875	49H0407
Sodium chloride (NaCl)	Ajax Chemicals	Auburn, NSW	465	70334315
Sodium dihydrogen orthophosphate (NaH_2PO_4)	BDH	Kilsyth, Victoria	10245	59137
Sodium dodecyl sulphate (SDS) 20%	Sigma-Aldrich	Missouri, USA	L4509	046K0085
Sodium hydroxide	Sigma-Aldrich	Missouri, USA	S8045	1310732
Sodium phosphate	Sigma-Aldrich	Missouri, USA	342483	7601549
Sodium thiosulphate	Sigma-Aldrich	Missouri, USA	S7026	7772987
Thiazolyl blue tetrazolium (MTT)	Sigma-Aldrich	Missouri, USA	M5655	03330DH
Trizma	Sigma-Aldrich	Missouri, USA	T4661	77861
TRIzol reagent	Ambion	CA, USA	15596026	47309

0.25% trypsin-EDTA solution	Sigma-Aldrich	Missouri, USA	T4049	126K2338
Tris-HCl	Sigma-Aldrich	Missouri, USA	T1503	074K5442
Triton X-100	Sigma-Aldrich	Missouri, USA	T-8787	110K0251
Trypan blue	Sigma-Aldrich	Missouri, USA	T-8154	725711
Trypsin	Fisher Scientific	CA, USA	SH3023601	J121841
Water for injections (sterile)	Astra Zeneca	Export Park, Adelaide, SA	825700	B308035 Sep 2011

Appendix VII: Recipes for Solutions

20 × Phosphate buffer saline (PBS)

NaCl (AJAX Chemicals; 160 g); KCl (4 g); $Na_2H_2PO_4$ (AJAX Chemicals; 28.8 g) and KH_2PO_4 (AJAX Chemicals; 4.8 g) were added to 900 ml of Milli-Q water. The pH was adjusted to 7.4 and then the volume was increased to 1 L with Milli-Q water. The stock solution was filter sterilized and stored at room temperature (RT) in a sterile 1 L glass Pyrex bottle.

1× Phosphate buffer saline (PBS)

50 ml of 20 × phosphate buffer saline (PBS) was added to 950 ml of Milli-Q water. The 1 × PBS was filtered and stored at RT in a sterile 1 L glass Pyrex bottle.

Crystal violet solution (0.5%)

Crystal violet (0.5g; Aldrich) was dissolved in a 50% methanol solution (Merck; 100 ml) and stored at RT in a glass Pyrex bottle in a fume hood until required.

Acetic acid solution (33%)

33 ml of acetic acid solution (APS Chemicals) was added to 67 ml of reverse osmosis water and stored in a 100 ml sterile glass Pyrex bottle at room temperature (RT).

Methylthiazol thiazolyl tetrazolium (MTT)

MTT cell-culture-tested (250 mg) was dissolved in 50 ml of sterile 1 × PBS to give a final concentration of 5 mg/ml. This MTT stock solution was filtered using

a sterile 0.22 μm filter (Sartorius) and under aseptic conditions, distributed into sterile 1.5 mL Eppendorf tubes and stored at -20°C until required.

Sodium dodecyl sulphate (SDS) in 0.02 M hydrogen Chloride (HCl)

200 ml of 20% SDS was prepared by adding SDS (40 g) to 0.02 M HCl (100 ml) with stirring and heat to dissolve powder. HCl 0.02 M was added to give a final volume of 200 ml.

0.02 M Hydrogen chloride (HCl)

Hydrogen chloride (12 M) was diluted in 1 L of Milli-Q water to a final concentration of 0.02 M by adding 1.66 ml of 12 M HCl to 998.33 ml of water. The solution was stored at RT in a glass Pyrex bottle.

Trypan blue solution (0.2%)

Trypan blue (0.2 g) was dissolved in 0.9% NaCl saline solution (100 ml) then filtered through Whatman grade I filter paper and stored at 4°C until required.

Sodium chloride solution 0.9% (NaCl)

A 100 ml 0.9% sodium chloride solution was prepared by dissolving 0.9 g of NaCl in ~90 ml of Milli-Q water by stirring. The volume was then increased to 100 ml with Milli-Q water, and the solution stored in a glass Pyrex bottle at RT.

Annexin V-FITC apoptosis detection kit

Annexin V-FITC apoptosis detection kit (BD Pharminutesgen™: 556547) was stored at 2–8ºC: it contained annexin V-FITC (51-65874X); propidium iodide (PI) staining solution (51-66211E) and annexin V binding buffer (51-66121E).

0.1% Sodium azide

0.1 ml of sodium azide (S8032) was added to 90 ml of sterile 1× PBS and mixed with stirring. The solution was then increased to 100 ml with PBS and stored in a glass Pyrex bottle at RT until required.

Propidium iodide (PI) for staining the nucleus of cells

A stock solution of PI (P4170) was prepared by dissolving PI (1 mg) in Milli-Q water (1 ml).

10 mg/ml of RNAse in Milli-Q water

10 mg of RNAse (Sigma; R-5503) was prepared by dissolving 10 mg of RNAse in 9 ml of Milli-Q water. The solution was mixed, then increased to 10 ml with Milli-Q water and stored at 4ºC until required.

Triton X-100 solution (0.1%)

1 ml of Triton X-100 was added to 90 ml of sterile 1 × PBS and mixed by stirring. The solution was then increased to 100 ml with PBS and stored in a glass Pyrex bottle at RT until required.

Caspase reagents

The Caspase-Glo® 3/7(G8090; Promega); Caspase-Glo® 8(G8200; Promega) and Caspase-Glo® 9(G8210; Promega) were stored at -20°C protected from light prior to use. For assays, the pre-equilibrated buffer (10 ml) was added to the lyophilized substrate (25°C) and mixed by gentle inversion to dissolve the substrate. Any remaining substrate not used on the day of the experiment was stored at 4°C

protected from light for three days (all experiments were performed within this time period).

200 × JC-1 stock solution (1 mg/ml)

200 µl of dimethyl sulfoxide (DMSO) (D8418) added from the bottle supplied with the kit to the vial containing the JC-1 dye (T4069). Then the vial was firmly closed and vortex for two minutes. The vial was left at RT for about 15 minutes to ensure the JC-1 dye was completed dissolved. The JC-1 solution containing the remaining solvent was transferred, the solution was mixed and stored at -20ºC.

1 × JC-1 staining buffer

This was prepared by a five-fold dilution of the JC-1 staining buffer 5 × (J3645) with Milli-Q water.

Protein determination reagent

A stock bicinchoninic acid (BCA) solution that contains protein standard (bovine serum albumin [BSA]) solution (P0914); bicinchoninic acid solution (B9643) and 4% (w/v) copper (II) sulphate pentahydrate (C2284). The BCA working reagent was prepared by mixing 50 parts of reagent A with 1 part of reagent B. Reagent A, without reagent B added, is stable for at least one year at RT in a closed container. The BCA working reagent (reagent A mixed with reagent B) is stable for one day. The protein standard solution was stored at 2–8 °C.

50 mM Ammonium acetate

3.854 g of ammonium acetate was dissolved in 900 mL water. The pH was adjusted to 7.0 and the volume then increased to 1000 mL, autoclaved and stored at room temperature (RT).

150 mM Sodium chloride

8.76 g of sodium chloride was added to 900 mL of water. The pH was adjusted to 7.8 and the solution was then increased to 1000 mL and stored in a glass Pyrex bottle at RT until required.

10 × Electrode (running) buffer

A 1 L 10 × running buffer solution was prepared by dissolving 30.3 g of Tris base; glycine (144.0 g) and 10.0 g SDS in ~90 mL of Milli-Q water. The volume was then increased to 1 L with Milli-Q water, the solution stored in a glass Pyrex bottle at 4°C.

1 × Electrode (running) buffer

To prepare 1 × running buffer, dilute 1:10 in Milli-Q water.

Loading/sample buffer

A stock solution was prepared by dissolving 0.5 M Tris-HCl (5.0 mL); 20% SDS (0.8 g); 100% glycerol (4.0 mL); 0.62 g dithiothreitol (DTT) and bromophenol blue (0.004 g) in ~9 mL of Milli-Q water by stirring. The volume was then increased to 10 mL with Milli-Q water, making 1 mL aliquots and stored at -20°C.

Fixative/stop solution

A fixative/stop solution was prepared by dissolving 30% ethanol in 10% acetic acid.

Sensitiser solution

1.2 mL 0.5% eriochrome black T (EBT) (0.15 g in 30 mL distilled water [dH_2O]) was added in 30% ethanol (100 mL). The solution was stored at RT in a glass Pyrex bottle.

Destain solution

30 mL ethanol was added to 70 mL of reverse osmosis water and stored at RT in a 100 mL sterile glass Pyrex bottle.

Silver solution

Silver solution was prepared by dissolving 100 µl of 37% formaldehyde and 0.25 g of silver nitrate in ~90 mL of distilled water. The volume was then increased to 100 mL with distilled water, and the solution stored at RT in a glass Pyrex bottle.

Developer solution

Developer solution was prepared by adding potassium carbonate (2 g); 1 M sodium hydroxide (1 mL); 37% formaldehyde (18.8 µl) and 1 M 0.2% sodium thiosulphate (0.1 g in 50 mL dH_2O) to distilled water (98 mL) by stirring and the solution stored at RT in a glass Pyrex bottle.

50% Acetonitrile/ammonium bicarbonate

50% acetonitrile/ammonium bicarbonate was prepared by adding 500 µl of 100% acetonitrile to 500 µl of 100 mM ammonium bicarbonate and stored in a glass Pyrex bottle at RT until required.

Trypsin diluent

The solution was prepared by adding 40 mM of ammonium bicarbonate in 10% acetonitrile and stored at RT until required.

1 M Tris-Cl

A 100 mL solution of Tris-Cl was prepared by dissolving 12.11 g of Trizma base (T01503) in 50 mL of Milli-Q water. The solution was mixed by stirring and the pH adjusted to 7.4. The solution was then increased to 100 mL, autoclaved and stored at RT until required.

0.5 M Ethylenediamine tetra acetic acid (EDTA)

The solution was prepared by adding 18.61 g of EDTA (E-5134) to 60 mL Milli-Q water and mixing vigorously with magnetic 'flea' (mixer or stirrer). The pH was then adjusted to 8.0 and the volume increased to 100 mL. The solution was then autoclaved and stored at RT.

1× TE (Tris-EDTA) buffer (200 mL)

0.4 mL of 0.5 M EDTA was added to 2 mL of 1 M Tris-Cl. The solution was then increased to 200 mL with Milli-Q water, autoclaved and stored at RT until required.

10 × TBE (Tris/Borate/EDTA) buffer

Tris (108 g; T-1503); boric acid (55 g; B-0252) and 20 mL of 0.5 M EDTA were added to 950 mL of Milli-Q water. The pH was adjusted to 8.0, and then the volume was increased to 1 L with Milli-Q water.

0.5 × TBE buffer

50 mL of 10 × TBE buffer was added to 950 mL of Milli-Q water and stored at RT in a sterile 1 L glass Pyrex bottle.

Sodium acetate buffer

408.24 g of sodium acetate was added to 800 mL of reverse osmosis water. The pH was adjusted to 5.2. The volume was increased to 1 L, then it was sterilized by autoclaving and the buffer was stored in a 1 L glass Pyrex bottle at RT until required.

Binding buffer

20 mM sodium phosphate (2.39 g), 0.5 M sodium chloride (29.2 g) and 30 mM imidazole (2.04 g) were added to 100 mL of Milli-Q water by stirring. The pH was adjusted to 7.4. The solution was stored at RT in a sterile glass Pyrex bottle until required.

Elution buffer

20 mM sodium phosphate (2.39 g); 0.5 M sodium chloride (29.2 g) and 500 mM imidazole (34.03 g) were added to 100 mL of Milli-Q water by stirring. The pH

was adjusted to 7.4. The solution was stored at RT in a sterile glass Pyrex bottle until required.

Appendix VIII

Table A8.1: IC_{50} values of *H. magnifica* venom extract *in vitro*

Extract Compound	Cell Type	IC_{50} (µg/ml)	
		MTT	Crystal Violet
H. magnifica	T47D	5.99	5.67
	MCF7	15.76	9.26
	184B5	6.74	14.70
	A549	11.14	22.91
	MRC5	18.17	24.28

Table A8.2: IC_{50} values of purified peptide from *H. magnifica in vitro*

Purified Peptide	Cell Type	IC_{50} (µg/ml)
		MTT
H. magnifica	T47D	6.97
	MCF7	5.28
	184B5	10.28
	A549	6.60
	MRC5	n/t

Note: n/t = not tested